

Electronic Thesis and Dissertation Repository

8-21-2012 12:00 AM

Disinfection of Low UV Transmittance Fluids: Fundamentals and Applications


Housyn Mahmoud, *The University of Western Ontario*

Supervisor: Dr. Ajay K. Ray, *The University of Western Ontario*

A thesis submitted in partial fulfillment of the requirements for the Doctor of Philosophy degree in Chemical and Biochemical Engineering

© Housyn Mahmoud 2012

Follow this and additional works at: <https://ir.lib.uwo.ca/etd>

 Part of the [Catalysis and Reaction Engineering Commons](#), and the [Environmental Engineering Commons](#)

Recommended Citation

Mahmoud, Housyn, "Disinfection of Low UV Transmittance Fluids: Fundamentals and Applications" (2012). *Electronic Thesis and Dissertation Repository*. 761.
<https://ir.lib.uwo.ca/etd/761>

This Dissertation/Thesis is brought to you for free and open access by Scholarship@Western. It has been accepted for inclusion in Electronic Thesis and Dissertation Repository by an authorized administrator of Scholarship@Western. For more information, please contact wlsadmin@uwo.ca.

**DISINFECTION OF LOW UV TRANSMITTANCE FLUIDS: FUNDAMENTALS
AND APPLICATIONS**

(Spine title: **Disinfection of Opaque Fluids with UV Light**)

(Thesis format: Monograph)

by

Housyn Mahmoud

Graduate Program in Engineering Science

Department of Chemical and Biochemical Engineering

A thesis submitted in partial fulfillment
of the requirements for the degree of
Doctor of Philosophy

The School of Graduate and Postdoctoral Studies
The University of Western Ontario
London, Ontario, Canada

© Housyn Mahmoud 2012

THE UNIVERSITY OF WESTERN ONTARIO
The School of Graduate and Postdoctoral Studies

CERTIFICATE OF EXAMINATION

Supervisor

Dr. Ajay K. Ray

Supervisory Committee

Dr. Hugo deLasa

Dr. Hassan Gomaa

Examiners

Dr. Dimitre Karmanev

Dr. Hassan Gomaa

Dr. Chao Zhang

Dr. Aiping Yu

The thesis by

Housyn Mahmoud

entitled:

**Disinfection of Low UV Transmittance Fluids:
Fundamentals and Applications**

is accepted in partial fulfillment of the
requirements for the degree of
Doctor of Philosophy

Date

Chair of the Thesis Examination Board

Abstract

Consumer demands for tasty, safe and healthier liquid foods and beverages. Chemical preservatives are usually added to foods to extend their shelf life and to protect against food borne pathogens. Application of ultraviolet (UV) light is gaining more attention as an alternative technology to disinfect fluids with low UV transmittance replacing classical chemical or thermal procedures due to growing negative public reaction over chemicals added. UV light irradiation has a positive consumer image as it is a physical non-thermal method efficient against microbial hazards, chemicals free cost effective and energy efficient methods and has been approved by regulatory agencies. While the use of UV light is well established for air and water treatment, its use for treating opaque fluids is limited due to low UV transmittance that restricts dose delivery, and consequently, efficient microbial inactivation. Appropriate UV reactor design that addresses effective mixing can reduce the interference of high UV absorbance and viscosity associated with liquid food products and therefore improves the inactivation efficiency. The flow pattern inside the reactor significantly influences the total applied UV dose distribution.

In this thesis, systematic study has been carried out with different size reactors (static Petri dish, Taylor-Couette and impinging jet) to understand the influence of mixing and exposure of UV light for disinfection using two UV sensitive microorganisms, Super-Hume and Para hydroxybenzoic acid (pHBA). Dimensional analysis was used to reduce the number of parameters by studying the effects of dimensionless groups on UV treatment process. The limitation of mixing effect in Petri dish was overcome through introduction flow instability and vortices in Taylor-Couette reactor by determining penetration depth of UV light in classical as well as wavy-wall Taylor-Couette reactor. Simulation results were validated with the experimental data for the disinfection of milk and pHBA solution. The effect of mixing on disinfection of low transmittance fluids was quantified and established. Finally, an Impinging Jet reactor was used for large scale treatment of blood water disinfection. It was found that alternation

between an irradiation period and dark mixing is the best approach for disinfection of opaque fluids.

Keywords:

Ultraviolet light, disinfection, UV dose, dose distribution, reduction equivalent dose, UV transmittance, UV absorber, UV reactor, log inactivation.

Acknowledgements

I would like to express my deeply felt of gratitude to those who helped me for the completion of this dissertation. Certainly, I would like to mention first my supervisor, Dr. Ajay K. Ray. I thank him for providing me with the opportunity to study under his guidance. His sound scientific advice and inspiration are deeply appreciated. In sincerely thank him for scarificing the time, effort and resourses to complete this job.

I am grateful to Torjan Technologies for funding this project and for making its labratories, testing facilities, and for the financial support. I like to earnestly thank Dr. Domenico Santoro, Dr. Jim Robinson and Dr. Mike Sages for their invaluable time in discussion on the various aspects of this project.

I want to thank the members of Chemical and Biochemical Engineering Department and the Faculty of Engineering for their support during my journey of study. Personal thanks to Mr. Souheil Afara for his continuous technical support and providing me with all kinds of help.

I am also thankful to my colleagues Panda Chowdhry, Ferdinando Crapulli, Dr. Po-Shun Chan, and Dr. Botao Beng for their assistance and cooperation throughout my stay here..

Finally, I would like to express special thanks to my uncles Rachad Haj-Toama and Fayez Fawzi for their unconditional support, and for my friends (Walid, Yasser, Youssef and Mohammad) for genuine understanding and eternal patience.

Dedication

I dedicate my dissertation to my beloved Father for all his love, care, and support throughout my life, and for my mother. Thank you for being always with me in every step of my life, without you I would not have been able to succeed.

Table of Contents

CERTIFICATE OF EXAMINATION	ii
Abstract	iii
Acknowledgements	v
Dedication	vi
Table of Contents	vii
List of Tables	xiv
List of Figures	xvi
Nomenclature	xx
Chapter 1	1
1 General Introduction	1
1.1 Background & Motivation	1
1.1.1 Ultra-Low UV Transmittance Fluids	3
1.1.2 Disinfection Methods	4
1.1.3 Mechanism of UV Disinfection	7
1.1.4 Methodology	9
1.2 Objectives and Scope	10
1.2.1 Research Objectives	10
1.2.2 Scope	10

1.3	Thesis Overview.....	11
1.4	References	12
	Chapter 2.....	14
2	Identification of UV Absorbing Compounds for Low UV Transmittance Fluids	14
2.1	Introduction	14
2.1.1	Super Hume	17
2.1.2	Coffee.....	18
2.1.3	Rhodamine B	18
2.1.4	Methylene Blue.....	19
2.1.5	Para- Hydroxybenzoic Acid (pHBA).....	20
2.1.6	Adnine.....	21
2.1.7	Preface results	22
2.2	Stability and Scattering of the UVT Modifiers	22
2.2.1	Abstract.....	22
2.2.2	Method	23
2.2.3	Tests details.....	24
2.2.4	Results.....	31
2.1	Sensitivity test	36
2.2	Conclusions	39

2.3	References	40
Chapter 3.....		41
3	Collimated Beam and Ultra Low UV Transmittance (Opaque) Fluids	41
3.1	Introduction	41
3.2	Collimated Beam's Dose Distribution and RED.....	45
3.3	Reducing dose distribution delivered for opaque sample under collimated beam 47	
3.3.1	Scattering, Alternated mixing direction effects	47
3.3.2	Pulse Irradiation (Light-Dark) Effects	52
3.4	Conclusions	53
3.5	References	54
Chapter 4.....		56
4	Dimensional Analysis of UV Disinfection in an Annular Reactor of Opaque Fluids 56	
4.1	Introduction	56
4.2	Definitions.....	56
4.2.1	Buckingham's PI theorem.....	56
4.2.2	Independent (Basic, or Primary) dimensional units.....	56
4.2.3	Dependent (Secondary Dimensional Units).....	56
4.3	Dimensional Analysis of an Annular Reactor.....	57

4.3.1	Dimensional Variables.....	58
4.3.2	Methodology: Pi-Groups Derivation	59
4.3.3	Dimensional Analysis and UV disinfection.....	60
4.3.4	PI Groups effects.....	62
4.4	Conclusions	68
4.5	References	70
Chapter 5.....		76
5	Taylor Couette Reactor	76
5.1	Introduction	76
5.2	Brief History of Taylor-Couette Flow.....	76
5.2.1	Taylor-Couette Flow without an Axial Flow	78
5.3	CFD Modeling of Taylor-Couette reactor for Opaque Fluids UV Disinfection	79
5.3.1	Taylor Couette Reactor	80
5.3.2	Mathematical Modeling	82
5.3.3	Measurements of UV incident radiation	85
5.3.4	Grid Independence Study.....	87
5.3.5	Actinometer Solution	88
5.3.6	Boundary conditions	90
5.4	Results and Discussion.....	91

5.4.1	Model Verification.....	91
5.4.2	Model Validation – Tracer Test.....	94
5.4.3	Model Validation – Steady State	95
5.4.4	Model prediction.....	96
5.4.5	Taylor Couette –Milk Disinfection test	99
5.5	Penetration depth effect.....	101
5.6	Modulate Taylor Couette reactor	104
5.7	Mixing efficiency.....	105
5.8	Conclusions	106
5.9	References	107
Chapter 6.....		108
6	Industrial Large Scale Reactor.....	108
6.1	Introduction	108
6.1.1	Measurment of UV Transmittance.....	109
6.1.2	Preliminary tests.....	110
6.1.3	The Pilot Test.....	113
6.2	Full Scale System of Reactors Validation Tests	114
6.2.1	Test Objectives.....	115
6.3	Collimated Beam Test.....	116

6.4	Microorganism Selection	116
6.5	Target Microorganism Study	117
6.5.1	Determining the D_{10} of the Targeted Virus (IHNV).....	117
6.5.2	Determining the Required Dose for the Treatment.....	118
6.5.3	Determining UV Dose–Response Curve of Test Microorganism	118
6.5.4	Test Technical Details.....	119
6.5.5	Blank Test	120
6.6	Short-Term Performance Test.....	120
6.7	Long-term performance test.....	120
6.8	Results and Discussion.....	121
6.8.1	Short-Term Performance Test.....	122
6.8.2	Long-Term Performance Test.....	122
6.9	Reactor Evaluation	124
6.10	Conclusions	125
6.11	References	125
Chapter 7	127
7	Conclusions and Recommendations	127
7.1	Major Contributions	128
7.2	Other Key Contributions	129

7.3	Recommendations for Future Work.....	129
	APPENDIX.....	130
A.	Appendix A: Dimensional Analysis of Annular Reactor	130
B.	Appendix B: Taylor Couette Reactor	138
B.1	Case Designs Two Different Dimensional Designs with Identical PI Groups	138
B.2	Disinfection Results	140
B.3	Milk Disinfection Test with Taylor Couette Reactor.....	141
B.4	UVT measurements' with integrating sphere.....	143
C.	Appendix C: Impinging Jet Validation test	144
C.1	Blank Test	144
C.2	RED Bias Factor.....	146
C.3	Dimensional Variables IJ reactor	148
C.4	Tanks Connections	148
C.5	Dimensional Groups.....	149
C.6	Mixing effect Joel J. Ducoste, Scott Alpert simulation	150
C.7	Reactor Efficiency.....	150
	Curriculum Vitae	152

List of Tables

Table 2-1:Summary of costs of 100L solution at targeted UVT for different	16
Table 2-2:Concentrations of the UVT modifiers based on the target absorbance of 8 cm^{-1}	23
Table 2-3:Summary of the stability tests of UVT modifiers	35
Table 3-1:Disinfection in 2% Milk with UV light emitted from Collimated Beam.....	46
Table 3-2:T1 UV Disinfection in 2% Milk with UV emitted from Collimated Beam.....	46
Table 3-3:MS2 Disinfection in pHBA with UV emitted from Collimated Beam with Petri dish mixed with alternated direction mode (CW-CCW)	48
Table 3-4:MS2 Disinfection in 2% Milk with UV emitted from Collimated Beam with Petri dish mixed with alternated direction mode (CW-CCW).....	48
Table 3-5:T1 Disinfection in pHBA with UV emitted from Collimated Beam with Petri dish mixed with alternated direction mode (CW-CCW)	48
Table 3-6:T1 Disinfection in 2% Milk with UV emitted from Collimated Beam with Petri dish mixed with alternated direction mode (CW-CCW)	48
Table 3-7:MS2 Disinfection in pHBA with UV emitted from Collimated Beam with Petri dish mixed with single direction mode	49
Table 3-8:MS2 Disinfection in 2% Milk with UV emitted from Collimated Beam with Petri dish mixed with single direction mode.....	49
Table 3-9:T1 Disinfection in pHBA with UV emitted from Collimated Beam with Petri dish mixed with single direction mode	49

Table 3-10:T1 Disinfection in 2% Milk with UV emitted from Collimated Beam with Petri dish mixed with single direction mode.....	50
Table 3-11:Scattering, Alternated mixing direction effect on Collimated Beam Irradiation	51
Table 3-12:RED Ratios: Scattering, Alternated mixing direction effect on Collimated Beam Irradiation	51
Table 3-13:MS2 Disinfection in 2% Milk with UV emitted from Collimated Beam in pulsation mode with Petri dish mixed with single direction mode.....	52
Table 3-14:T1 Disinfection in 2% Milk with UV emitted from Collimated Beam in pulsation mode with Petri dish mixed with single direction mode.....	52
Table 4-1:Identical PI Groups values for different dimensional designs	60
Table 4-2:Simulation Results of Dimensional Analysis.....	62
Table 4-3:Effect of Reynolds Number on UV Disinfection of PI Groups	63
Table 4-4:Effect of Lamp Aspect Ratio on UV Disinfection of PI Groups.....	64
Table 4-5:Effect of Absorption Thickness on UV Disinfection of PI Groups	64
Table 4-6:Effect of UV Power on UV Disinfection of PI Groups.....	65
Table 5-1: Boundary conditions.....	90
Table 6-1:: Log Inactivation	124

List of Figures

Figure 1-1:Upper: Representation of UV Transmittance.....	4
Figure 1-2:UV Inactivates Microorganisms by DNA Disrupting Technologies	8
Figure 1-3:Different UV Treatment Technologies	9
Figure 2-1:Coffee, SuperHume, and pHBA are examples of commonly used as UV absorbing materials in UV reactor validation	15
Figure 2-2:Superhume UVA vs. concentration	17
Figure 2-3:Coffee UVT vs. concentration (Malley et al., 2001)	18
Figure 2-4:Molar extinction coefficient spectrum of Rhodamine B dissolved in ethanol (omlc).....	19
Figure 2-5:Molar extinction coefficient spectrum of Methylene Blue dissolved in water(omlc).....	20
Figure 2-6:pHBA Absorbance vs. concentration.....	21
Figure 2-7:Absorbance stability of the UVT modifiers against UV irradiation	31
Figure 2-8:Absorbance stability of the UVT modifiers against time	32
Figure 2-9:Absorbance stability of the UVT modifiers against pH agents.	33
Figure 2-10:Absorbance stability of pHBA before and after pH adjusted to ≈ 7	33
Figure 2-11:Absorbance measurements of pHBA, SuperHume and coffee	34
Figure 2-12:Survival test for MS2 and T1 in four different UVT modifiers.....	36
Figure 2-13:Sensitivity test for MS2 in Super Hume	37

Figure 2-14:Sensitivity test for T1 in Super Hume.....	38
Figure 2-15:Sensitivity test for MS2 in pHBA	38
Figure 2-16:Sensitivity test for T1 in pHBA.	39
Figure 3-1:Schematic of collimated beam device.....	42
Figure 3-2:MS2 Dose Response Behavior.....	44
Figure 3-3:T1 Dose Response Behavior	44
Figure 4-1:Schematic representation of an annular UV reactor	57
Figure 4-2:PI Goupd relative effect on UV Disinfection in an Annular Reactor	66
Figure 4-3:Microorganisms Concentration Profile for Four Different Cases.....	67
Figure 5-1:Taylor Center section of the fluid column with laminar axisymmetric Taylor vortices at $Ta = 1.16 Ta_{cr}$ (from Koschmieder, 1979)	77
Figure 5-2:Schematic Representation of UV Taylor-Couette Reactor	81
Figure 5-3:UV Irradiance Measurements' setup.....	86
Figure 5-4:UV Irradiance Measurements Data obtained from X911 UVC Radiometer ..	86
Figure 5-5:Normalized Velocity profiles at Different Quad elements along Thickness ..	88
Figure 5-6:Absorbed Energy vs. Absorbance	89
Figure 5-7:Stable Solution – Radial Velocity Profile Comparison	92
Figure 5-8:Unstable Solution – Radial Velocity Profile Comparison	93
Figure 5-9:Breakthrough Curve with Passive Tracer	94

Figure 5-10:Steady State Model Validation	95
Figure 5-11:Prediction of First Order Inactivation Curve	97
Figure 5-12:Average dose/D10 vs. Relative error	98
Figure 5-13:MS2/T1 Survival Test in Milk (96Hours).	99
Figure 5-14:MS2-Milk Sensitivity Test.....	100
Figure 5-15:MS2-Milk Sensitivity Test.....	100
Figure 5-16:Log Inactivation Comparison CFD Vs Experimental Data	101
Figure 5-17:Dimensionless Penetration Depth Effects.....	102
Figure 5-18:Dimensionless Penetration Depth Effects.....	102
Figure 5-19:Penetration Depth Effects in Taylor Couette Reactor.....	103
Figure 5-20:RED in Modulate Taylor Couette Reactor.....	104
Figure 5-21:Energy Consumption per Different Reactors Raw Milk.....	105
Figure 5-22:Energy Consumption per Different Reactors Pasteurized Milk.....	105
Figure 6-1: Simplified Model Geometry IJ Reactor U.S. Pat. No. 7,166,850.....	108
Figure 6-2:UVT measurement using DRA-30 Lab Sphere fixed on Varian Spectrophotometer Cary 100	109
Figure 6-3:Blood Water Stability Test.....	110
Figure 6-4:T1/MS2 UV disinfection Curves	111
Figure 6-5:Reduction Equivalent Dose IJ Reactor	111

Figure 6-6:Impinging Jet Reactor	112
Figure 6-7:Experimental Layout used during Bioassay Experiment	113
Figure 6-8:T1 Counts vs. Operating Time	114
Figure 6-9: Schematic of Effluent’s Treatment System	114
Figure 6-10:IJ-UV Reactors.....	115
Figure 6-11:T1 Performance Curve for Walcan's Plant Effluent 2009	116
Figure 6-12:Dose-Response Curves for IHN and VHS Virus	117
Figure 6-13:T1 Dose-Response Curves in Plant’s Effluent (“Composite”) and in Clean Water (“PBW”).....	118
Figure 6-14:T1 Dose-Response Curve in Clean Water	119
Figure 6-15:Schematic of Reactor Long-Term Test.....	121
Figure 6-16:T1UV RED for 50, 75 & 100 gpm Flow Rates Measured at Six Outlets...	122
Figure 6-17:T1 RED for 50 gpm Flow Rate.....	123
Figure 6-18:T1 RED for 84 gpm Flow Rate.....	123

Nomenclature

A	Absorbance [-]
Abs	Absorbance[-]
AT	Absorption Thickness[-]
C	Concentration [Counts/m ³]
D	UV dose [J/m ²]
D_s	Specific Dose[-]
I_0	Irradiance at the sleeve surface [W/m ²]
$I_\lambda(\vec{r})$	UV Irradiance [W/m ²]
I_{ave}	Average Irradiance [W/m ²]
K_d	Free-swimming microorganism inactivation rate constant [m ² /W/log]
k_{or}	Inactivation constant of microorganism per log inactivation[m ² /W/log]
L	Path length [m]
MS2	Bacteriophage MS2 [Counts/m ³]
N_0	Microorganism Initial count [Counts/m ³]
N	Microorganism count [Counts/m ³]
N_d	Free-swimming microorganism initial concentration [Counts/m ³]

P	Lamp Power [W]
PP7	Bacteriophage PP7 [Counts/m ³]
Q	Volumetric Flow Rate [m ³ /s]
R17	Bacteriophage R17 [Counts/m ³]
R	Radius [m]
Re	Reynolds' number [-]
r_i	Inner radius [m]
Rt	Retention time [s]
\vec{s}	Direction Vector
T1	Bacteriophage T1 [Counts/m ³]
TC	Taylor Couette [-]

Greek letters

α	Absorption coefficient
Γ	Diffusive coefficient
δ	Gap [m]

ε	Molar absorptivity (extinction coefficient) of the absorber [1/cm/M]
μ	Dynamic Viscosity [kg/m/s]
λ	Light wavelength of radiation [nm]
ν	Kinematic Viscosity [m ² /s]
ρ	Density [kg/m ³]
σ	Scattering coefficient [1/m]
Φ	Geometrical Phase Function
Ω	Angular Velocity [rad/s]

Acronyms

CBR	Collimated Beam Reactor
CFSTR	Continues Flow Stirred Tank Reactor
DO	Discrete Ordinate
E. Coli	Escherichia Coli
HRT	Hydraulic Retention Time
IHNV	IHN Virus
LP	Low Pressure
LPHO	Low Pressure High Output

LSA	Lignan Sulfanate
MP	Medium Pressure
p-HBA	Para-Hydroxybenzoic acid
RED	Reduction Equivalent Dose
ST	Scattering thickness
RTE	Radiative Transfer Equation
UDS	User defined Scalar
UV	Ultraviolet Light
UVT	Ultraviolet Transmittance
VHSV	VHS Virus

Chapter 1

1 General Introduction

1.1 Background & Motivation

In an increasingly regulated and safety-conscious society, the food, beverage and brewing industries have to meet more stringent standards of quality. Microbial growth due to contaminated water or ingredients can cause discoloration, fusty flavors and reduced shelf-life. The threat of contamination is further increased as manufacturers respond to demands for less chemical additives and preservatives for appetizing and safe liquid foods. Effective microbial disinfection of the entire process is therefore essential. While thermal food preservation processes have a long history of successful application, they suffer from important drawbacks, including the potential to change the nutritional properties, taste, or odor of these food items. Other non-conventional disinfection systems rely on the use of chemicals to provide the needed dose to reach the desired level of inactivation. However, this approach has a number of disadvantages such as the potential formation of disinfection byproducts and, at times, the increased water toxicity. An alternate non-chemical approach is to use Ultra-Violet (UV) radiation. Exposure of fluid to UV radiation inactivates microorganisms and bacteria contained within the fluid. Furthermore, UV treatment has the advantages of (i) easy to operate with all process arrangement, (ii) reduced footprint, (iii) the ability to control and (iv) monitor the irradiance at certain location, (v) lower operating cost

Disinfecting very low transmittance fluid with ultraviolet (UV) germicidal irradiation has been neglected in spite of that ultraviolet based technologies have seen rapid growth over the past decade. Since the demonstration of the UV ability to disinfect bacteria and viruses through damaging its nucleic acid and make them unable to reproduce itself instead of the classical disinfection methods like chlorination etc. The problem behind the reluctance of the scientists and engineers in exploring was mainly because of fast attenuation of the UV light within such fluids and because of the non-homogenous

composition of such fluid, which lead to several problems. These problems are the lack of a disinfectant residual and a direct method to monitor the optical properties of low UV transmittance fluids and disinfection performance and as consequence an accurate model of irradiance field. In chemical disinfection systems, accurate predictions of reactor performance can be yielded using the information of disinfectant concentration and the residence time distribution. However, in UV disinfection systems, the radiation intensity field typically is characterized by strong spatial gradients. In addition, transport behavior (*i.e.*, fluid mechanics) within these systems can be quite complex. Therefore, particles (*i.e.*, microorganisms) will pass through the UV reactor with different trajectories and receive different UV doses. UV dose, defined as the time-integral of the UV intensity history delivered to a particle, is the master variable in photochemical processes. Knowledge of the dose distribution is necessary to fully characterize the performance of the system. To date, it is not possible to monitor dose distribution. Therefore, it is required to operate the system under validated operation conditions (*i.e.*, lamp output power, water transmittance, and flow rates) and to monitor these parameters during operation in order to protect public health.

As environmental regulations have been more severe and the concerns regarding chemical treatment methods was continued to rise, the need for more environmentally solution became an issue. The use of UV technology for disinfecting low UV transmittance (UVT) fluids came back to be attractive option for defeating the undesired parts of the classical methods.

A mathematical model for UV lamp intensity was developed along with a model for the reflected and refracted intensity inside the UV lamp sleeve. The dose received by any microbe passing through this field can then be computed and the disinfection rate of a population of microbes passing through this field could have been evaluated.

Different types of reactors are selected to enable us to construct a complete idea about the scenery of disinfection problem of Ultra Low Ultraviolet Transmittance (UL-UVT) fluids. These reactors are: Petri dish reactor (PMR reactor), annular gap, Taylor-

Couette (TC), and Impinging Jet (IJ) reactor. The factors which are going to be included in this study can be divided into four main categories: Geometrical (reactor dimensions), Optical (fluid absorption, scattering, etc), Kinetic (microbial disinfection rate constants), and Hydraulic (flow rate, viscosity, density, etc).

Computer code was used to allow us to study of the parameters to determine which factors are critical to the design of effective systems and how these factors are inter-related. This program will be used to generate enough data sets by using proper design of experiment. These data sets are, in turn, analyzed to assess these parameters. The result will enable us to determine the factors which affect the disinfection directly and in turn play major role in design of more effective UV systems.

1.1.1 Ultra-Low UV Transmittance Fluids

Using ultraviolet (UV) light for drinking water disinfection dates back to 1906 in Marseille France. In the United States first full scale application started in Henderson, Kentucky was in 1916. Over the years, UV costs have declined as researchers develop and use new UV methods to disinfect water and later wastewater. Currently over 10,000 facility based on UV irradiation technology are working around the world. In spite of the huge success UV Technology achieved in the field of drinking-waste water treatment, researcher's are still hesitating to apply this technology to opaque fluids.

By definition opaque means not transmitting or reflecting light or radiant energy; impenetrable to sight, however to be more precise the UV transmittance of drinking water is in the range of 75-95% or in terms of absorbance it is less than 0.1 as some researchers like to express it. For wastewater the UV transmittance is 45-65% and for low UV transmittance fluids it is around 10%, while it goes down to less than 0.1% to what we called Ultra-Low (UL-UVT) fluids.

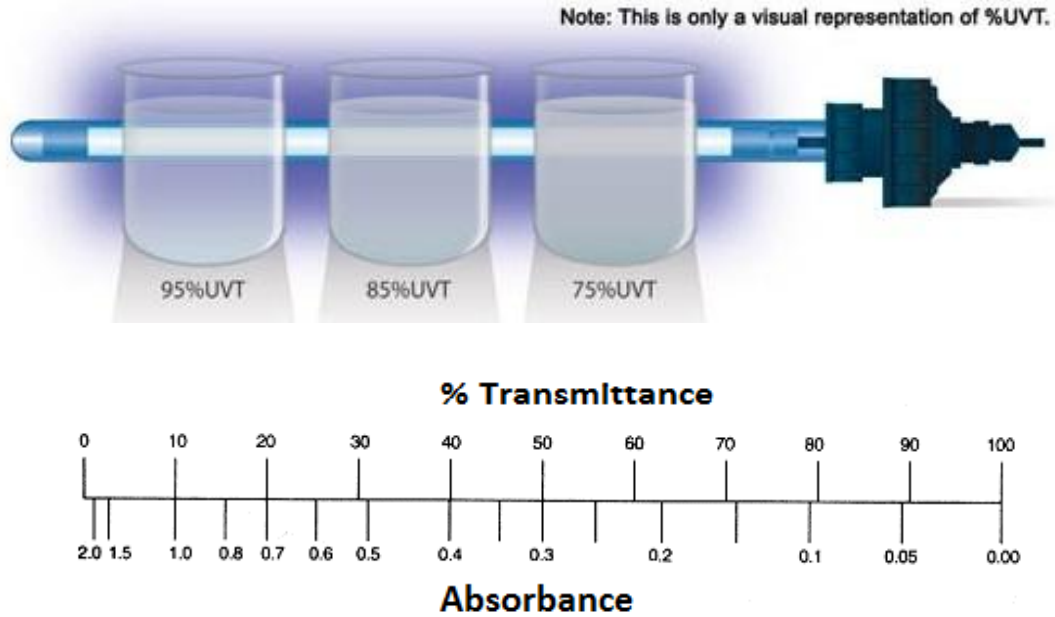


Figure 1-1:Upper: Representation of UV Transmittance.

Lower: Relation between Transmittance -Absorbance

The challenges associated with applying the UV in disinfection of such fluids with UV irradiation were:

1. The ability of the UV light to penetrate such fluids in depth and disinfect highly contaminated liquids such milk, juices, blood, etc.
2. The restriction on the elevation of the treated fluid temperature and also on the fluid optical properties.
3. The ability to treat all microorganisms present in fluids including fungus and biocide resistant mycobacterium.

1.1.2 Disinfection Methods

Disinfection, as applied to water treatment, wastewater treatment and food processing; is a process by which, pathogenic microorganisms are inactivated to provide public health protection. There are two common types of methods to achieve disinfection:

1. Chemical disinfection such as chlorination
2. Physical disinfection such as pasteurization and ultraviolet (UV) disinfection.

The traditional disinfection method is chlorination. The main problems associated with chlorination are residual chlorine compounds and the danger of handling chlorine. Dechlorination and other safety requirements increase the cost of chlorine based disinfection while the cost of UV disinfection has been reduced because new and efficient UV disinfection systems have been developed. Currently, the cost of the two processes is similar for wastewater disinfection (Water Environment Federation, 1996). Furthermore, because of residual chlorine compounds, chlorination is mainly used for processing of water or wastewater, and it is seldom used for processing of liquid foods such as juices or Milk.

Among physical disinfection methods, thermal pasteurization has been used for processing of foods for many years. Because it is a thermal method, the flavour of foods is affected and some nutritional components, which are sensitive to heat, are destroyed during the disinfection process.

Outbreaks of food-borne illness associated with the consumption of unpasteurized juice and apple cider have resulted in a rule published by the U.S. Food and Drugs Administration (FDA) in order to improve the safety of juice products. The rule (21 CFR120) requires manufacturers of juice products to develop a Hazard Analysis and Critical Control Point (HACCP) plan and to achieve a 5-log reduction in the numbers of the most resistant pathogens (US FDA, 2000).

UV disinfection is one of the promising methods to reach the 5-log reduction of Pathogen. Compared with traditional disinfection methods such as pasteurization and chlorination, UV disinfection has following advantages:

1. UV disinfection is a physical method, it leaves no harmful chemical residuals.
2. UV disinfection is a non-thermal method, the flavour of food is not affected. Nutritional components, which are sensitive to heat, are not destroyed by the UV disinfection process or are destroyed less than by pasteurization.

However, like other photochemical reaction systems, UV disinfection has a unique and intrinsic characteristic since radiation energy is absorbed by the fluid in which the micro organisms are suspended leading to non-uniform fluence rates.

The simplified form of the radiative transfer equation is Lambert-Beer's law,

$$I = I_0 \exp(-\alpha \cdot l) \quad (1-1)$$

Where:

I , fluence rate at path length l , mW/cm²;

I_0 , incident fluence rate, mW/cm²;

α , absorbance coefficient, cm⁻¹;

l , path length, cm.

From equation (1-1), the radiation fluence rate decreases exponentially with the path length from the radiation source. In other words, the non-uniform disinfection rates caused by the non-uniformity of fluence rate can severely limit disinfection efficiency especially when liquid foods with high absorption coefficients are treated. The non-uniform disinfection rates present a big challenge when designing UV disinfection reactors. The application of UV to opaque fluids disinfection is the main topic of this study.

1.1.3 Mechanism of UV Disinfection

Light is characterized by its wavelength. UV has wavelengths between 200 – 400 nm and can be further divided into UVA (320-400 nm), UVB (280-320 nm) and UVC (200-280 nm). Approximately 85% of the output from low-pressure mercury arc lamps is monochromatic at a wavelength of 254 nm (Water Environment Federation, 1996).

$$E_{\lambda} = \frac{hC}{\lambda_w} A_v \quad (1-2)$$

Where:

E_{λ} , radiant energy at a given wavelength λ_w , kJ/Einstein;

C, speed of light, 3×10^8 m/s;

h, Planck's constant, 6.626×10^{-34} J·s;

λ_w , wavelength, m;

A_v , Avogadro's number, 6.023×10^{23} photons/Einstein.

Therefore, radiant energy at $\lambda_w = 254$ nm has 472 kJ/Einstein. In a photochemical reaction, one Einstein represents one “mole”. It should be noted that 472 kJ/Einstein or 472 kJ/mole is greater than the bond energies of several important bonds in microbial systems. For example, the C-H bond is about 401-414 kJ/mole and the C-C bond is about 347-355 kJ/mole. Both proteins and nucleic acids are effective absorbers of UVC. This absorption causes genetic damage and thus disinfection of bacteria and viruses; therefore, UVC light is also referred to as germicidal radiation. DNA (Deoxyribonucleic acid) consists of a sequence of four constituent bases known as purines (adenine and guanine) and pyrimidines (thymine and cytosine). They are linked together in a double-stranded helix. When UVC radiation is absorbed by the 4 pyrimidine bases (mainly thymines), it permits a unique photochemical reaction, which leads to dimerization of adjacent pyrimidines (formation of a chemical bond between the pyrimidines). Most of the time, the dimerization happens with thymines as shown in Figure 1, but cytosine dimers and thymine-cytosine heterodimers can also be formed. This disruption in the structure of the

DNA makes it unable to replicate when the cell undergoes mitosis. This is the fundamental mechanism of UV disinfection (Jagger, 1967).

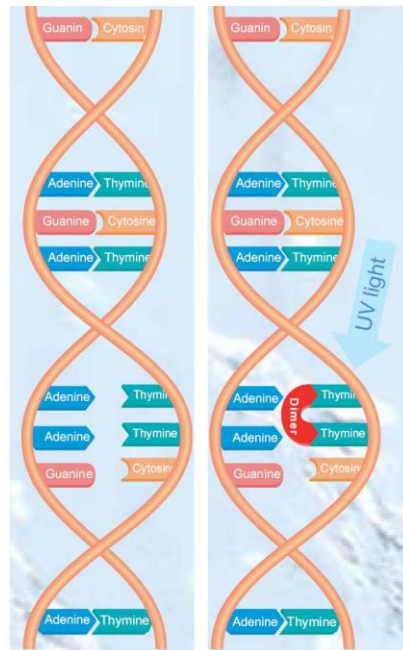


Figure 1-2:UV Inactivates Microorganisms by DNA Disrupting Technologies

We examined several possibilities with regards to the design of Ultra-Low UVT fluids reactors such as static mixers, reactors with fluid instability (Taylor-Couette, Dean Vortices reactor), and thin layer reactors (impinging jet) and we found certain practical features with each one. The thin layer reactor depends mainly on treating thin layers of fluid of a total thickness of the same order of magnitude as the UV light penetration depth or less, while the reactors in which flow instability was introduced depend on enhancing mixing of the treated fluid through vortices. Taylor-Couette reactor is one example where that mixing is introduced through flow instability which is controlled by rotation speed of one or both cylindrical surface of an annular reactor. The last proposed reactor used in this study is Impinging Jet reactor where fluid to be treated is forced to reach very close to the UV lamp surface instead of the classical methods, which relies on ability of UV light penetration.

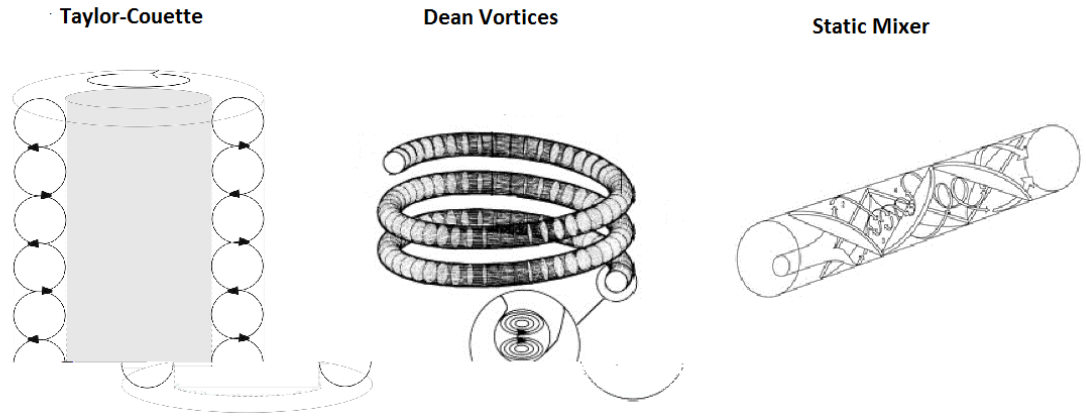


Figure 1-3: Different UV Treatment Technologies

1.1.4 Methodology

To analyze all the reactors, It has been found that large number of variables influence the reactor performance. Governing partial differential equations depends on numerous variables that include geometrical as well as their process variables which need to be solved. In evaluating the sensitivity of all these variables on reactor performance experimentally will be extremely time consuming and will be expensive, whereas CFD will be computationally expensive and it also not guaranteed that we will be able to generalize our results. However, we know from Buckingham Pi Theorem that any equation of the mathematical physics can be written in non-dimensional form, and the several variables can be combined into dimensionless groups thereby reducing number of variables to be studied saving time and money for bioassay tests in real size UV reactor. Hence, CFD studies in non dimensional space using dimensionless groups and variables will save time and resources for prediction of reactor performance. These study in non dimensional space will provide knowledge of better understanding of the disinfection performance of the UV reactors and later on for scaling-up of such reactors.

1.2 Objectives and Scope

1.2.1 Research Objectives

The objective of this work is to develop a comprehensive method for designing reactors systems for disinfection of ultra low UV transmittance fluids and to identify the differences in operating principles and ways to improve and optimize their performances.

1.2.2 Scope

The scope of this research includes the following steps:

1. Identification of model UV absorbing compounds for low UV transmittance Fluids.
2. Identification of criteria when collimated beam is used to study ultra low UVT fluids.
3. Development of dimensional analysis to reduce number of physical parameters and study the sensitivity and the interactions of dimensionless groups on reactor performance.
4. Development of a numerical model describing the intensity field for UL-UVT fluids and several reactors considered.
5. Selecting the proper mathematical model for microbial response and analysis, and simulation of the disinfection problem.
6. Validation of mathematical models with experimental results.
7. Optimization of performance of UL-UVT reactor systems.
8. Identify the key factors affecting disinfection of very low UV transmittance fluids.

1.3 Thesis Overview

This thesis includes seven chapters and follows the “monograph format” as mentioned in the Thesis Regulation Guide by the School of Graduate and Postdoctoral Studies (SGPS) of the Western University.

Chapter 2 entitled “Identification of UV absorbing compounds for low UV transmittance Fluids” introduces several model UV absorbers, determination of criteria and evaluation of the suitability of these to be used in UV reactors for validation.

Chapter 3 entitled “Collimated beam and ultra low UV transmittance fluids”. In this chapter we focus on identifying the main criteria to be taking into consideration when collimated beam is used to study ultra low UV transmittance fluids.

Chapter 4 entitled “Dimensional analysis of UV disinfection in annular reactor of opaque fluids”. It illustrates briefly the Buckingham Pi theorem and its application to reduce the number of variables to be studied for UV disinfection of low UV transmittance fluids.

Chapter 5 entitled “Taylor Couette reactor”. In this chapter, the concept of Taylor Couette flow and flow instability is introduced that increases mixing with in the reactor for treatment of ultra low UV transmittance fluid. Dimensional analysis was applied to reduce the number of physical parameters to be studies. Both numerical simulation using CFD and verification of simulation results was validated experimentally.

Chapter 6 entitled “Industrial large-scale Impinging Jet reactor”, which represents how we applied the lessons learned from the previous chapters to study the disinfection of blood water in industrial-scale reactor.

Chapter 7 summarizes the key conclusions of this research and suggests some ideas for future research based to be conducted.

1.4 References

Andereck, C. D., Liu, S. S., Swinney, H. L., Flow regimes in a circular Couette system with independently rotating cylinders, *Journal of Fluid Mechanics* 164, p. 155-183(1986).

Baier, G., Graham, M. D., Two-fluid Taylor-Couette flow: experiments and linear theory for immiscible liquids between corotating cylinders. *Physics of Fluids* 10, 3045-3055 (1998).

Baier, G., Grateful, T. M., Graham, M. D., Lightfoot, E. N., Prediction of mass transfer in spatially periodic systems. *Chemical Engineering Science* 54, 343-355 (1999).

Becker, K. M., Kaye, J., Measurements of diabatic flow in an annulus with an inner rotating cylinder. *Journal of Heat Transfer* 84, 97 (1962).

Bird, R. B., Stewart, W. E., Lightfoot, E. N., *Transport Phenomena*, Wiley, New York (2002).

Blatchley, E. R., Dumoutier, N., Halaby, T. N., Levi, Y., Laine J. M., Bacterial responses to ultraviolet irradiation, *Water Science and Technology* 43, 179-186 (2001).

Chandrasekhar, S., The hydrodynamic stability of viscid flow between coaxial cylinders., *Proceedings of the National Academy of Sciences of the United States of America*, 46, 141-143 (1960).

Chiu, K., Lyn, D. A., Savoye, P., Blatchley, E. R., Effect of UV system modification on disinfection performance. *Journal of Environmental Engineering*, 125, 7-16 (1999).

Chung, K. C., Astill, K. N., Hydrodynamic instability of viscous-flow between

rotating coaxial cylinders with fully developed axial flow, *Journal of Fluid Mechanics* 81, 641-655 (1977).

Cohen S., Marom, D. M., Experimental and Theoretical study of a rotating annular flow reactor. *Chemical Engineering Journal* 27, 87-97 (1983).

Coles, D., Transition in circular Couette flow. *Journal of Fluid Mechanics* 21, 385-425 (1965).

Collins, H. F., Selleck, R. E., Process kinetics of wastewater chlorination, SERL Report, Univ. of Calif., Berkeley, 72-75 (1972).

Davey, A., DiPrima, R. C. and Stuart, J. T. On the instability of Taylor vortices. *Journal of Fluid Mechanics* 31, 17-52 (1968).

Davidson, P. A. *Turbulence: An Introduction for Scientists and Engineers*, Oxford University Press (2004).

Chapter 2

2 Identification of UV Absorbing Compounds for Low UV Transmittance Fluids

2.1 Introduction

The Ultra Violet Transmittance (UVT) of a medium plays an important role in delivering specific dose in Ultra Violet (UV) reactor. To ensure reactor performance and the specified dose delivery to a certain fluid, it is best to carry out reactor validation either at the test facility or at the manufacturer plant; however water or in more general testing fluid should have UVT representative of the final destination treated fluid.

During validation the UVT of testing fluid is changed to match the designated one by adding UV absorbing components. One of the important aspects in selecting the UV absorber is equivalency between its absorbing spectrum and treated fluid, especially in case of polychromatic medium pressure (MP) lamp. The mismatching in the absorbing spectrum leads to deviation in validation results in any reactor if MP lamp is used. However, this is not an issue if low pressure LP or lower pressure high output LPHO lamps are used since these are monochromatic lamp (Figure 2.1).

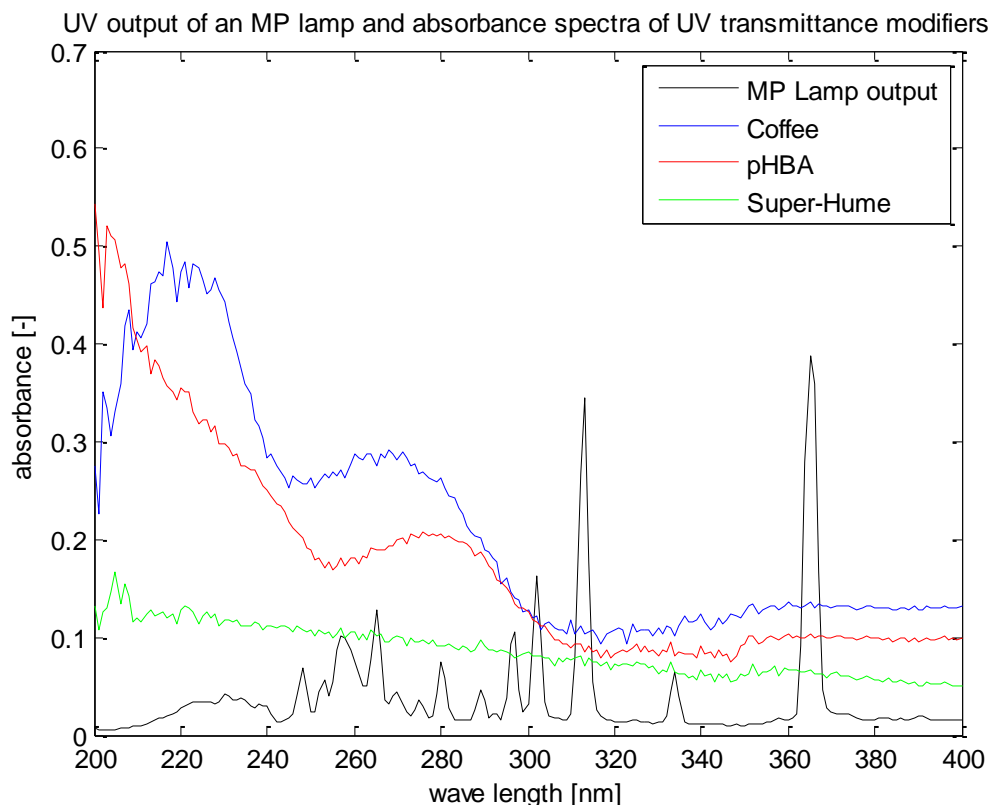


Figure 2-1: Coffee, SuperHume, and pHBA are examples of commonly used as UV absorbing materials in UV reactor validation

Table 2.1 lists nine modifiers, Lignan Sulfanate (LSA) has been proven to inactivate phages MS2, R17 and PP7 (Fallon et al., 2007). There is limited information about using tea and sugar as UVT modifiers from literatures. The required amounts for 100 liter solution at target UVT and costs were estimated using extinction coefficients and solubility from literatures for Rhodamine B, Methylene Blue and Adenine. SuperHume, coffee and Hydroxybenzoic acid (pHBA) were also estimated using extrapolation of available data of UVA as function of concentration.

Table 2-1: Summary of costs of 100L solution at targeted UVT for different

Modifier	Ability to reach the target UVT ($10^{-8}/\text{cm}$)	Amount per 100L	Unit Price	Cost for 100L at target UVT	Note
SuperHume¹	Not sure	0.3 L	\$10/gallon	\$1	
Coffee¹	Not sure	0.025 lb	\$20/kg	\$1	
Rhodamine B²	Yes	15 g	\$386.25/100g	\$60	Toxic; irritating
Methylene Blue²	Yes	20 g	\$76.43/25g	\$65	
pHBA¹	NA	10 g	\$33.58/kg	\$0.5	
Adenine²	NA	10 g	\$77.97/25g	\$30	Irritating; low solubility
Tea	NA	NA			
Sugar	NA	NA			Potentially high viscosity
LSA					Inactivate MS2

¹ Based on the extrapolation on the UVA v.s. concentration curves from literatures.

² Based on extinction coefficients and solubility from literatures.

2.1.1 Super Hume

Super Hume required amount was obtained from calibration curve data illustrated in Figure(2-2)

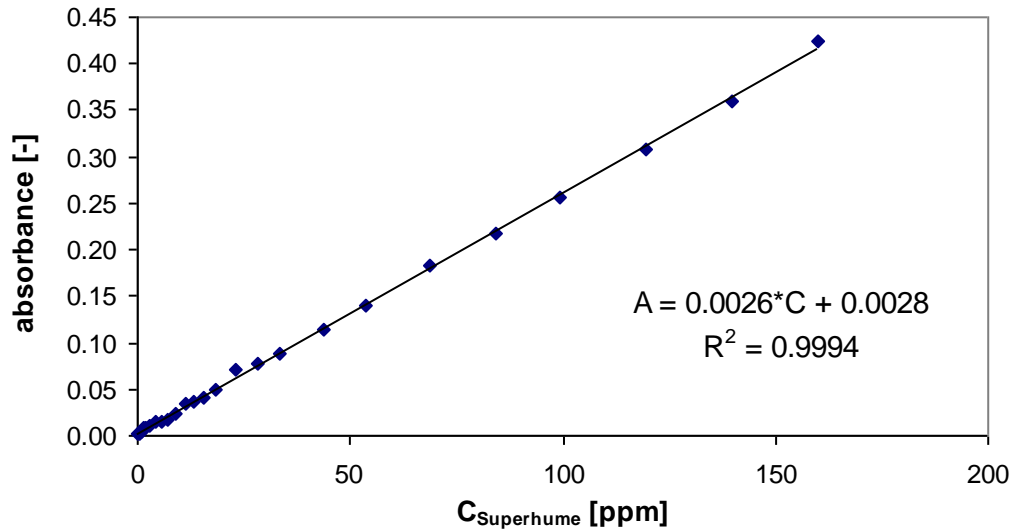


Figure 2-2:Superhume UVA vs. concentration

$$\begin{aligned} C &= (A - 2.7832 \times 10^{-3}) / (2.5816 \times 10^{-3}) = (8 - 2.7832 \times 10^{-3}) / (2.5816 \times 10^{-3}) \\ &= 3097.8 \text{ ppm} = 3.0978 \text{ g/L} = 309.78 \text{ g/100L} = (309.78 \text{ g/100L}) / (1050 \text{ g/L}) \\ &= 0.2950 \text{ L/100L} \end{aligned}$$

Where: A is the required Absorbance.

2.1.2 Coffee

Coffee required amount was obtained from calibration curve data illustrated in Figure(2-3)

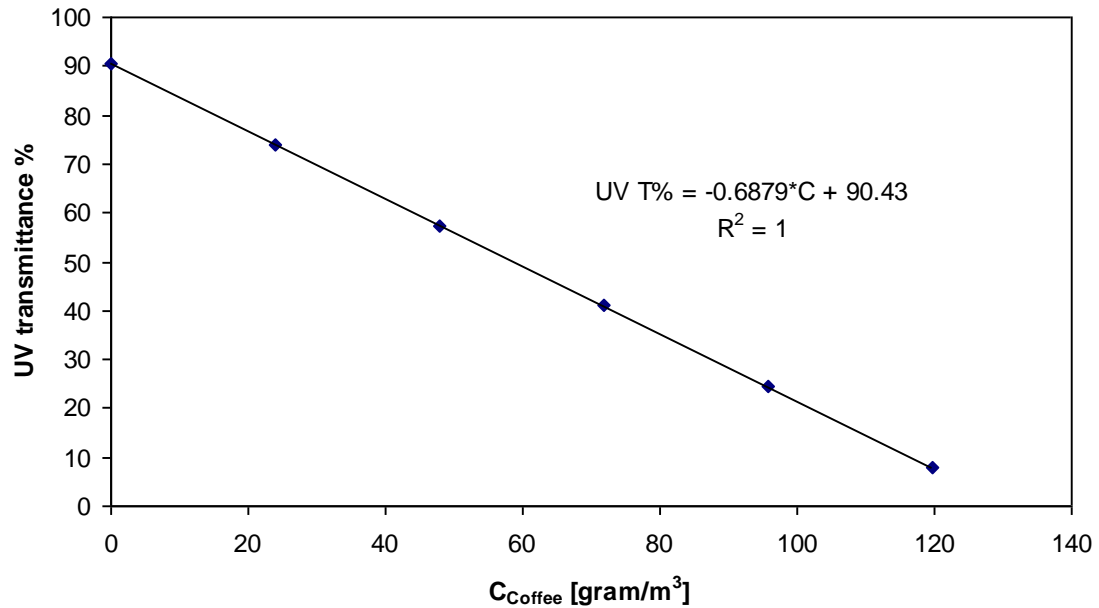


Figure 2-3: Coffee UVT vs. concentration (Malley et al., 2001)

$$C = (T-90.43)/-68.8 = 11.75\text{g}/100\text{L}$$

2.1.3 Rhodamine B

Rhodamine B required amount was calculated after molar extinction coefficient was determined from spectra illustrated in Figure (2-4)

Solubility: 50 g/L

Molar weight: 479.02 g/mol

Price: \$386.25 /100g (Fisher)

Toxic by inhalation and digestion; Irritating to skin and eyes

Extinction coefficient: 26003 cm⁻¹M⁻¹

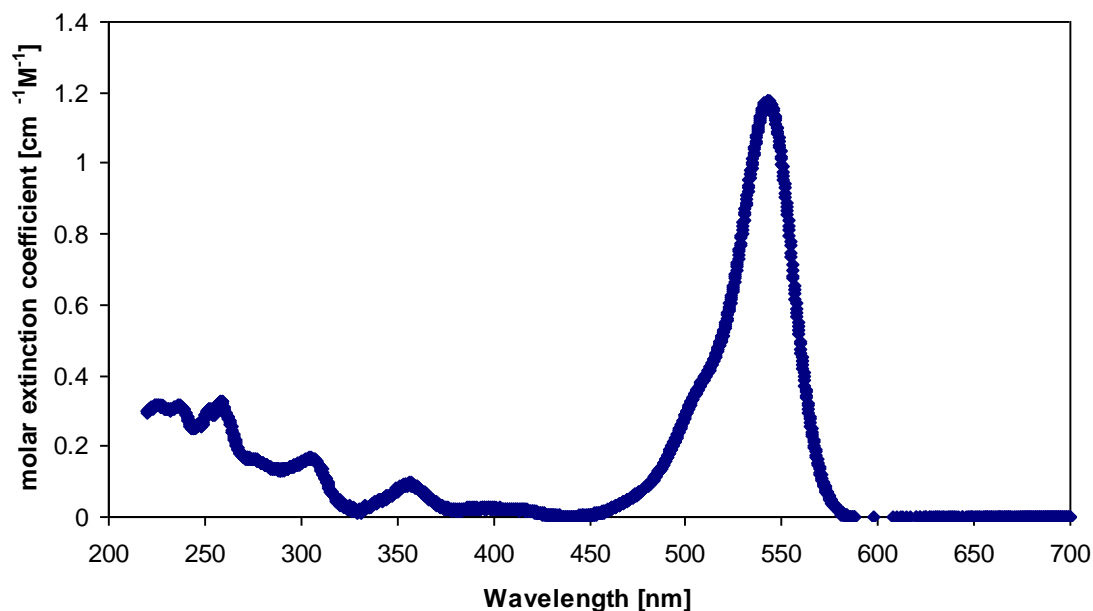


Figure 2-4: Molar extinction coefficient spectrum of Rhodamine B dissolved in ethanol (omlc)

$$A = \epsilon CL$$

Where A: Absorbance

ϵ : Molar absorptivity (extinction coefficient) of the absorber

C: Molar concentration of absorbing species in the material

L: The distance the light travels through the material (i.e., the path length)

$$C = A / (\epsilon * L) = 8 / (26003 * 1) = 3.077 \times 10^{-4} \text{ M} = (3.077 \times 10^{-4} * 479.02) \text{ g/L}$$

$$= 0.1474 \text{ g/L} = 14.74 \text{ g/100L}$$

2.1.4 Methylene Blue

Methylene Blue required amount was calculated after molar extinction coefficient was determined from spectra illustrated in Figure (2-5)

Solubility: Easily soluble in cold water

Molar weight: 319.85 g/mol

Price: \$76.43/25g (Fisher)

Extinction coefficient: $12457 \text{ cm}^{-1}\text{M}^{-1}$

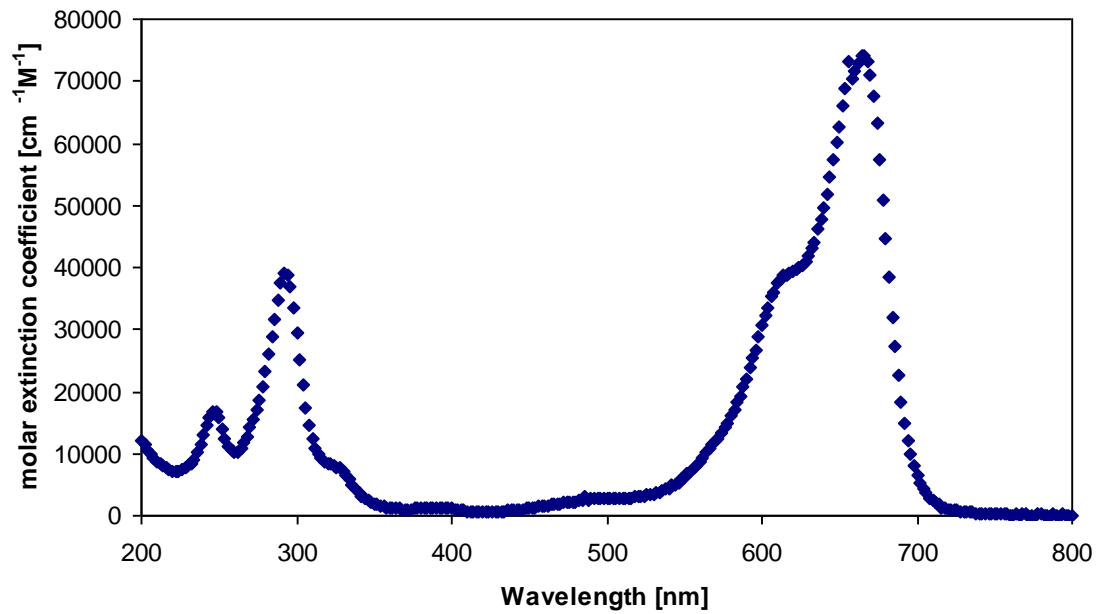


Figure 2-5: Molar extinction coefficient spectrum of Methylene Blue dissolved in water (omlc)

$$A = \epsilon CL$$

Where A: Absorbance

ϵ : Molar absorptivity (extinction coefficient) of the absorber

C: Molar concentration of absorbing species in the material

L: The distance the light travels through the material (i.e., the path length)

$$C = A / (\epsilon * L) = 8 / (12457 * 1) = 6.4221 \times 10^{-4} \text{ M} = 6.4221 \times 10^{-4} * 319.85 \text{ g/L} = 20.54 \text{ g/100L}$$

2.1.5 Para- Hydroxybenzoic Acid (pHBA)

para-Hydroxybenzoic acid required amount was obtained from calibration curve data illustrated in Figure(2-6)

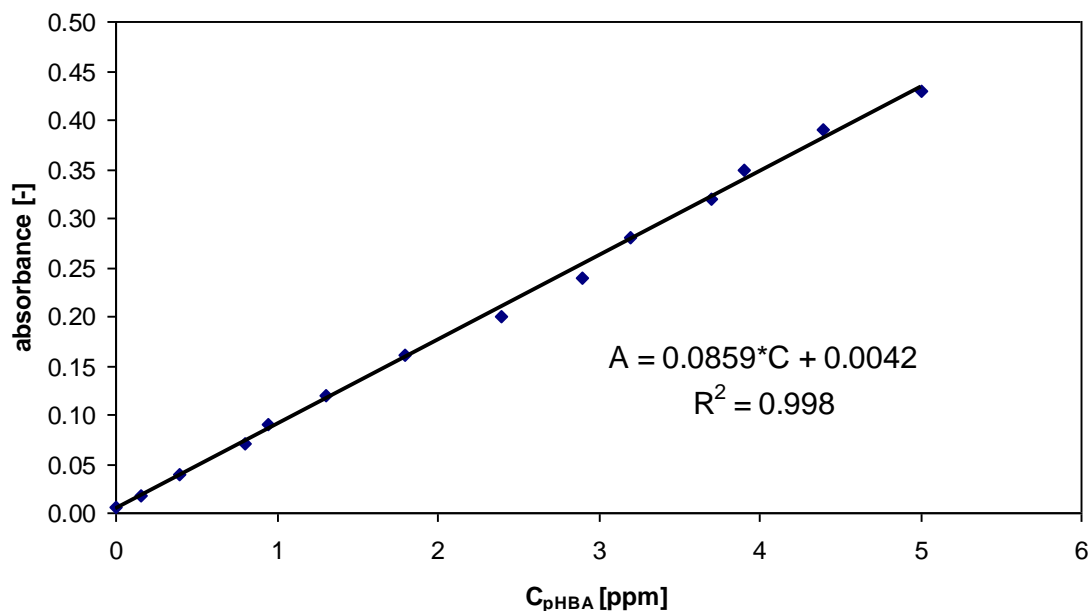


Figure 2-6:pHBA Absorbance vs. concentration

$$A = \epsilon CL$$

Where A: Absorbance

ϵ : Molar absorptivity (extinction coefficient) of the absorber

C: Molar concentration of absorbing species in the material

L: The distance the light travels through the material (i.e., the path length)

$$C = A / (\epsilon * L) = (8.42 \times 10^{-3}) / (8.59 \times 10^{-2}) = 92.86 \text{ ppm} = 9.286 \text{ g/100L}$$

2.1.6 Adnine

Adnine required amount was calculated after molar extinction coefficient was determined from spectra illustrated reported by [omlc]

Soluble in hot water; very slightly soluble in cold water

Molar weight: 135.13 g/mol

Price: \$77.97/25g (Fisher)

Irritating to skin and eyes

Extinction coefficient: $11983 \text{ cm}^{-1}\text{M}^{-1}$

(http://omlc.org.edu/spectra/PhotochemCAD/abs_html/adenine.html)

$$A = \epsilon CL$$

Where A: Absorbance

ϵ : Molar absorptivity (extinction coefficient) of the absorber

C: Molar concentration of absorbing species in the material

L: The distance the light travels through the material (i.e., the path length)

$$\begin{aligned} C &= A /(\epsilon *L) = 8/(11983*1) = 6.6761 \times 10^{-4} \text{ M} = (6.6761 \times 10^{-4} * 135.13) \text{ g/L} \\ &= 0.09021 \text{ g/L} = 9.02 \text{ g/100L} \end{aligned}$$

2.1.7 Preface results

Based on the calculation presented above pHBA, Coffee, tea, sugar and superhume were considered to be investigated in our study.

2.2 Stability and Scattering of the UVT Modifiers

2.2.1 Abstract

The stability of five UVT modifiers (i.e. pHBA, SuperHume, tea, coffee and sugar) were tested with respect to absorbance stability against UV irradiation, time, temperature and pH agents. The pHBA, SuperHume and coffee were relatively stable against all these variables. However, the absorbance of pHBA dropped to 0.25 units per mm right after adding NaOH, it became stable right away and remained stable at least up

to 72 hours. Of these three UVT modifiers, pHBA solution had the minimal scattering character.

2.2.2 Method

The UVT modifiers were prepared based on the target absorbance of 8 cm^{-1} (or 0.8 mm^{-1}) and the concentrations of the modifiers are listed in Table 2-2.

Table 2-2: Concentrations of the UVT modifiers based on the target absorbance of 8 cm^{-1}

UVT modifier	Concentration	pH	Absorbance (cm^{-1})
pHBA	80 mg/L	3.45	7.2199
SuperHume	2 mL/L	10.3	7.9906
Tea	1 bags/L	4.85	14.3814
Coffee	1.1 g/L	4.84	7.4668
Sugar	1 kg/L	-	0.4457

The absorbance measurement was conducted using Cary100 with 1-mm-path cuvette at the entrance port of the integrating sphere. The pH was measured using a pH meter, and the pH was adjusted to around 7 using HCl and/or NaOH solutions. The UV irradiation for all modifiers was measured for 2 hours and 20 minutes. For the scattering test, each selected modifier was measured using Varian Carry50 spectrophotometer and Varian Cary100 spectrophotometer equipped with Labsphere DRA-30 Integrating Sphere with new and standard cuvettes.

2.2.3 Tests details

2.2.3.1 Effect of UV modifier on UV sensitivity of challenge organism

2.2.3.1.1 Purpose

The purpose of this test is to determine whether the UV sensitivity of the microbial surrogates remains the same after contacting with the solution of UVT modifiers.

The idea is to expose the challenge organism to the UV modifier at the target concentration for an extended period, then evaluate the UV sensitivity of the organism. Since it is difficult to apply precise doses at low UVT, the solution will be diluted back to higher UVT before exposing to UV. The assumption is that any coating or chemical modification of the organism will not be reversible in the short time required for dilution and UV exposure.

2.2.3.1.2 Materials

1. Microbial surrogates (MS2 and T1)
2. UVT modifier solution
3. pH modifiers, NaOH and HCl

2.2.3.1.3 Apparatus

4. 50 ml beaker
5. 500 ml beaker
6. 500 ml graduated cylinder
7. 10 ml Pipette
8. pH meter
9. Collimated-beam device
10. Magnetic stirring bar and plate
11. Petri dish (diameter of 5.6 cm)

12. Timer

2.2.3.1.4 General ideas of this test

1. Each type of surrogates will be tested in DI water with pH buffer (control samples) and in solution of UVT modifier with pH adjusted to 7 (target samples).
2. The surrogates used in the “target samples” should first contact with the UVT modifier at $UVT = 10^{-6} \text{ \%/cm}$ overnight in a fridge, and then will be diluted to have $UVT = 90 \text{ \%/cm}$.
3. The absorbance of 10^{-6} \%/cm and 90 \%/cm is 8 and 0.045757. Based on the Beer’s law, the absorbance is proportional to the concentration. Therefore, the dilution factor = $8/0.045757 = 175$ time.
4. Replicate each sample.

2.2.3.1.5 Procedure

1. Combine MS2 stock, UV modifier and pH modifier to a final 10 mL volume, where $pH = 7$, $UVA = 8$, and the titer of MS2 = 1.75×10^9 pfu/mL.
Mix T1 stock and the modifier to a final 10 mL solution, where $pH = 7$, $UVA = 8$, and the titer of MS2 = 1.75×10^9 pfu/mL.
2. Put two solutions in a fridge overnight.
3. Measure the petri-dish factor for the collimated-beam device.
4. Take 2 mL of the solution and add 348 mL of DI water to it (for MS2 and T1 separately).
5. Measure absorbance of the diluted solutions (should be around 90 \%/cm).
6. Calculated required time of doses of 20, 40, 60, 80 and 100 mJ/cm^2 (for MS2) and 5, 10, 15, 20, 25 mJ/cm^2 (for T1).
7. Take 50 mL of the diluted solution to a petri dish for each sample.
8. Conduct and collect CB samples at doses of 0, 20, 40, 60, 80 and 100 mJ/cm^2 for MS2, and 0, 5, 10, 15, 20 and 25 mJ/cm^2 for T1.
9. Repeat steps 5 to 9 for replicates.

10. Prepare 350 mL of MS2 and T1 solutions separately in buffered DI water with a titer of 10^7 pfu/mL.
11. Repeat steps 6 to 10 for the control samples.
12. Store samples in a cooler with blue ice pack, and send it to GAP for analysis.

2.2.3.2 Fouling Test

2.2.3.2.1 Purpose

Fouling on quartz sleeves generally affect the performance of UV reactors. We want to make sure that the candidate UV absorber will not change the quartz sleeve transmittance during the short contact period of the test.

2.2.3.2.2 Materials

1. pH adjusting agents: NaOH or HCl solution
2. quartz Coupon (Fred Pella or other)
3. UV absorber

2.2.3.2.3 Apparatus

Cary 50 with sleeve holder

2.2.3.2.4 Procedure

1. Prepare a stock of the UV absorber in milli-Q water to an absorbance of 8
2. and adjust the pH to 6.8 – 7.2 using pH adjusting agent, measuring the pH using a conventional pH probe

3. Measure the transmittance of new quartz coupon using Cary 100 at ten points across the coupon
4. Immerse the quartz coupon in the a pan filed with the UV absorber
5. Wait for 2 hours
6. Remove the quartz coupon from the solution and rise with DI
7. Allow the coupon to dry
8. Measure the UV-transmittance at ten points across the coupon

2.2.3.3 Scattering Test

2.2.3.3.1 Purpose

The purpose of this test is to assure that the UV absorber has minimum scattering to the degree which considered negligible

2.2.3.3.2 General ideas of this test

The test will utilize two spectrophotometers, one designed to collect both transmitted and forward scattered light, and the other designed to collect only transmitted light. By comparing the readings of the two devices when measuring the same sample, it will be possible to estimate the degree of scattering of the sample. If the two readings are within a small tolerance of each other, the fluid can be assumed to be non-scattering.

2.2.3.3.3 Materials

UV absorber solution with absorbance of 8, with pH adjusted

2.2.3.3.4 Apparatus

1. UV-VIS spectrophotometer Cary 50
2. UV-VIS spectrophotometer Cary 100 with integrating sphere

3. 0.5mm cuvette

2.2.3.3.5 Procedure

1. Set the zero and full-scale readings of both spectrophotometers using an opaque card and a 0.5mm cuvette filled with milli-Q water as references.
2. Fill the 0.5mm cuvette with the absorber solution
3. Mount the cuvette at the entrance pupil of the integrating sphere, and record the transmittance or absorbance at 254nm
4. Move the same cuvette and absorber to the Cary 50 spectrophotometer, and measure the absorbance at 254nm
5. Compare the two readings

2.2.3.4 Survival Test

2.2.3.4.1 Purpose

This test is aimed to assure that UV absorber and other additives do not contribute to the disinfection of the challenging micro organism. In UV disinfecting validation test all the care should be given to assure that UV is the only disinfection factor. The concept is to spike the challenge organisms into both a low-UVT solution and a control solution of water, then enumerate the viable organisms after 24 hours.

2.2.3.4.2 Materials

1. DI water
2. UVT modifier
3. pH adjusting agents, NaOH or HCl
4. Microbial surrogates (MS2 and T1)

5. Vial tubes, beakers, pipettes

2.2.3.4.3 Apparatus

1. Refrigerator
2. Stirring plate and magnetic stirrer
3. pH meter

2.2.3.4.4 Procedure

1. Fill 2 beakers with 100 ml of DI water
2. Place the beakers on stirring plates
3. Add the UVT modifier according to the calibration curve to get UVT $10^{6\%}$ to one of the solutions
4. Stir for 5 minutes
5. Add pH adjusting agent according to the pre-determined correcting test to the low-UVT solution to reach a target pH of 7.
6. Stir for 5 minutes, then check the pH and adjust as necessary to reach the target.
7. Spike each of the 100 ml solutions with both challenge organisms to get concentration of the order of 10^6 - 10^8 pfu/mL
8. Keep very gentle stirring for 10 minutes
9. Place the beaker s in the refrigerator for 24 hours
10. Gently stir the solutions for 10 minutes
11. Collect 10 ml sample from each beaker and send them to microbial lab for enumeration.

2.2.3.5 Stability Test

2.2.3.5.1 Purpose

The purpose of this test is to make sure that UV absorber transmittance will remain constant under several factors UV irradiance, temperature, time.

2.2.3.5.2 Materials

1. UVT modifier solution
2. pH modifiers: NaOH or HCl solutions
3. Cuvettes

2.2.3.5.3 Apparatus

1. Refrigerator
2. Collimated-beam device
3. Magnetic stirring bar and plate
4. Petri dish (diameter of 5.6 cm)
5. UV-VIS spectrophotometer Cary 100 with integrating sphere
6. UV-VIS spectrophotometer Cary 50
7. Thermometer
8. Timer

2.2.3.5.4 Procedure

1. Prepare 2 liters of the UVT absorber solution with UVT 10^{-6} %
2. Adjust the pH of the solution to 6.9 to 7.1

3. Place 500 ml in the refrigerator and measure the transmittance and pH every hours
4. Expose a sample of 5 ml to a dose of 100 mJ/cm² and measure the transmittance and pH
5. Take a sample of 200 ml and increase the temperature to 35°C allow enough time for the sample temperature to stabilize then measure the transmittance and the pH

2.2.4 Results

Figure 2.7 shows that pHBA, SuperHume and coffee are relatively more stable while tea and sugar were not with respect to UV irradiation. Therefore, pHBA, SuperHume and coffee were selected for stability tests against time, temperature and pH adjustment.

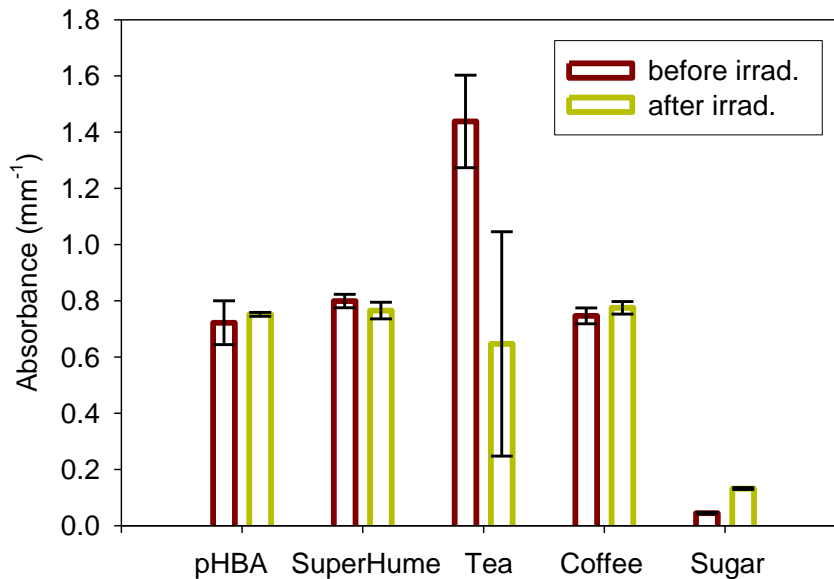


Figure 2-7: Absorbance stability of the UVT modifiers against UV irradiation (2 hours and 20 minutes under the collimated-beam device).

Figure 2.8 shows that all of them are stable against time and temperature. After pH is adjusted to around 7, absorbance of SuperHume and coffee remained stable, while that of pHBA dropped to 0.25 units per mm as shown in Figure 2.9. However, the absorbance of pHBA remained stable after the initial drop as shown in Figure 2.10.

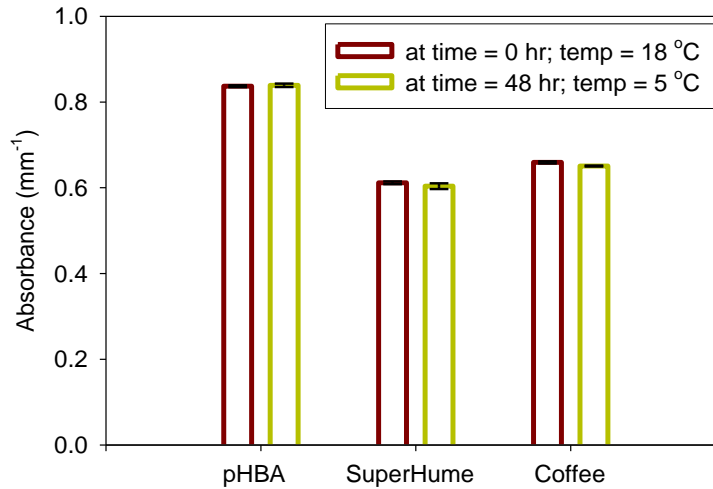


Figure 2-8: Absorbance stability of the UVT modifiers against time (from 0 to 48 hours) and temperature (from 18 °C to 5 °C).

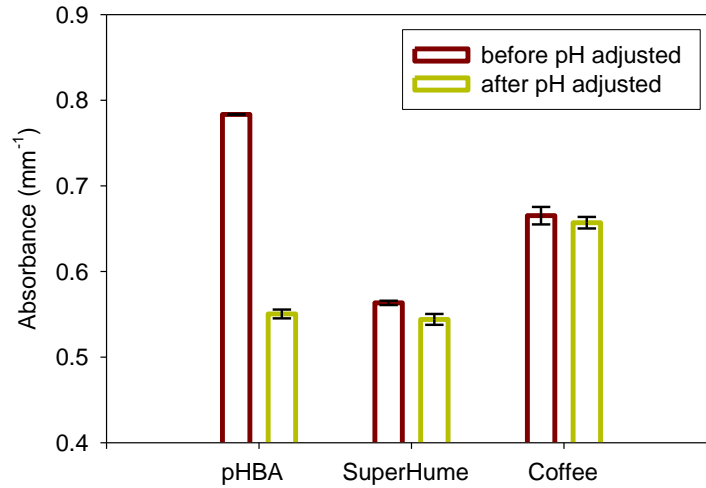


Figure 2-9: Absorbance stability of the UVT modifiers against pH agents.

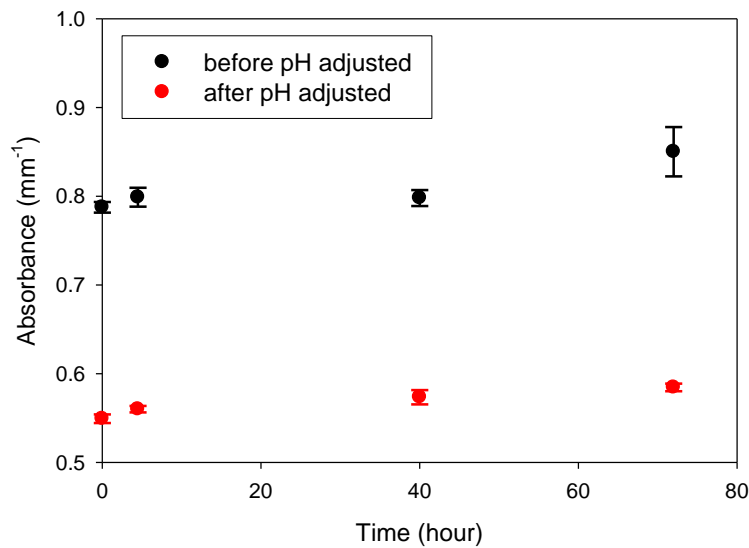


Figure 2-10: Absorbance stability of pHBA before and after pH adjusted to ≈ 7 .

The pHBA, SuperHume and coffee were tested for scattering characteristics by comparing their absorbance measurements using new cuvette designed to be located directly at the outer wall of the reactor and give wide range of path lengths with Cary100 and standard cuvettes with Cary100 and Cary50. The three measurements of pHBA were close to each other, showing the minimal scattering character as shown in Figure 2.11.

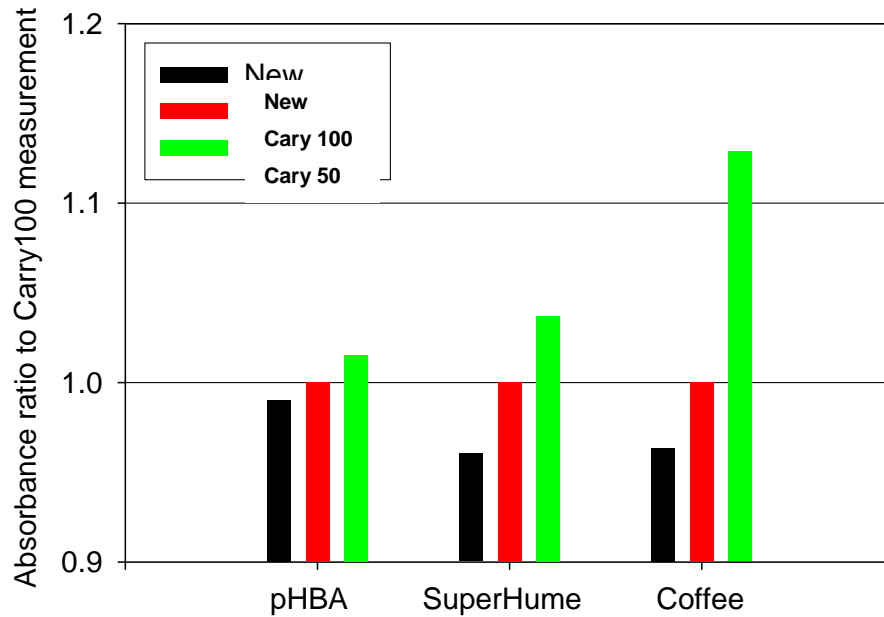


Figure 2-11: Absorbance measurements of pHBA, SuperHume and coffee using new cuvette with Cary100 and standard cuvettes with Cary100 and Cary50. All the measurement was normalized to the measurement by the standard cuvette with Cary100.

2.2.4.1 Termination

The sugar failed to reach the target absorbance, while pHBA, SuperHume, tea and coffee passed. The tea and sugar failed in the stability test against UV irradiation, so only pHBA, SuperHume and coffee were used in the stability tests against time, temperature and pH adjustment. These three modifiers passed all the stability tests as summarized in Table 2.3, however coffee eliminated to keep the best two for the final survival sensitivity tests.

Table 2-3: Summary of the stability tests of UVT modifiers

UVT modifier	Target absorbance	UV irradiation	time	temperature	pH agents	Scattering
pHBA	passed	passed	passed	passed	passed	passed
SuperHume	passed	passed	passed	passed	passed	passed
Tea	passed	failed	-	-	-	-
Coffee	passed	passed	passed	passed	passed	eliminated
Sugar	failed	failed	-	-	-	-

This test is aimed to assure that UV absorber and other additives do not contribute to the disinfection of the challenging microorganism. In UV, disinfecting validation test all the care should be given to assure that UV is the only disinfection factor. The concept is to spike the challenge organisms into both a low-UVT solution and a control solution of water, then enumerate the viable organisms after certain time counts from starting the validation test until samples get processed in the microbial laboratory.

1 ml of MS2-coliphage stock and 1 ml of T1-coliphage stock were added together to 1L DI water. 1 ml from this diluted stock was added to 35 ml of each UVT modifier solution (with pH adjusted to around 7) and DI water (as a control sample). Samples were stored in a fridge for 2 days and sent to microbial laboratory GAP EnviroMicrobial Services for analysis. The result is shown in Figure 2.12.

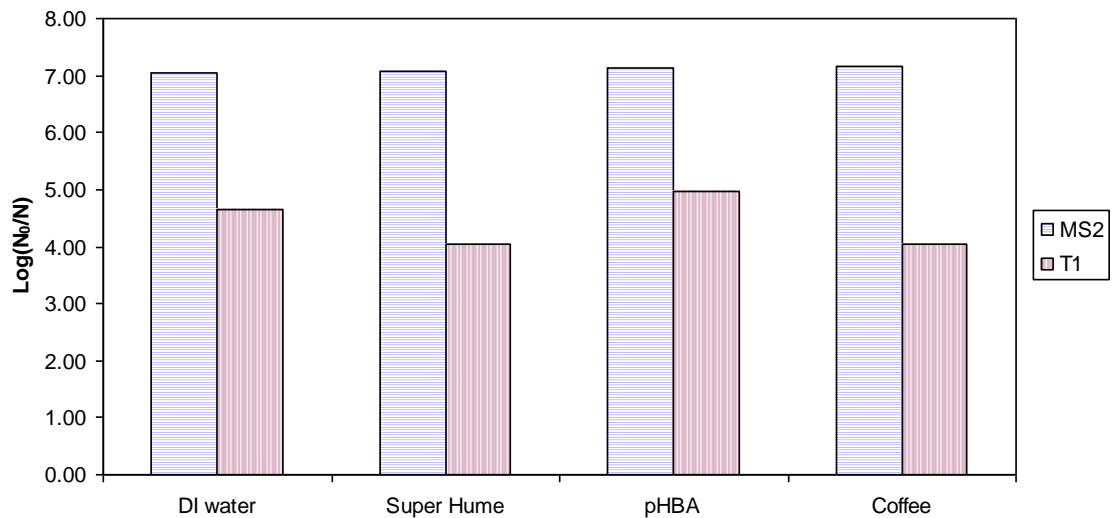


Figure 2-12: Survival test for MS2 and T1 in four different UVT modifiers after 48 hours.

2.1 Sensitivity test

The purpose of this test is to determine whether the UV sensitivity of the microbial surrogates remains the same after contacting with the solution of UVT modifiers.

The idea is to expose the challenge organism to the UV modifier at the target concentration for an extended period, then evaluate the UV sensitivity of the organism. Since it is difficult to apply precise doses at low UVT, the solution will be diluted back to higher UVT before exposing to UV. The assumption is that any coating or chemical modification of the organism will not be reversible in the short time required for dilution and UV exposure.

The challenge organisms MS2-coliphage and T1-coliphage were exposed to the UV modifier at the target concentration $UVT = 10^{-6} \text{ \%}/\text{cm}$ for an extended period (48 hours), then the solution was diluted back to higher UVT before exposing to UV. The assumption is that any coating or chemical modification of the organism will not be

reversible in the short time required for dilution and UV exposure, so if there is any effect that will be captured in this test. The sensitivity of the microorganisms was also estimated in clean water and was compared.

The results, which are illustrated in the following figures 2.13, 2.14, 2.15 and 2.16-showed no, effect on the sensitivity of both microorganisms MS2-coliphage and T1-coiphage in superhume and slightly change in pHBA.

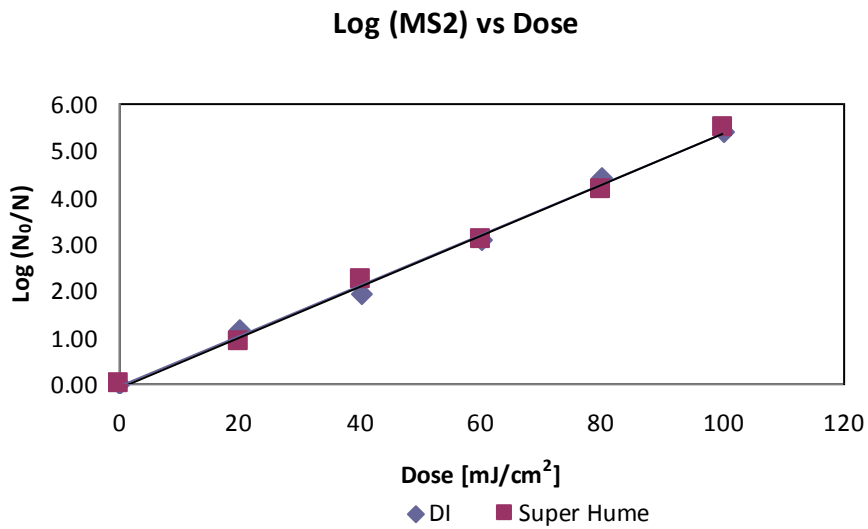


Figure 2-13: Sensitivity test for MS2 in Super Hume

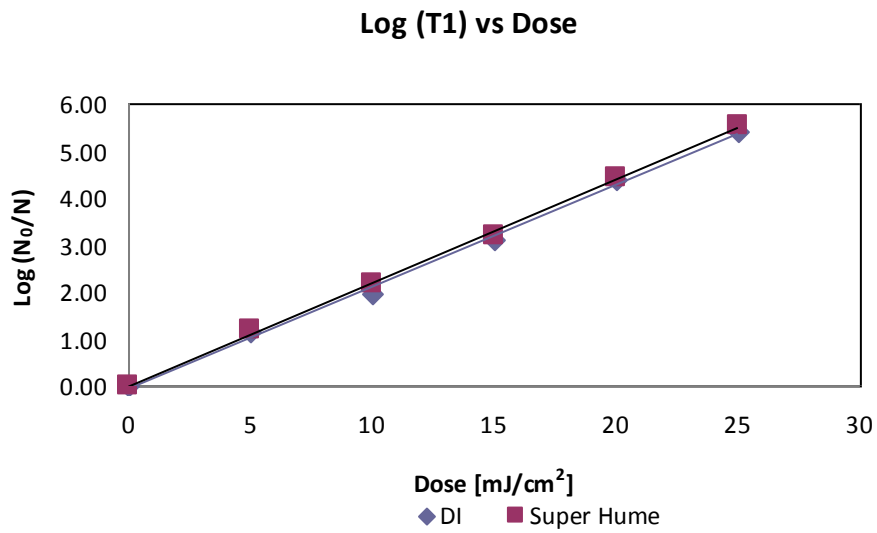


Figure 2-14: Sensitivity test for T1 in Super Hume.

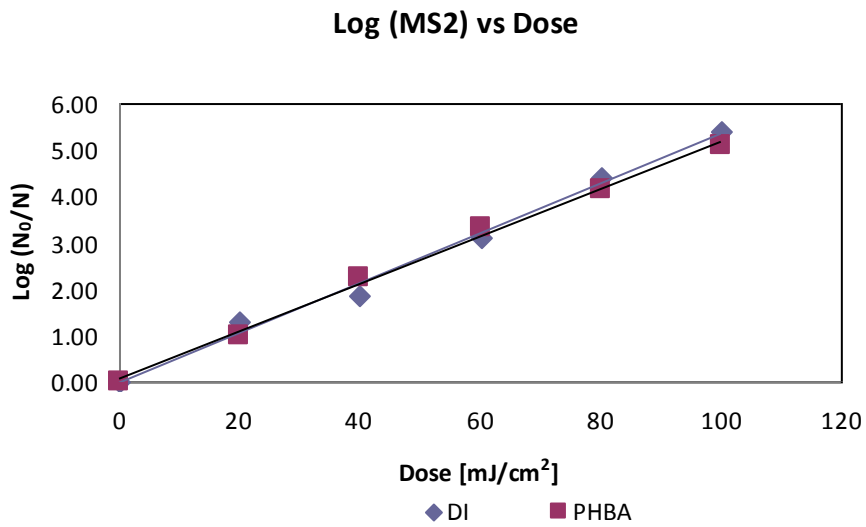


Figure 2-15: Sensitivity test for MS2 in pHBA

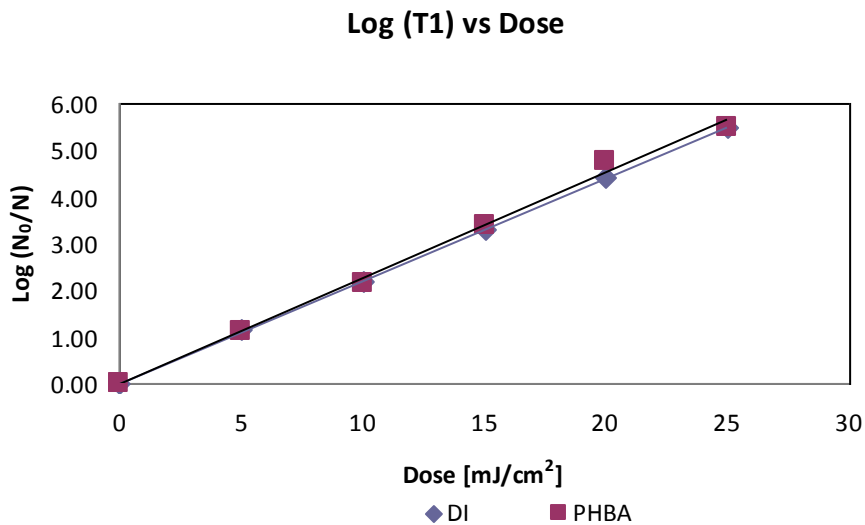


Figure 2-16: Sensitivity test for T1 in pHBA.

2.2 Conclusions

1. Two UV absorbers were capable of surviving complete set of tests, Hydroxybenzoic acid and Super Hume.
2. Hydroxybenzoic acid showed minimum scattering effects, however it showed reduction in absorbance once pH is adjusted.
3. Super Hume came second as UV absorber with scattering effects; however, it was first with all other tests
4. The results of this study showed more scattering effects for the coffee, which used widely in UV validation in the past; however , it remain valid candidate for high and medium UV transmittance tests.
5. The difference in the pH environment of each UV absorber makes it more suitable to specific microorganism than other

2.3 References

Bolton, J.R., Linden, K.G. JD, Standardization of Methods for fluence (UV Dose) Determination in Bench-scale UV Experiments, Journal of Environmental Engineering Science, ASCE 129(3)p. 209(2003).

Fallon, K.S., Hargy, T.M., Mackey, E.D., Wright, H.B., Clancy, J.L., Development and characterization of nonpathogenic surrogates for UV reactor validation, Journal of American Water Works Association, 99:3, p. 73-82(2007).

Fallon, K.S., Hargy, T.M., Mackey, Clancy, J.L., Stability of Bacteriophage MS2 Used in a UV Reactor Validation Study, IUVA News 6:2, p. 21 (2004).

USEPA Ultraviolet Disinfection Guidance Manual, Draft EPA 815-D-03-007, Washington

Oregon Medical Laser Center

<http://omlc.ogi.edu/spectra/PhotochemCAD/html/rhodamineB.html>

Chapter 3

3 Collimated Beam and Ultra Low UV Transmittance (Opaque) Fluids

3.1 Introduction

UV irradiance is the most applied physical disinfection process for water and wastewater. In all applications collimated beam apparatus was used for the generation of fluence UV dose inactivation response data for different pathogens in order to determine comparative UV susceptibility as well as investigation of the photochemical degradation of contaminants.

The reactor usually consists of a low mercury UV lamp with a radiation peak at 253.7 nm wavelength. The UV radiation is collimated through a black painted tube which is approximately the same size of the Petri dish. Samples are placed in a Petri dish directly below the collimated UV beam. In this process, microorganisms are inactivated by penetration of UV light to the outer membrane of the cell and damaging the DNA due to formation of thymine dimers, which prevent the microorganism from DNA transcription and replication, and eventually leading to cell death (Miller et al., 1999). Mixing is an important parameter that deserves attention for determining the microbial inactivation rate in fluids. As the collimated beam impinges the air-liquid interface, these rays are partially reflected and transmitted through the liquid. Mixing produces concave-upward liquid surfaces, and consequently, the fraction of light reflected by the surface as well as the refraction angles of transmitted light were taken into account and a formula of UV average intensity was developed (Kuo et al., 2003; Morowitz, 1950). Once UV average dose is calculated, it is possible to relate it to inactivation of microorganisms and determine the inactivation constant.

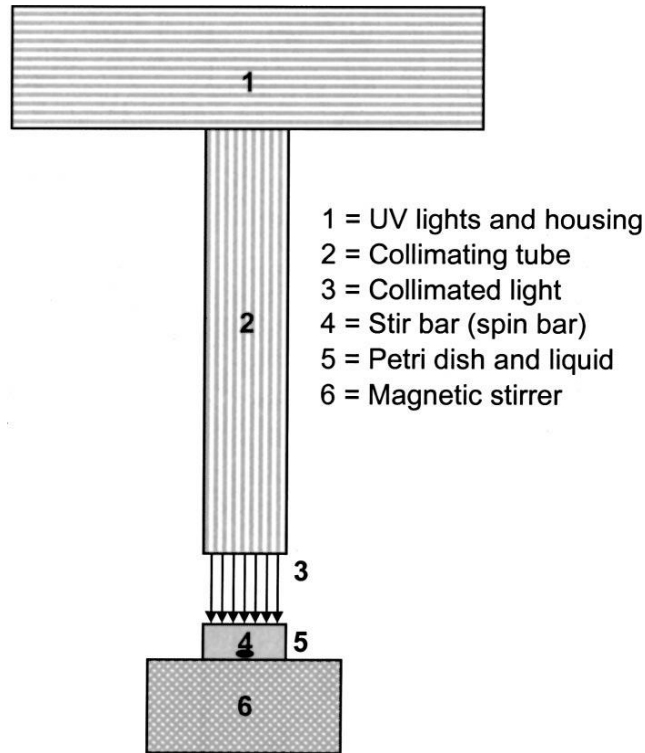


Figure 3-1: Schematic of collimated beam device.

This apparatus has been designed to apply a uniform, measurable UV radiation field to a small sample of fluid. By exposing fluid samples containing a population of a given organism to this quantified radiation field for various exposure times, various doses may be applied and the organism response to UV may be determined. By finding the dose corresponding to the same level of reduction as was found in the reactor, the Reduction-Equivalent Dose RED may be determined [1].

Real UV reactors are imperfect devices, and do not apply the exact same UV dose to each element of fluid that passes through the reactor. However; applies a distribution of doses to the treated fluid, due to the velocity field and the non-uniform radiation field in a real reactor. The level of disinfection of a given organism in a real reactor will depend on the distribution of dose values and on the sensitivity of the organism. The resulting performance is generally quantified in terms of a Reduction-Equivalent Dose (RED), which is the single-valued UV Dose that would result in the same disinfection performance, for particular organism, in case of idealized dose was applied.

The mixing of the fluid sample during collimated beam test found to guarantee single average dose all over the fluid particles. However this assumption of the ability of the classical mixing of collimated beam apparatus to achieve uniform dose in case of low UV transmittance fluid was not tested. Without proper mixing, fluid further from the lamp will receive a lower dose than that close to the free surface. Which results in a strong intensity gradient in the fluid. In an imperfect collimated beam where the mixing is not sufficient, the inactivation is less than what it supposes to be and the Reduction Equivalent Dose is lower than the applied average dose to the fluid medium. As a result the response of the target chemical or microbe will be lower than that predicted under the assumption of perfect mixing. Kuo et al. suggested, without an explanation, that if a liquid sample of low transmittance is being used, the depth of the water should be adjusted so that the calculated minimum intensity is still more than 50% of the intensity at the free surface. Applying his rule of thumb for a liquid of UVT 30% results in total liquid depth of 5mm which seems very small compared with the volume of the smallest stir bars, making this guideline difficult to apply to fluids with low UVT.

The main purpose of our work is to determine the conditions which allow us to consider the results of the collimated beam tests are meaningful when low UV transmittance fluids are under consideration.

This study is based on well known concept of the bioassay Reduction Equivalent Dose RED variation, which depends on UV sensitivity of the challenge microbes and dose distribution delivered by a reactor(In our case the Petri dish under the collimated-beam apparatus). Two challenge microbes with different UV sensitivity were used in this study. Alternation of mixing via rotation directions (i.e. clockwise and counter clockwise) was evaluated. Continuous and Intermittent irradiation (with continuous mixing) were also tested.

The preliminary test was carried out in clean water to determine the dose response curve for both MS2-coliphage and T1-coliphage. Dose required to cause one log

inactivation (D_{10}) values were 20.02 (Figure 3.2) and 5.66 (Figure 3.3) mJ/cm^2 for the previously mentioned microorganisms respectively.

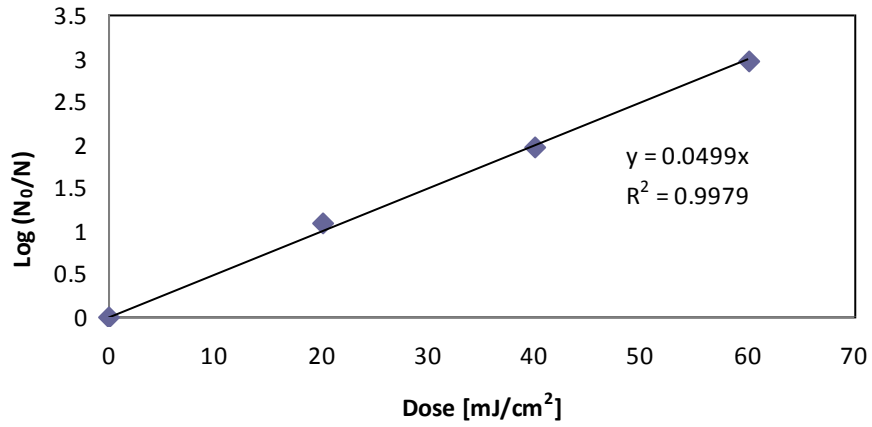


Figure 3-2:MS2 Dose Response Behavior

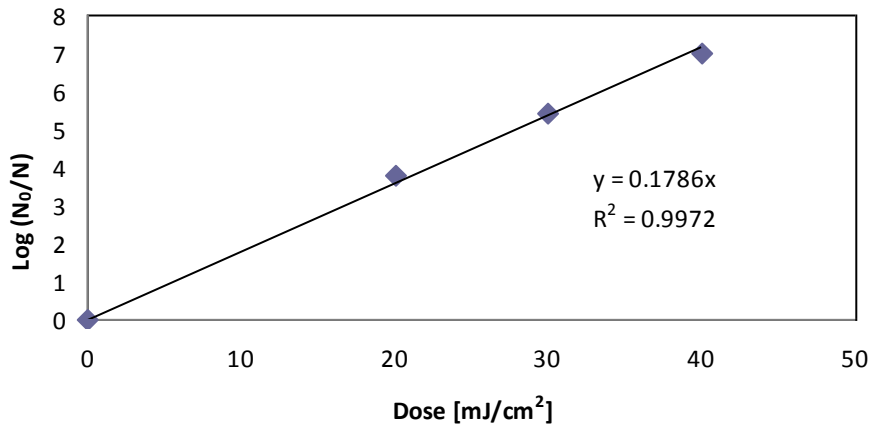


Figure 3-3:T1 Dose Response Behavior

3.2 Collimated Beam's Dose Distribution and RED

Milk was selected as a best representative of opaque fluid. MS2 and T1 were used as challenging microorganisms and spiked into the milk. Gentle mixing was applied for 5 minutes. Initial concentration samples were collected at the beginning of the test (each sample point was collected in triplicate). 40 minutes irradiation were also collected after the test and analyzed for both microorganisms results were summarized in tables 3.1 and 3.2

Table 3-1: Disinfection in 2% Milk with UV light emitted from Collimated Beam

	MS2				20.012			
Sample Name	Dilution Log	PFU	Calculated Full Conc'n	Ave-Calculated Full Conc'n	Log10(MS2)	InActiv. log	log I	RED
			PFU_MS2/ml					
M0	-6	270	270000000	270000000	8.43	0		
MC 40_1	-6	106	106000000	106000000	8.03	0.41	0.41	8.13
MC 40_2	-6	114	114000000	114000000	8.06	0.37	0.37	7.49

Table 3-2: T1 UV Disinfection in 2% Milk with UV emitted from Collimated Beam

	T1				5.66			
Sample Name	Dilution Log	PFU	Calculated Full Conc'n	Ave-Calculated Full Conc'n	Log10(T1)	InActiv. log	log I	RED
			PFU_T1/ml					
M0	-6	201	201000000	201000000	8.30	0		
MC 40_1	-5	206	206000000	206000000	7.31	0.99	1.12	6.33
MC 40_2	-5	181	181000000	181000000	7.26	1.05	1.17	6.64

The test results showed two different values of RED depending on the microorganism type $RED_{MS2} / RED_{T1} \approx 1.28$ the matter, which confirms that the mixing in the Petri dish was not able to overcome the huge intensity gradient of the UV light in the milk sample. As a result, dose distribution was not avoidable under collimated beam in case of opaque fluids.

3.3 Reducing dose distribution delivered for opaque sample under collimated beam

3.3.1 Scattering, Alternated mixing direction effects

The drawback of classical mixing was addressed above. Initial proposal was to generate more rigorous mixing in opaque fluid samples under collimated beam, however that was terminated because of contravening with important rule set by Bolton, which was the necessity of maintaining the free surface of the fluid flat and perpendicular to the light irradiation direction.

Hydroxybenzoic Acid pHBA as non-scattering opaque fluid representative (described in the previous chapter).milk ad traditional scattering fluid representative were considered in the new test to determine relative role of scattering to absorption of fluids in producing the intensity gradient of UV light.

Stirring plate featured with the possibility of controlling the rotation speed, direction as well as duration to enhance the mixing in the Petri-dish was implemented.

Table 3-3:MS2 Disinfection in pHBA with UV emitted from Collimated Beam with Petri dish mixed with alternated direction mode (CW-CCW)

Sample Name	MS2		Bouble Mixing Direction		Log I	RED
	Dilution Log	PFU	Calculated Full Conc'n	Log10(MS2)		
			PFU_MS2/ml			
PHBAA-0-MS2	-7	38	380000000	8.580	0.000	
PHBAA-20-MS2-1	-5	29	2900000	6.462	2.117	41.62
PHBAA-20-MS2-2	-5	41	4100000	6.613	1.967	38.33
PHBAA-20-MS2-3	-5	36	3600000	6.556	2.023	39.56

Table 3-4:MS2 Disinfection in 2% Milk with UV emitted from Collimated Beam with Petri dish mixed with alternated direction mode (CW-CCW)

Sample Name	MS2		Bouble Mixing Direction		Log I	RED
	Dilution Log	PFU	Calculated Full Conc'n	Log10(MS2)		
			PFU_MS2/ml			
Milka-0-MS2	-6	289	289000000	8.461	0.000	
Milka-20-MS2-1	-5	122	12200000	7.086	1.375	25.89
Milka-20-MS2-2	-5	61	6100000	6.785	1.676	32.11
Milka-20-MS2-3	-5	96	9600000	6.982	1.479	28.02

Table 3-5:T1 Disinfection in pHBA with UV emitted from Collimated Beam with Petri dish mixed with alternated direction mode (CW-CCW)

Sample Name	T1		Bouble Mixing Direction		Log I	RED
	Dilution Log	PFU	Calculated Full Conc'n	Log10(MS2)		
			PFU_MS2/ml			
PHBAA-0-T1	-5	238	238000000	7.377	0.000	
PHBAA-20-T1-1	0	3	3	0.477	6.899	35.96
PHBAA-20-T1-2	0	34	34	1.531	5.845	29.55
PHBAA-20-T1-3	0	166	166	2.220	5.156	25.54

Table 3-6:T1 Disinfection in 2% Milk with UV emitted from Collimated Beam with Petri dish mixed with alternated direction mode (CW-CCW)

Sample Name	T1		Bouble Mixing Direction		Log I	RED
	Dilution Log	PFU	Calculated Full Conc'n	Log10(MS2)		
			PFU_MS2/ml			
Milk 0-T1	-6	51	51000000	7.708	0.000	
Milka-20-T1-1	-3	30	30000	4.477	3.230	15.07
Milka-20-T1-2	-2	180	18000	4.255	3.452	16.22
Milka-20-T1-3	-2	276	27600	4.441	3.267	15.26

Table 3-7:MS2 Disinfection in pHBA with UV emitted from Collimated Beam with Petri dish mixed with single direction mode

Sample Name	MS2		Single Mixing Direction		Log I	RED
	Dilution Log	PFU	Calculated Full Conc'n	Log10(MS2)		
			PFU_MS2/ml			
PHBAC-0-MS2	-6	180	180000000	8.255	0.000	
PHBAC-20-MS2-1	-4	141	1410000	6.149	2.106	41.37
PHBAC-20-MS2-2	-4	161	1610000	6.207	2.048	40.11
PHBAC-20-MS2-3	-4	198	1980000	6.297	1.959	38.15

Table 3-8:MS2 Disinfection in 2% Milk with UV emitted from Collimated Beam with Petri dish mixed with single direction mode

Sample Name	MS2		Single Mixing Direction		Log I	RED
	Dilution Log	PFU	Calculated Full Conc'n	Log10(MS2)		
			PFU_MS2/ml			
MilkC-0-MS2	-6	289	289000000	8.461	0.000	
MilkC-20-MS2-1	-5	178	17800000	7.250	1.210	22.58
MilkC-20-MS2-2	-5	175	17500000	7.243	1.218	22.72
MilkC-20-MS2-3	-5	190	19000000	7.279	1.182	22.01

Table 3-9:T1 Disinfection in pHBA with UV emitted from Collimated Beam with Petri dish mixed with single direction mode

Sample Name	T1		Single Mixing Direction		Log I	RED
	Dilution Log	PFU	Calculated Full Conc'n	Log10(MS2)		
			PFU_MS2/ml			
PHBAC-0-T1	-5	238	23800000	7.377	0.000	
PHBAC-20-T1-1	0	21	21	1.322	6.054	30.80
PHBAC-20-T1-2	-1	39	390	2.591	4.786	23.44
PHBAC-20-T1-3	0	1	1	0.000	7.377	38.98

Table 3-10:T1 Disinfection in 2% Milk with UV emitted from Collimated Beam with Petri dish mixed with single direction mode

Sample Name	T1		Single Mixing Direction		Log I	RED
	Dilution Log	PFU	Calculated Full Conc'n	Log10(MS2)		
			PFU_MS2/ml			
Milk 0-T1	-6	51	51000000	7.708	0.000	
MilkC-20-T1-1	-3	13	13000	4.114	3.594	16.96
MilkC-20-T1-2	-2	35	3500	3.544	4.164	20.01
MilkC-20-T1-3	-2	95	9500	3.978	3.730	17.68

The reduction equivalent dose values were summarized in table 3.11. RED remained microbe dependent, and was independent of the fluid type. This confirm that Alternated direction of mixing (CW-CCW), in not sufficient to overcome the mixing problem in opaque fluids. It also backed up the assumption of absorption nature of the light intensity gradient, in more than scattering one. Since no significant difference in RED ratios of pHBA comparing to milk ones, were detected as showed in table 3.12

Table 3-11:Scattering, Alternated mixing direction effect on Collimated Beam Irradiation

	Single Direction						Double Direction					
	MS2			T1			MS2			T1		
pHBA	41.37	40.11	38.15	30.80	23.44	38.98	41.62	38.33	34.56	35.96	29.55	25.54
		Average	39.88		Average	31.07		Average	38.17		Average	30.35
		Stdev	1.62		Stdev	7.77		Stdev	3.53		Stdev	5.26
2% milk	22.58	22.72	22.01	16.96	20.01	17.68	25.89	32.11	28.02	15.07	16.22	15.26
		Average	22.44		Average	18.22		Average	28.67		Average	15.52
		Stdev	0.38		Stdev	1.59		Stdev	3.16		Stdev	0.62

Table 3-12:RED Ratios: Scattering, Alternated mixing direction effect on Collimated Beam Irradiation

Ratio MS2/T1UV			
Single Direction		Double Direction	
pHBA	1.28	pHBA	1.26
2% Milk	1.23	2% Milk	1.85

3.3.2 Pulse Irradiation (Light-Dark) Effects

The idea of this test was built on the concept, which states that the total delivered dose is equal to the sum of all doses delivered during different periods. This test was designed to divide the irradiation time to several equal periods and alternate in between each two irradiated periods with an equal period of dark mixing (i.e., without irradiation).

Tables 3.13 and 3.14 shows the reduction equivalent dose calculated for Pulsed irradiation condition.

Table 3-13:MS2 Disinfection in 2% Milk with UV emitted from Collimated Beam in pulsation mode with Petri dish mixed with single direction mode

	MS2				20.012			
Sample Name	Dilution Log	PFU	Calculated Full Conc'n	Ave- Calculated Full Conc'n	Log10(MS2)	InActiv. log	log I	RED
			PFU_MS2/ml					
M0	-6	270	270000000	270000000	8.43	0		
MA 40_1	-6	124	124000000	124000000	8.09	0.34	0.34	6.76
MA 40_2	-6	124	124000000	124000000	8.09	0.34	0.34	6.76

Table 3-14:T1 Disinfection in 2% Milk with UV emitted from Collimated Beam in pulsation mode with Petri dish mixed with single direction mode

	T1				5.66			
Sample Name	Dilution Log	PFU	Calculated Full Conc'n	Ave- Calculated Full Conc'n	Log10(T1)	InActiv. log	log I	RED
			PFU_T1/ml					
M0	-6	201	201000000	201000000	8.30	0		
MA 40_1	-5	189	189000000	189000000	7.28	1.03	1.15	6.54
MA 40_2	-5	167	167000000	167000000	7.22	1.08	1.21	6.84

The resulted ratio of MS2_RED/T1_RED varied between 0.99 and 1.033, which showed great improvement in the mixing under collimated beam., This could be explained by the fact that dark mixing time was allowing the mixing to continue without adding additional UV dose thereby allowing more randomizing in mixing of fluids .Once irradiated again, the new dose is delivered to different particles than the one if irradiation

was done without a dark period. The repetition in alternating between light and dark periods led to reducing in the dose distribution and as consequence more accurate kinetic results for irradiation of opaque fluids under collimated beam.

The drawback of this method is that it doubles the irradiation time, which is originally very long time in case of fluids with low transmittance. This might lead to the risk of fluid evaporation, which leads to change in optical properties of fluids with time. Proper attention to this fact was given during this test through monitoring sample depth and designing the test within the duration of no significant evaporation.

3.4 Conclusions

1. Disinfecting of low transmittance fluid under collimated beam is more complex than classical fluids
2. The scattering of the low transmittance fluids played minor role in generating light gradient comparing to the absorption
3. Proper mixing under Collimated was considered in light of combining the hydraulic of the fluid with the light gradient the matter that brought wider concept than traditional mass mixing of fluids.
4. Pulsed irradiation was capable of delivering UV dose with narrower distribution.

3.5 References

- Bolton, J. R., Linden, K. G., Standardization of Methods for Fluence (UV Dose) Determination in Bench-Scale UV Experiments, *Journal of Environmental Engineering*, 129(3): p. 209-215 (2003).
- Ducoste, J., Liu, D., Linden, K., Alternative Approaches to Modeling Fluence Distribution and Microbial Inactivation in Ultraviolet Reactors: Lagrangian versus Eulerian, *J. Envir. Engrg.* 131(10), p.1393-1403 (2005).
- Gehr, R., Collimated beam tests: their limitations for assessing wastewater isinfectability by UV, and a proposal for an additional evaluation parameter, *Journal of Environmental Engineering and Science*, 6, p. 265-270 (2007).
- Jin, S., Linden, K., Ducoste, J., Liu, D., Impact of lamp shadowing and reflection on the fluence rate distribution in a multiple low-pressure UV lamp array, *Water Research*, 39(12), p. 2711-2721(2005).
- Kuo, J., Chen, C., Nellor, M., Standardized Collimated Beam Testing Protocol for Water/Wastewater Ultraviolet Disinfection, *Journal of Environmental Engineering*, 129(8), p. 774-779 (2003).
- Lyn, D. A., Blatchley, E. R., III, Numerical computation fluid dynamics-based models of ultraviolet disinfection channels, *J. Environ. Eng. (Reston, VA, U.S.)*, 131(6), p. 838-850 (2005).
- Morowitz, H. J., Absorption effects in volume irradiation of microorganisms, *Science*, 111, p. 229-230 (1950).
- Patankar, S. V., *Numerical Heat Transfer and Fluid Flow*, Hemisphere, Washington D.C. 1980.

Qualls, R. G., Johnson J. D., Bioassay and dose measurement in UV disinfection, *Appl Environ Microbiol.*, 45(3)p. 872–877 (1983).

Sozzi, D. A., Taghipour, F., UV Reactor Performance Modeling by Eulerian and Lagrangian Methods, *Environmental Science & Technology*, 40(5), p. 1609-1615 (2006).

Chapter 4

4 Dimensional Analysis of UV Disinfection in an Annular Reactor of Opaque Fluids

4.1 Introduction

Dimensional analysis is a technique for decreasing the number of experimental variables, affecting certain physical phenomenon. The Buckingham PI theorem concludes a formal method of conducting dimensional analysis (Buckingham, 1915)

4.2 Definitions

4.2.1 Buckingham's PI theorem

The theorem states that if we have a physically meaningful equation involving a certain number, n , of physical variables, and these variables are expressible in terms of k independent fundamental physical quantities, then the original expression is equivalent to an equation involving a set of $p = n - k$ dimensionless parameters constructed from the original variables.

4.2.2 Independent (Basic, or Primary) dimensional units

The basic units are the set of independent units, which cannot be derived from another set of units. For example, time (sec), length (m), and mass (kg) are basic units, the values of which are determined through experiments. The number of basic units in a particular problem is problem specific, which depends on the physical process under consideration.

4.2.3 Dependent (Secondary Dimensional Units)

The units, which can be derived from the basis units, are called dependent or secondary units. For example, velocity can be derived from primary units of time and length.

4.3 Dimensional Analysis of an Annular Reactor

The dimensional analysis was applied on thin film annular UV reactor because that reactor decreases the path length to avoid the problems associated with lack of penetration. Figure 4.1

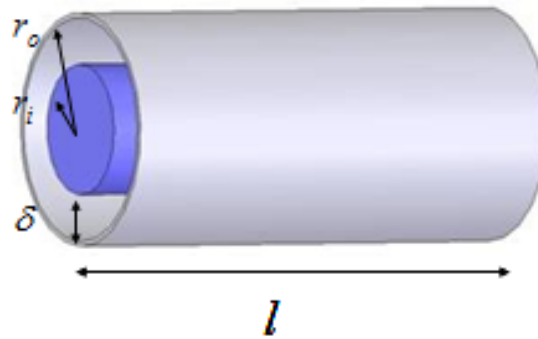


Figure 4-1: Schematic representation of an annular UV reactor

The dimensional equations governing the process of UV disinfection are the following:

The continuity equation.

$$\nabla \cdot (\rho \vec{v}) = 0 \quad (4-1)$$

The Navier-Stokes equation for incompressible fluid in absence of gravity.

$$\nabla \cdot (\rho \vec{v} \vec{v}) = -\nabla p + \nabla \cdot (\mu [(\nabla \vec{v} + \nabla \vec{v}^T)]) \quad (4-2)$$

Where, p is the static pressure, μ is dynamic viscosity

UV Irradiance equation

$$\operatorname{div}(I_{\lambda}(\vec{r}, \vec{s})\vec{s}) + (a_{\lambda} + \sigma_s)I_{\lambda}(\vec{r}, \vec{s}) = \frac{\sigma_s}{4\pi} \int_0^{4\pi} I_{\lambda}(\vec{r}, \vec{s}') \Phi(\vec{s}, \vec{s}') d\Omega' \quad (4-3)$$

Where, $I_{\lambda}(\vec{r}, \vec{s})$ The spectral irradiance (W/m^2) with the wave length λ acting on small area normal to the direction \vec{s} , at a location \vec{r} ; a_{λ} is the spectral absorbance m^{-1} , σ_s is the scattering coefficient m^{-1} ; usually independent of λ , the integration variable Ω' is the solid angle ;and Φ is a geometrical phase function.

4.3.1 Dimensional Variables

The dimensional variables involved in the problem categorized in the following groups:

4.3.1.1 Geometrical Variables

- Annular gap (delta, δ)
- Reactor Length (L)
- Sleeve Radius (ri)

4.3.1.2 Fluid Variables

- Dynamic Viscosity (μ)
- Density (ρ)
- Volumetric Flow Rate (Q)

4.3.1.3 Optical Variables

- Absorption coefficient (α)
- Scattering coefficient (σ)

- Lamp power (P)

4.3.1.4 Disinfection Variables

- Free-swimming microbes inactivation rate constant (Kd)
- Free-swimming microbes initial concentration (Nd)

4.3.2 Methodology: Pi-Groups Derivation

Given the number of variables involved in the problem (e.g., 11) and the number of fundamental units describing those variables (e.g., 4), a system of equations for each dimensional variable can be derived using the following generalized expression:

$$\Pi_i = L \cdot Q \cdot \mu \cdot N_d \cdot [free\ Variable] \quad (4-4)$$

Where:

- L is the reactor length [m]
- Q is the volumetric flow rate [m³/s]
- μ is the dynamic viscosity [kg/s/m]
- Nd is the free-swimming microbes concentration [Counts/m³]
- Free dimensional variable of interest

In the previous expression, it can be noticed that four (4) repeating variables were arbitrarily selected in a way that they do not form a dimensionless group. A system of algebraic equations was built after to give a power-law monomial in mass, length, time and microbial counts.

$$[L]^a \left[\frac{L^3}{T} \right]^b \left[\frac{M}{T L} \right]^c \left[\frac{Count}{L^3} \right]^d [F.V.D] = M^0 L^0 T^0 Count^0 \quad (4-5)$$

If this procedure was repeated for each of the non-repeating dimensional variables (i.e., excluding the repeating variables), a dimensionless group can be identified for each non-repeating dimensional variables considered. Now we will apply this procedure to develop a set of non-dimensional Pi-groups for the annular reactor.

4.3.3 Dimensional Analysis and UV disinfection

The model equations are simulated using CFD package and the log inactivation was calculated. The dimensional variables and pi-groups are illustrated in Table 4.1 and

Table 4-1: Identical PI Groups values for different dimensional designs

Variables	Case Number			
	1	2	3	4
Density	1.00E+03	5.00E+02	1.00E+02	5.00E+02
Dynamic Viscosity	1.00E-03	2.00E-04	2.00E-04	2.00E-04
Volumetric Flow Rate	5.00E-04	1.00E-03	5.00E-04	1.00E-03
Inner Radius	1.00E-01	5.00E-01	5.00E-02	5.00E-01
Outer Radius	1.10E-01	5.50E-01	5.50E-02	5.50E-01
Reactor Length	1.00E+00	1.00E+00	2.00E+00	2.00E+00
Absorption Coeff.	1.00E+02	2.00E+01	2.00E+02	2.00E+01
Scattering Coeff.	1.00E+02	2.00E+01	2.00E+02	2.00E+01
Lamp power	4.00E+01	1.60E+02	8.00E+02	1.60E+02
Inactivation Rate constant1	1.00E-02	1.00E-03	1.00E-03	1.00E-03
Inactivation Rate constant2	5.00E-03	5.00E-04	5.00E-04	5.00E-04

Gap	1.00E-02	5.00E-02	5.00E-03	5.00E-02
Cross section area	6.60E-03	1.65E-01	1.65E-03	1.65E-01
Reactor Volume	6.60E-03	1.65E-01	3.30E-03	3.30E-01
Residence time1	1.32E+01	1.65E+02	6.60E+00	3.30E+02
Aver. Velocity	7.58E-02	6.06E-03	3.03E-01	6.06E-03
Surface Area	6.28E-01	3.14E+00	6.28E-01	6.28E+00
Boundary Intensity(Fluence Rate)	6.37E+01	5.09E+01	1.27E+03	2.55E+01
Volumetric average Intensity	3.83E+01	3.07E+01	7.67E+02	1.53E+01
Mass flow rate	5.00E-01	5.00E-01	5.00E-02	5.00E-01
Dimensionless Group				
Reynolds Number	1.52E+03	1.52E+03	1.52E+03	1.52E+03
Lamp Aspect Ratio	1.00E+01	1.00E+01	1.00E+01	1.00E+01
Absorption Thickness	1.00E+00	1.00E+00	1.00E+00	1.00E+00
Scattering Thickness	1.00E+00	1.00E+00	1.00E+00	1.00E+00
Specific Dose	9.52E-01	9.52E-01	9.52E-01	9.52E-01
UV Power	1.25E-01	1.25E-01	1.25E-01	1.25E-01

Table 4-2:Simulation Results of Dimensional Analysis

Design	Microbs Inlet count	Dose	Microb #1 Outlet count	Microb #2 Outlet count	Log (I) Microb #1	Log (I) Microb #2
1	1.00E+08	5.95E+02	4.45E+06	1.78E+07	1.35E+00	7.50E-01
2	1.00E+08	5.95E+03	4.60E+06	1.74E+07	1.34E+00	7.52E-01
3	1.00E+08	5.98E+03	4.47E+06	1.82E+07	1.35E+00	7.47E-01
4	1.00E+08	5.96E+03	4.40E+06	1.79E+07	1.36E+00	7.48E-01

Table 4.2 shows the disinfection of two microbes, which was the same for all four cases, the matter that proves the validity of our methodology of analyzing the disinfection of opaque fluid with UV light.

The Pi-groups as identified above via dimensional analysis were able to describe similarities among very different annular reactor designs.

Dimensional analysis can be considered a promising approach to generate further understanding of the role of individual dimensionless groups, as well as to support reactor design.

4.3.4 PI Groups effects

We adjusted the dimensional parameter of the disinfection problem of UV in annular reactor to generate several designs were the group subject of study was allowed to be changed. Tables 4.3-4.6 report Reynolds' number, Aspect ratio, absorption thickness and UV power respectively.

Table 4-3: Effect of Reynolds Number on UV Disinfection of PI Groups

Re	Design	Microbs Inlet Count	Dose	Microb#1 outlet count	Microb#2 outlet count	Log(I) Microb #1	Log(I) Microb #2
14	1	1.00E+08	6.88E+02	8.17E+07	8.52E+07	8.79E-02	6.94E-02
72	2	1.00E+08	6.88E+02	8.09E+07	8.45E+07	9.22E-02	7.30E-02
145	3	1.00E+08	6.88E+02	8.06E+07	8.43E+07	9.34E-02	7.40E-02
723	4	1.00E+08	6.88E+02	8.22E+07	8.56E+07	8.54E-02	6.73E-02
1447	5	1.00E+08	6.88E+02	8.15E+07	8.51E+07	8.87E-02	7.00E-02

Table 4-4:Effect of Lamp Aspect Ratio on UV Disinfection of PI Groups

AR	Design	Microbs Inlet Count	Dose	Microb#1 outlet count	Microb#2 outlet count	Log(I) Microb#1	Log(I) Microb#2
5	1	1.00E+08	6.88E+01	9.20E+07	9.41E+07	3.63E-02	2.63E-02
6	2	1.00E+08	6.88E+01	9.18E+07	9.40E+07	3.72E-02	2.70E-02
7	3	1.00E+08	6.88E+01	9.11E+07	9.35E+07	4.04E-02	2.91E-02
8	4	1.00E+08	6.88E+01	9.13E+07	9.36E+07	3.97E-02	2.86E-02
9	5	1.00E+08	6.88E+01	9.09E+07	9.34E+07	4.12E-02	2.97E-02

Table 4-5:Effect of Absorption Thickness on UV Disinfection of PI Groups

AT	Design	Microbs Inlet Count	Dose	Microb#1 outlet count	Microb#2 outlet count	Log(I) Microb#1	Log(I) Microb#2
0.50	1	1.00E+08	9.11E+02	4.02E+05	5.17E+06	2.40E+00	1.29E+00
1.00	2	1.00E+08	5.95E+03	4.29E+06	1.73E+07	1.37E+00	7.62E-01
1.50	3	1.00E+08	4.38E+03	1.41E+07	3.24E+00	8.49E-01	7.49E+00
2.00	4	1.00E+08	3.44E+03	2.56E+07	4.46E+07	5.92E-01	3.51E-01

Table 4-6:Effect of UV Power on UV Disinfection of PI Groups

UV power	Design	Microbs Inlet Count	Dose	Microb#1 outlet count	Microb#2 outlet count	Log(I) Microb#1	Log(I) Microb#2
1.00	1	1.00E+09	981	8.38E+08	8.65E+08	0.077	0.063
0.50	2	1.00E+09	2000	8.10E+08	8.38E+08	0.092	0.077
0.33	3	1.00E+09	3072	7.92E+08	8.21E+08	0.101	0.086
0.25	4	1.00E+09	4146	7.79E+08	8.09E+08	0.108	0.092
0.20	5	1.00E+09	5202	7.69E+08	8.00E+08	0.114	0.097

Results reported above were summarized in Figure 4.2. Reynolds number sounds to have the least weighted factor however, the analyzing of the data of the designed cases shows that lamp power increased to maintain the same level of disinfection.

The most affective two groups were Absorption thickness and specific dose; however, they work oppositely, followed by Aspect ration and UV power

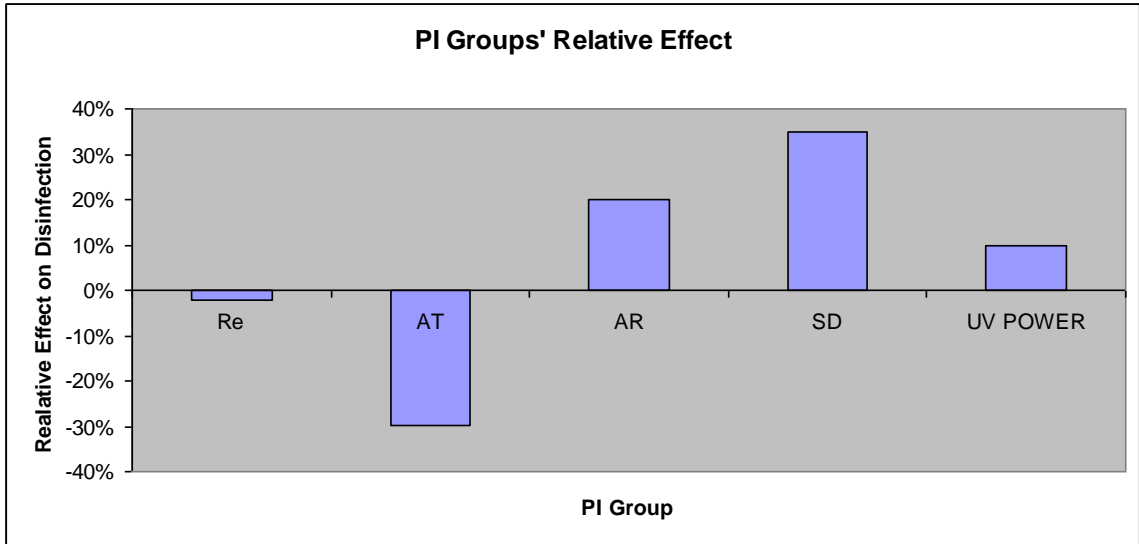


Figure 4-2:PI Goupd relative effect on UV Disinfection in an Annular Reactor
Re:Reynolds number; AT: Absorption thickness; AR: Aspect ratio; SD: Specific Dose

The microorganism concentration profiles of four cases were depicted in Figure 4.3 these cases were different in the dimensional domain however similar in the dimensionless one. This matter proves the validity Dimensional Analysis technique to analyze UV disinfection problem. The complete verification and validation of the CFD simulation is provided in the coming chapter.

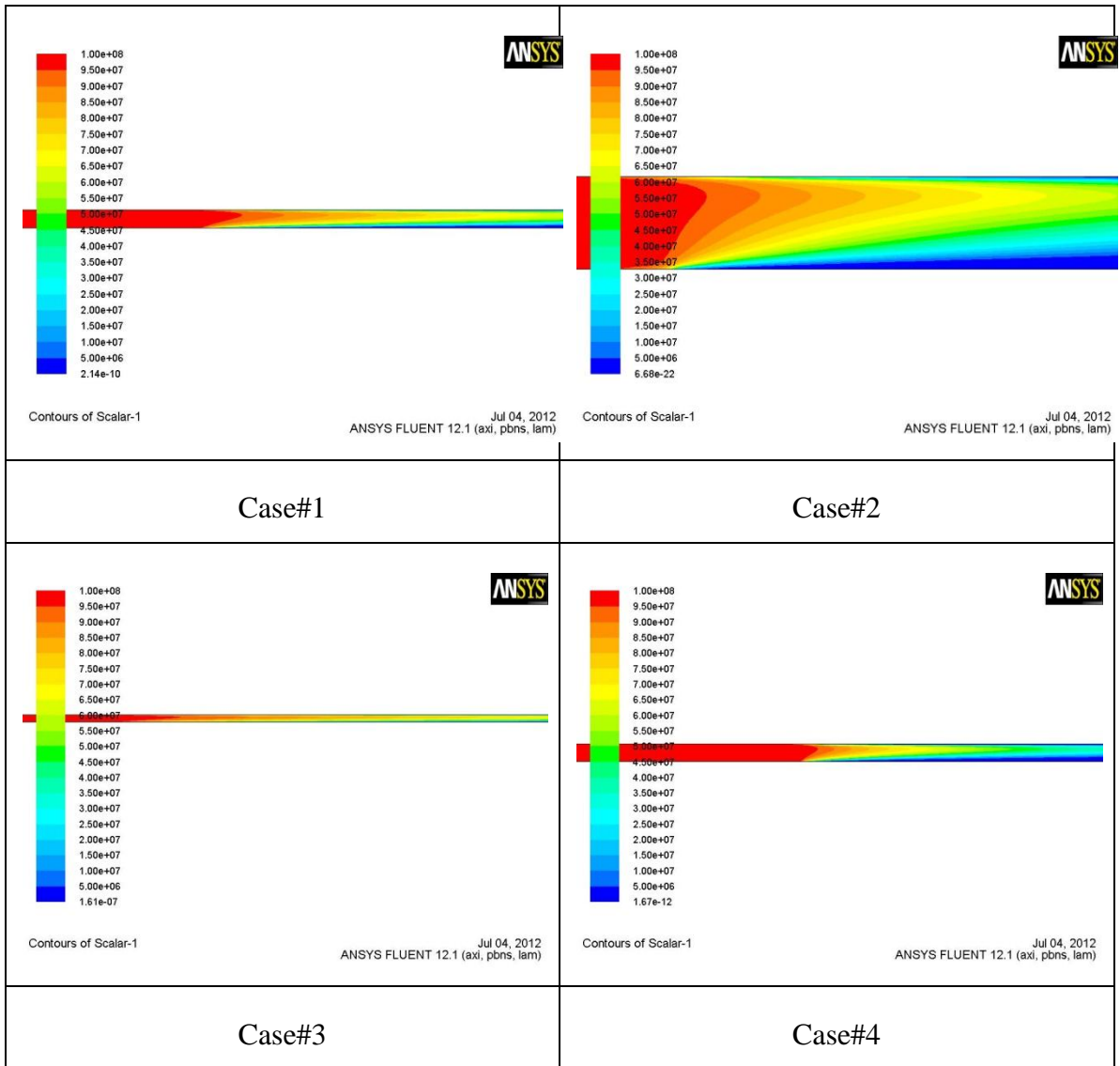


Figure 4-3: Microorganisms Concentration Profile for Four Different Cases

4.4 Conclusions

1. Numerical application of dimensional analysis resulted in the following PI groups (Reynolds number, Absorption thickness, Aspect ratio, Specific Dose and Relative UV power).
2. Disinfection is inversely proportional to both Absorption Thickness and Reynolds number with relative weights of 32%,4% respectively .
3. Disinfection is directly proportional to Specific dose, Aspect ratio and specific UV power with relative weights of 38%,24%,11% respectively .
4. Scattering thickness is PI group which appears if scattering took into consideration.

4.5 References

Abu-Ghararah Z. H., A Numerical Model for estimating average Light Intensity in Annular Ultraviolet Disinfection Reactor, *Environmental Technology*, 18p. 929–936 (1997).

Bolton, J. R., Calculation of ultraviolet fluence rate distributions in an annular reactor: significance of refraction and reflection, *Journal of Water Research*, Vol 34 Issue 13, p. 3315-3324 (2000).

DiPrima, R. C., Pridor A., The stability of viscous-flow between rotating concentric cylinders with an axial flow. *Proceeding of the Royal Society of London. Series A, Mathematical and Physical Sciences* 366, 555-573 (1979).

Donnelly, R. J., Experiments on the stability of viscous flow between rotating cylinders. I. Torque measurements. *Proceeding of the Royal Society of London. Series A, Mathematical and Physical Sciences* 246, 312-325 (1958).

Donnelly, R. J., Experiments on the stability of spiral flow between rotating cylinders. *Proceedings of the National Academy of Sciences of the United States of America* 46, 1150 (1960).

Fasel, H., Booz, O., Numerical investigation of supercritical Taylor-vortex flow for a wide gap. *Journal of Fluid Mechanics* 138, 21-52 (1984).

Fenstermacher, P. R., Swinney, H. L., Gollub, J. P., Dynamical instabilities and the transition to chaotic Taylor vortex flow. *Journal of Fluid Mechanics* 94, 103- 128 (1979).

Forney, L. J., Skelland, A. H. P., Morris, J. F., Holl, R. A., Taylor vortex column: Large shear for liquid-liquid extraction. *Separation Science and Technology* 37, 2967-2986 (2002a).

Forney, L. J., Pierson, J. A., Goodridge, C. F., Development of an advanced UV disinfection technology. Ann. Rep. for Food-PAC, Atlanta, GA (2002b).

Forney, L. J., Goodridge, C. F., Pierson, J. A., Ultraviolet disinfection: Similitude in Taylor-Couette and channel flow. *Environmental Science and Technology* 37, 5015-5020 (2003a).

Forney, L. J., Pierson, J. A., Optimum photolysis in Taylor-Couette flow. *AIChE Journal* 49, 727-733 (2003b).

Forney, L. J., Pierson, J. A., Photolytic reactors: Similitude in Taylor-Couette and channel flows. *AIChE Journal* 49, 1285-1292 (2003c).

Forney, L. J., Pierson, J. A., Ye, Z., Juice irradiation with Taylor-Couette flow: UV inactivation of *Escherichia coli*. *Journal of Food Protection* 67, 2410-2415 (2004).

Forney, L. J., Pierson, J. A., Giorges, A., Photon absorption in modified Taylor-Couette flow: Theory and experiment. *Industrial & Engineering Chemistry Research* 44, 5193-5198 (2005a).

Forney, L. J., Ye, Z., Giorges, A., Fast competitive reactions in Taylor-Couette flow. *Industrial & Engineering Chemistry Research* 44, 7306-7312 (2005b).

Fox, R. O., *Computational Models for Turbulent Reacting Flows*. Cambridge University Press (2003).

Froment, G. F., Bischoff, K. B., *Chemical Reactor Analysis and Design*, John Wiley & Sons, New York (1990).

- Goldstein, S., The stability of viscous fluid flow between rotating cylinders. Proceedings of the Cambridge Philosophical Society 33, 41-61 (1937).
- Gravas, N., Martin B. W., Instability of viscous axial-flow in annuli having a rotating inner cylinder. Journal of Fluid Mechanics 86, 385 (1978).
- Gu, Z. H., Fahidy, T. Z., Characteristics of Taylor vortex structure in combined axial and rotating flow. The Canadian Journal of Chemical Engineering 63, 710-715 (1985).
- Gu, Z. H., Fahidy, T. Z., The effect of geometric parameters on the structure of combined axial and Taylor-vortex flow. The Canadian Journal of Chemical Engineering 64, 185-189 (1986).
- Haim, D., Pismen, L. M., Performance of a photochemical reactor in the regime of Taylor-Gortler vortical flow. Chemical Engineering Science 49, 1119-1129 (1994).
- Hasoon, M. A., Martin, B. W., The stability of viscous axial flow in an annulus with a rotating inner cylinder. Proceedings of the Royal Society of London Series A, Mathematical and Physical Sciences 352, 351-380 (1977).
- Howes, T., Rudman, M., Flow and axial dispersion simulation for traveling axisymmetric Taylor vortices. AIChE Journal 44, 255-262 (1998).
- Hoyer, O., Testing performance and monitoring of UV systems for drinking water disinfection. Water Supply 16, 424-429 (1998).
- Ikeda, E., Maxworthy, T., Spatially forced corotating Taylor-Couette flow. Physical Review E 49, 5218-5224 (1994).
- Jagger, J., Introduction to Research in Ultra-Violet Photobiology. Prentice-Hall Inc., Englewood Cliffs, NJ (1967).
- Jones, C. A., The transition to wavy Taylor vortices. Journal of Fluid Mechanics 157, 135-162 (1985).

Kataoka, K., Doi, H., Hongo, T., Futagawa, M., Ideal plug-flow properties of Taylor vortex flow. *J. Chem. Eng. Japan* 8, 472-476 (1975).

Kataoka, K., Doi, H., Komai, T., Heat-mass transfer in Taylor vortex flow with constant axial-flow rates. *International Journal of Heat and Mass Transfer* 20, 57(1977).

Kaye, J., Elgar, E. C., Modes of adiabatic and diabatic fluid flow in an annulus with an inner rotating cylinder. *Transactions of ASME* 80, 753-765 (1958).

Koschmieder, E. L., Turbulent Taylor vortex flow. *Journal of Fluid Mechanics* 93, 515-527 (1979).

Koutchma, T., Parisi, B., Biodosimetry of *Escherichia coli*' UV inactivation in model juices with regard to dose distribution in annular UV reactors'. *Journal of Food Science* 69 E14-E22 (2004a).

Koutchma, T., Keller, S., Chirtel, S., Parisi, B., Ultraviolet disinfection of juice products in laminar and turbulent flow reactors. *Innovative Food Science & Emerging Technologies* 5 179-189 (2004b).

Kowalski, W. J., Design and optimization of UVGI air disinfection system, PhD thesis, Pennsylvania State University (2001).

Kucuk, S., Unluturk, S., Arastoopour, H., Koutchma, T., Modeling of UV dose distribution in a thin-film UV reactor for processing of apple cider, *Journal of Food Engineering* , 11, p. 125-136 (2004).

Launder, B. E., Spalding, D. B., *Lectures in Mathematical Models of Turbulence*. Academic Press, London, England (1972).

Lord Rayleigh On the dynamics of revolving fluids. *Proc. Roy. Soc. London. A* 93, 148-154 (1916).

- Lueptow, R. M., Dotter, A., Min, K., Stability of axial flow in an annulus with a rotating inner cylinder. *Physics of Fluids* 4, 2446-2455 (1992).
- Lyn, D. A., Chiu, K., Blatchley, E. R., Numerical modeling of flow and disinfection in UV disinfection channels. *Journal of Environmental Engineering*, 125, 17-26 (1999).
- Lyn, D. A., Blatchley, E. R., Numerical computational fluid dynamics-based models of ultraviolet disinfection channels. *Journal of Environmental Engineering*, 131, 838-849 (2005).
- Mallock, A., Experiments of fluid viscosity. *Proceeding of the Royal Society of London. Series A, Mathematical and Physical Sciences* 183, 41-56 (1896).
- Marchisio, D. L., Barresi, A. A., Fox, R. O., Simulation of turbulent precipitation in a semi-batch Taylor-Couette reactor using CFD. *AIChE Journal* 47, 664-676 (2001).
- Middleman, S., *An Introduction to Mass and Heat Transfer: Principles of Analysis and Design*, John Wiley & Sons, Inc., New York (1998).
- Min, K., Lueptow, R. M., Circular Couette flow with pressure driven axial flow and a porous inner cylinder. *Experiments in Fluids* 17, 190-197 (1994).
- Pudjiono, P. I., Tavare, N. S., Garside, J., Nigam, K. D. P., Residence time distribution from a continuous Couette flow device. *Chem. Eng. J.* 48, 101-110 (1992).
- Puma, G. L., Reactors using suspended solid photocatalysts, *Chemical Engineering Research and Design*, 83(A7): 820–826 July 2005.
- Radata, Inc. (2006) A UV System for Everyone. [Online] http://www.radata.com/wtest/infopacket/treatment/wedeco_uv.pdf.
- Rafique, M., Lami, S. S., Flow regimes and vortex competition in modified Taylor-Couette system: Inner Rotating wavy cylinder coaxial with a smooth stationary outer cylinder, 12th International Couette-Taylor Workshop, Evanston, IL (2001).

Resende, M. M., Vieira, P. G., Sousa R., Giordano, R. L. C., Giordano R. C., Estimation of Mass Transfer Parameters in a Taylor-Couette-Poiseuille Heterogeneous Reactor. *Brazilian Journal of Chemical Engineering* 21, 175-184 (2004).

Rotz, C. A., Suh, N. P., Vortex motion induced by V-grooved rotating cylinders and their effect on mixing performance. *Journal of Fluid Mechanics* 101, 186-192 (1979).

Sczechowski, J. G., Koval, C. A., Noble R. D., A Taylor vortex reactor for heterogeneous photocatalysis. *Chemical Engineering Science* 50, 3163-3173 (1995).

Severin, B. F., Suidan, M. T., Engelbrecht, R. S., Kinetic modeling of U. V. disinfection of water. *Water Research* 17, 1669-1678 (1983).

Severin, B. F., Suidan M. T., Rittmann B. E., Engelbrecht, R. S., Inactivation kinetics in a flow-through UV reactor, *Journal WPCF* 56, 164-169 (1984).

Taghipour, F., Ultraviolet and ionizing radiation for microorganism inactivation. *Water Research* 38, 3940-3948 (2004).

Chapter 5

5 Taylor Couette Reactor

5.1 Introduction

In general, a bench-lab scale collimated beam reactor (CBR) is used for studying the disinfection of microorganisms with UV light. For the opaque fluids that have high absorption (such as apple juice, orange juice, wine) and scattering coefficients (such as milk) even with the stirring bar, a uniform fluence cannot be guaranteed. This is an important requisite to calculate the microbial inactivation rate. Since the collimated beam test procedure is not appropriate for these food products because of the weak penetration of UV light through the sample, unless special procedure was adopted like we seen in chapter two. It was necessary to develop another lab-scale reactor in order to provide adequate mixing and uniform dose delivery to the fluid. This reactor can be based on Taylor-Couette flow.

5.2 Brief History of Taylor-Couette Flow

The study of Taylor-Couette flow began Couette (1890) experimented with two long concentric cylinders with the inner cylinder fixed and the outer cylinder rotating. He observed by experiments that the torque sustaining the steady rotation increased linearly with angular velocity of the outer cylinder, Ω_2 , if Ω_2 was less than a critical value. However, the torque increased sharply when Ω_2 was greater than the critical value. Couette concluded that the change from steady laminar flow to turbulent flow resulted in the abrupt increase in the torque.

Afterwards, Mallock (1896) confirmed Couette's observation and extended Couette's experiments to the case with the inner cylinder rotating. He showed an important difference between the two cases:

(1) If the outer cylinder was fixed with the inner cylinder rotating, the flow was stable until the rotation of the outer cylinder produces turbulence.

(2) If the inner cylinder was fixed with the outer cylinder rotating, the flow was always unstable at all speeds tested.

Lord Rayleigh (1916) realized the role of angular momentum in promoting instability, and the Rayleigh criterion was proposed, i.e., the flow of in viscid fluid is stable when the cylinders rotate in the same direction and equation below is met:

$$\Omega_2 R_2^2 = \Omega_1 R_1^2 \quad (5-1)$$

Where: Ω_2 and Ω_1 are angular velocities of the outer and inner cylinder respectively, and R_2 and R_1 are radii of the outer and inner cylinder respectively.

Taylor (1923) extended the works of Couette, Mallock and Rayleigh, and verified his calculations experimentally with very long cylinder. Taylor also observed the appearance of the toroidal vortices (now known as Taylor or Taylor-Couette vortices) under some circumstances. Figure 5.1

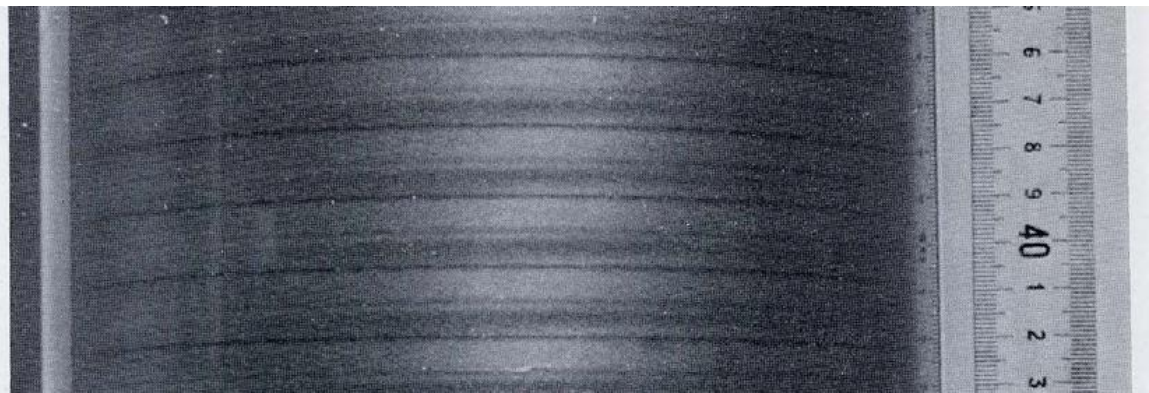


Figure 5-1: Taylor Center section of the fluid column with laminar axisymmetric Taylor vortices at $Ta = 1.16 Ta_{cr}$ (from Koschmieder, 1979)

5.2.1 Taylor-Couette Flow without an Axial Flow

When pressure-driven Poiseuille flow (axial flow) is superimposed on Taylor-Couette flow, the shear instability caused by the axial flow and the centrifugal instability caused by the circular Couette flow cause a transition from laminar Couette-Poiseuille flow to axial flow with toroidal Taylor vortices (sometimes called Taylor-Couette-Poiseuille flow in many references in order to differentiate from Taylor-Couette flow without an axial flow). The combination of the two different instabilities forms a rich variety of flow regimes depending on the flow conditions (Lueptow et al., 1992). Taylor-Couette-Poiseuille flow can be found in several engineering applications, including rotating machinery, heat and mass transfer and journal bearings.

Taylor-Couette-Poiseuille flow (abbreviated as Taylor-Couette flow below for brevity) was first studied by Goldstein (1937) though his results were proven wrong afterwards by many researchers. Later, an axisymmetric disturbance in a narrow annular gap was applied to analyze Taylor-Couette-Poiseuille flow numerically (Chandrasekhar, 1960, DiPrima, 1960). Then, wide annular gaps were considered (Hasoon and Martin, 1977, DiPrima and Pridor, 1979, Fasel and Booz, 1984). Their research showed that toroidal Taylor vortices advanced downstream with the axial flow. If the assumption of the axisymmetric disturbance was removed and the disturbance was assumed to be nonaxisymmetric, a new regime, pairs of helical vortices, was predicted (Chung and Astill, 1977, Takeuchi and Jankowski, 1981, Ng and Turner, 1982).

Many experiments (Kaye and Elgar, 1958, Donnelly, 1960, Becker and Kaye, 1962, Snyder, 1962, Schwarz, 1964, Kataoka et al., 1977, Gravas and Martin, 1978, Sorour and Coney, 1979, Takeuchi and Jankowski, 1981, Buhler and Polifke, 1990, Lueptow et al., 1992) were carried out to confirm these numerical results and to find new regimes. Figure 1.9 is Lueptow's results where there were mainly seven flow regimes, namely:

- 1) Taylor vortices
- 2) Wavy vortices
- 3) Random wavy vortices
- 4) Modulated wavy vortices
- 5) Turbulent modulated wavy vortices
- 6) Turbulent wavy vortices
- 7) Turbulent vortices

5.3 CFD Modeling of Taylor-Couette reactor for Opaque Fluids UV Disinfection

As the treatability of liquid foods by UV depends on their optical properties as well as the interplay between mixing and light gradients, high shear systems such as the Taylor-Couette UV reactor have lately gained considerable attention as they may represent a viable solution for the irradiation of such fluids.

In this chapter, a detailed numerical analysis of opaque fluids UV disinfection in a lab-scale Taylor-Couette reactor was conducted. Initially lamp power was measured by using radiometer. The fluence rate distribution was simulated using ANSYS Fluent and the radiative transfer equations (RTE) was solved using the discrete ordinates (DO) radiation model . Transport processes were numerically investigated using a 2d axis-symmetric CFD code, which was validated with breakthrough and steady state tests designed and conducted using a user defined scalar and a model photochemical reaction. The model prediction was validated with passive and reactive tracer tests.

5.3.1 Taylor Couette Reactor

The Taylor-Couette reactor used in this study was built by Trojan Technologies (London, Ontario). The system includes an UV lamp, protective quartz sleeve, and a power supply. The single low pressure, germicidal UV lamp was positioned along the central axis of two concentric cylinders. The inner cylinder, made by quartz (thickness = 0.6 cm) is rotating along the central axis while the external cylinder is fixed. The length of the reactor is 19.86 cm. The gap formed by the 2 cylinders is 0.33 cm wide and there the fluid takes place. The schematic representation of the UV reactor used is shown in Figure 5.2.

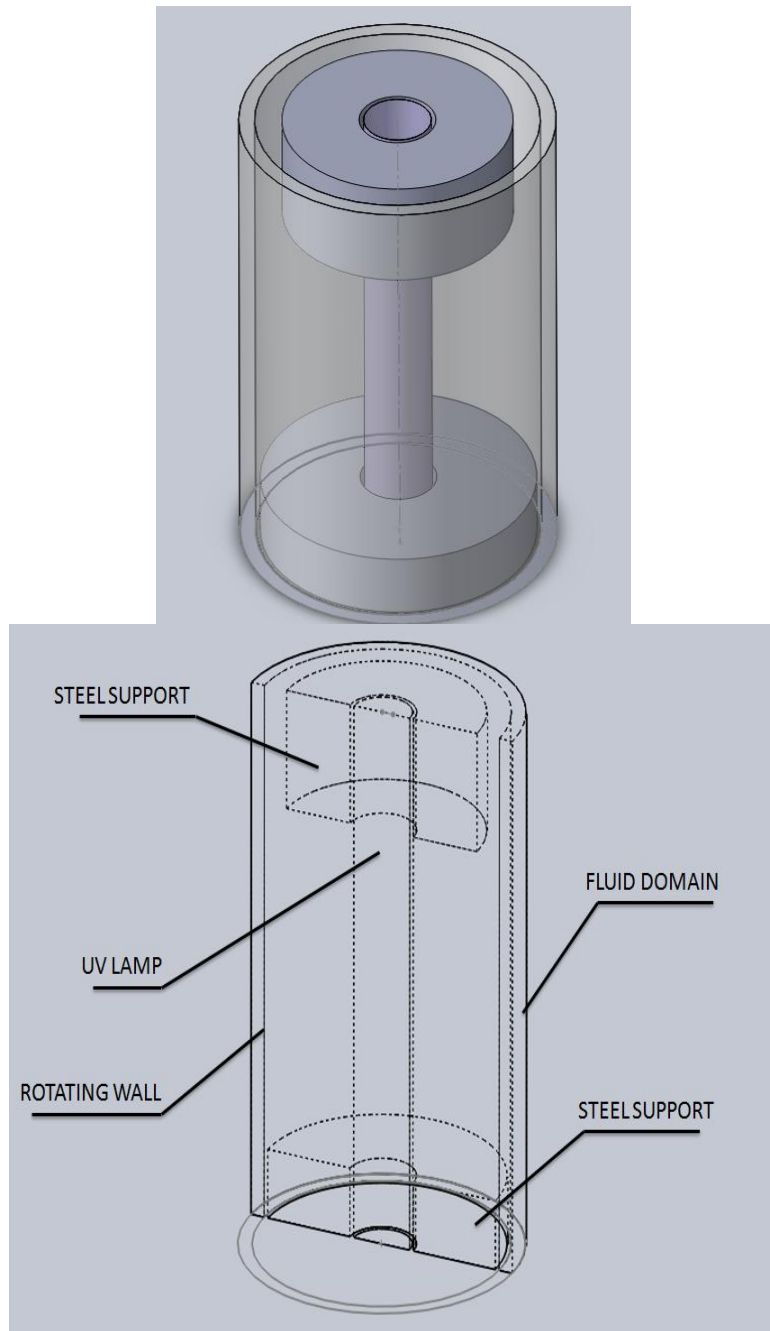


Figure 5-2: Schematic Representation of UV Taylor-Couette Reactor

A peristaltic pump was used during the experiments to control the mass flow rate of treated fluid in the reactor. The flow rate of the pump was varied from 100 ml/min to 600 ml/min. The range of axial Reynolds number was varied from 2.6 to 14.9 indicating that the flow pattern in the reactor was within the laminar flow regime.

5.3.2 Mathematical Modeling

The flow has been modeled in two-dimensions because the problem was found to be axi-symmetrical, including the prediction of the circumferential (or swirl) velocity. Hence, in the present case, two dimensional simulations have been performed for an axi-symmetric swirling flow between two concentric cylinders. The Navier-Stokes equations for an incompressible, constant viscosity liquid can be written in cylindrical coordinates as follows:

5.3.2.1 Continuity:

$$\frac{\partial(\rho v_z)}{\partial z} + \frac{1}{r} \frac{\partial}{\partial r} (r(\rho v_r)) = 0 \quad (5-2)$$

5.3.2.2 Momentum conservation equation:

The momentum conservation equation can be derived for 2D incompressible flow without any source term in cylindrical coordinates as follows.

Axial Component:

$$\frac{1}{r} \frac{\partial(r\rho v_z^2)}{\partial z} + \frac{1}{r} \frac{\partial(r\rho v_r v_z)}{\partial r} = -\frac{\partial p}{\partial r} + \frac{1}{r} \frac{\partial}{\partial r} \left(r\mu \left(2 \frac{\partial v_z}{\partial z} - \frac{2}{3} (\nabla \cdot \vec{V}) \right) \right) \quad (5-3)$$

Radial Component:

$$\begin{aligned} \frac{1}{r} \frac{\partial(r\rho v_z v_r)}{\partial z} + \frac{1}{r} \frac{\partial(r\rho v_r^2)}{\partial r} = -\frac{\partial p}{\partial r} + \frac{1}{r} \frac{\partial}{\partial z} \left(r\mu \left(\frac{\partial v_r}{\partial z} + \frac{\partial v_z}{\partial r} \right) \right) \\ + \frac{1}{r} \frac{\partial}{\partial r} \left(r\mu \left(2\frac{\partial v_r}{\partial z} - \frac{2}{3}(\nabla \cdot \vec{V}) \right) \right) - 2\mu \frac{v_r}{r^2} + \frac{2\mu(\nabla \cdot \vec{V})}{3r} + \frac{\rho v_g^2}{r} \end{aligned} \quad (5-4)$$

$$\text{Where : } (\nabla \cdot \vec{V}) = \frac{\partial v_z}{\partial z} + \frac{\partial v_r}{\partial r} + \frac{v_r}{r}$$

Tangential Component:

$$\frac{1}{r} \frac{\partial(r\rho v_z v_g)}{\partial z} + \frac{1}{r} \frac{\partial(r\rho v_r v_g)}{\partial r} = \frac{1}{r} \frac{\partial}{\partial z} \left(r\mu \left(\frac{\partial v_g}{\partial z} \right) \right) + \frac{1}{r^2} \frac{\partial}{\partial r} \left(r^3 \mu \frac{\partial}{\partial r} \left(\frac{v_g}{r} \right) \right) - \frac{\rho v_r v_g}{r} \quad (5-5)$$

In swirling flows, the conservation of angular momentum has a tendency to create free vortex flow in which the angular velocity increases as the radius decreases. In an ideal vortex flow, the centrifugal forces created by a circumferential motion are in equilibrium with the radial pressure gradient,

$$\frac{\partial p}{\partial r} = \frac{\rho \Omega^2}{r} \quad (5-6)$$

As the distribution of angular momentum in non ideal vortex evolves, the form of this radial pressure gradient changes, driving radial and axial flows, in response to highly non uniform pressures that result therein.

5.3.2.3 Scalar transport equations:

In ANSYS FLUENT there is the possibility to introduce an arbitrary scalar (ϕ) as user-defined-scalar (UDS). Fluent solves the following transport equation for single phase flow in Cartesian coordinates considering the convective and diffusion contributions (Ansys Fluent, 2009):

$$\frac{\partial \rho \phi}{\partial t} + \frac{\partial}{\partial x_i} \left(\rho u_i \phi - \Gamma \frac{\partial \phi}{\partial x_i} \right) = S_\phi \quad (5-7)$$

Where: Γ and S_ϕ are the diffusion coefficient and source term for the scalar equation.

5.3.2.4 Radiation model

The general radiative transfer equation (RTE) for an absorbing, emitting and scattering medium at position \vec{r} in direction \vec{s} is the following partial differential equation (Ansys Fluent, 2009):

$$\frac{dI(\vec{r}, \vec{s})}{ds} + (a + \sigma_s)I(\vec{r}, \vec{s}) = an^2 \frac{\sigma T^4}{\pi} + \frac{\sigma_s}{4\pi} \int_0^{4\pi} I(\vec{r}, \vec{s}') \phi(\vec{s} \cdot \vec{s}') d\Omega' \quad (5-8)$$

In this problem, such equation should be simultaneously solved for the three adjacent media, namely air, quartz and liquid using the appropriate initial boundary conditions.

Scattering of UV light was neglected in both liquid and air domains. Appropriate boundary conditions were assigned to semi-transparent walls to ensure that the light transmitted across the quartz was diffusely and isotropically re-emitted in the fluid region. The approach used in this study allowed a simplification of the RTE since the fluid scattering coefficient could now be set to zero:

$$\frac{dI(\vec{r}, \vec{s})}{ds} + aI(\vec{r}, \vec{s}) = 0 \quad (5-9)$$

where α is the absorption coefficient of the three media (air, quartz, liquid).

The discrete ordinates (DO) radiation model was used to solve the radiative transfer equations (RTE) for a finite number of discrete solid angles, associated with a vector direction \vec{s} fixed in global Cartesian coordinates system.

5.3.2.5 UV Inactivation Kinetics

The first order inactivation model is the simplest approach. It assumes that the inactivation rate changes with respect to pathogen concentration, N , and the fluence, I , such that

$$\frac{dN}{dt} = -kIN \quad (5-10)$$

where k is the first order inactivation constant and I is the fluence. The parameter k is based on the amount of radiation absorbed by the fluid and delivered to molecules or microorganisms and indicates the amount of radiant energy required to drive the reaction.

The first-order inactivation reaction was defined as the pseudo-first order model (Severin et al., 1983). Considering k and I as constants, it is possible to integrate Equation (5-10) obtaining

$$\frac{N}{N_o} = e^{-kIt} \quad (5-11)$$

5.3.3 Measurements of UV incident radiation

After UV lamp was turned on for 15 minutes, an X911 UVC-Meter Radiometer equipped with an UV-3718-4 detector (Gigahertz-Optik, Turkenfeld, Germany) was used to measure the incident radiation fluence rate of UV lamp along the vertical direction on external surface of inner quartz cylinder (Figure 5.3). The measurements were conducted in triplicate calculating the average and standard deviation. For this UV lamp the average fluence rate measured was about 2.29 ± 0.11 mW/cm². In order to obtain a non-saturation value of UV dose in the treated fluid during actinometer test, a doped sleeve was installed around the UV lamp decreasing the amount of radiation emitted. The average value of fluence rate measured by the radiometer was about 0.05 ± 0.001 mW/cm². The resulted emission of UV radiation was decreased of about 98% (Figure 5.4).



Figure 5-3:UV Irradiance Measurements' setup

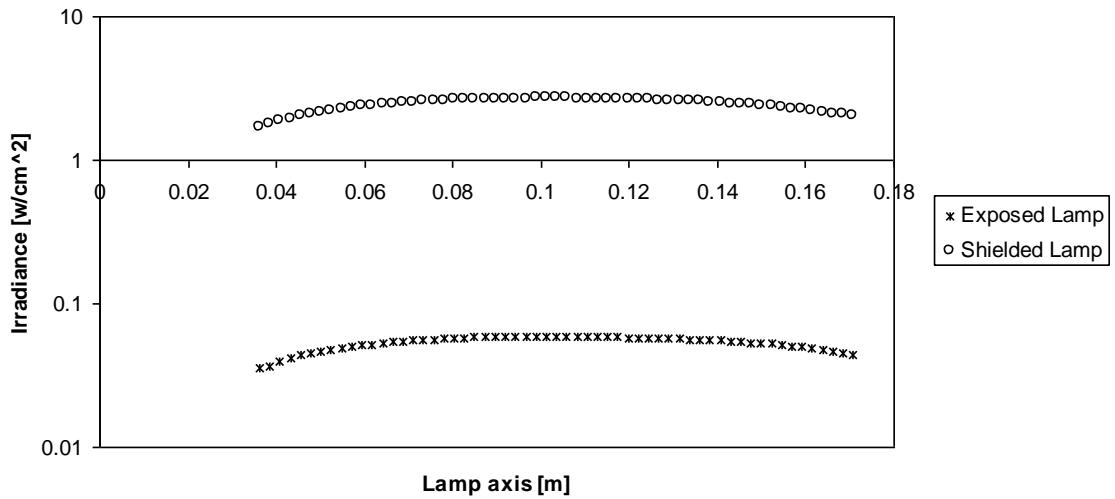


Figure 5-4:UV Irradiance Measurements Data obtained from X911 UVC Radiometer

Following the data collection using the radiometer, the radiation model was implemented in ANSYS FLUENT using a DO model with theta and phi division equal to

8 and theta and phi pixels equal to 4. The lamp was considered as radiation emitting surface with diffuse radiation equal to 11 W/m^2 according to experimental data. Second Order Upwind was used as solution method for DO radiation and the optical properties of the other materials are described in Table 5.1.

5.3.4 Grid Independence Study

The geometry for the Taylor-Couette reactor was considered axi-symmetric along the axis of rotation. Gambit version 2.4.6 was used to draw and describe the geometrical properties of the reactor. Grid independence studies were carried out on a representative 2D cross-section of the UV reactor to determine the minimum number of elements needed to accurately solve the velocity field. Figure 5.5 shows the normalized velocity profiles along radial direction at different quad elements. The chosen grids in fluid domain for grid independence tests were: 5x100, 10x200, 20x400, 30x600, 40x800.

Simulations were carried out without any mass flow inlet but only considering the rotation of internal cylinder ($Ta = 1743$). It was observed that the solution of velocity field, obtained from the grid with 20 quad elements along the thickness, is grid independent (the error compared with the solution with 30 quad elements is less than 1%). With an aspect ratio 1:1 the entire geometry was divided into 473,602 quad elements.

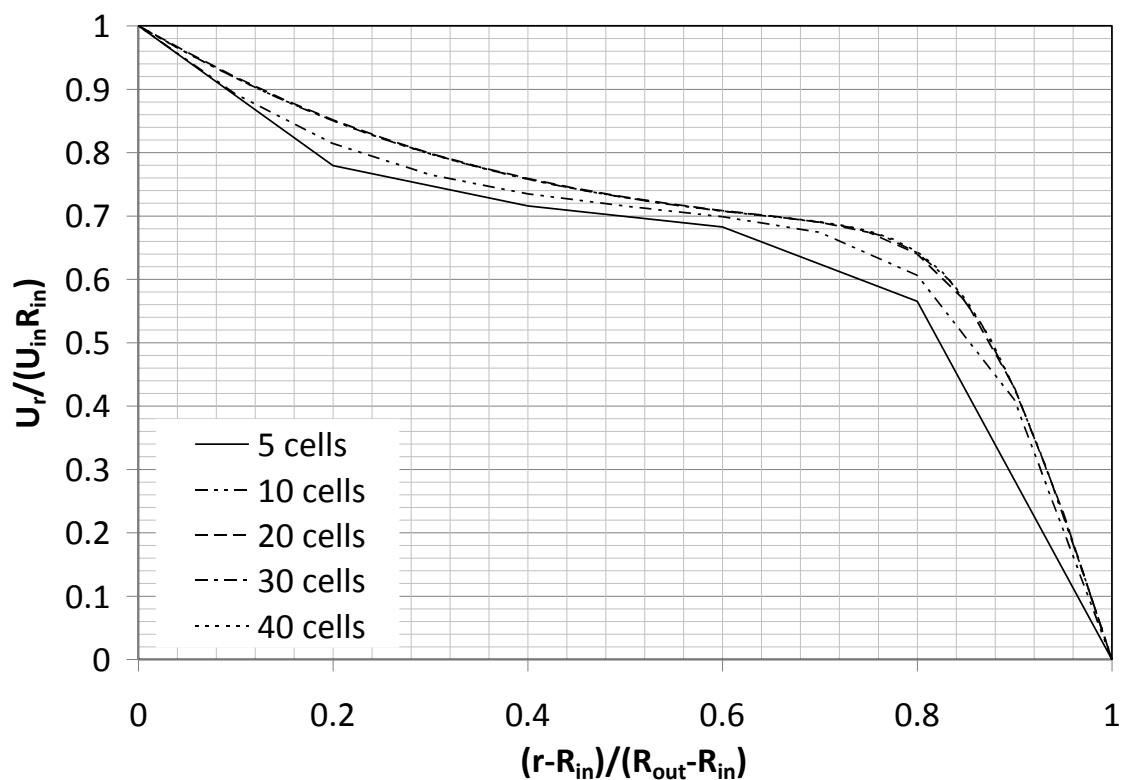


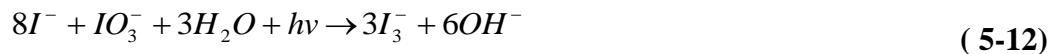
Figure 5-5: Normalized Velocity profiles at Different Quad elements along Thickness

5.3.5 Actinometer Solution

The iodide/iodate actinometer was used to determine incident photon flow emitted from the UV lamp into TC reactor. This commonly used low pressure UV lamp has two advantages, which are known quantum yield at 253.7 nm as well as independence from ambient light.

The actinometer consists of mixture of 0.6M of potassium iodide (KI) and 0.1M of potassium iodate (KIO_3) in 0.01M sodium tetraborate hydrate ($Na_2B_4O_7 \cdot 10H_2O$) buffer solution at pH 9.2. The iodide-iodate solution absorbs the UV radiation which induces photolysis of iodide ion with iodine atoms and hydrated electrons as primary

photoproducts. The hydrated electrons are instantaneously scavenged by the iodate ions, whereas the iodine atoms react with the excess of iodide ions forming the tri-iodide complex. The overall photochemical reaction is provided below:



The amount of UV light absorbed by the actinometer is proportional to the amount of photo-product (tri-iodide I_3^-) formed. The tri-iodide complex exhibits a defined absorption band in the UV-A spectral region with a maximum at 352 nm, characterized by a molar absorption coefficient $\epsilon_{352nm} = 27.636 M^{-1}cm^{-1}$. The quantum yield of the iodide/iodate actinometer at 253.7 nm was reported in literature as 0.73 mol/Einstein.

Samples of 3, 5, 10 mL contained de-ionized water and actinometer at dilution rate 1:20 were irradiated under collimated beam apparatus at different exposure time (0-2-4-6-8-10 min) and the absorption of the final solution was measured at 352nm with Varian Cary50 UV-Vis Spectrophotometer (Varian Inc.). The experimental data were fitted by a second order polynomial curve obtaining a relation between absorbance and absorbed energy (Figure 5.6). The fitted curve was used in ANSYS FLUENT to reproduce the actinometer test (wash-out test).

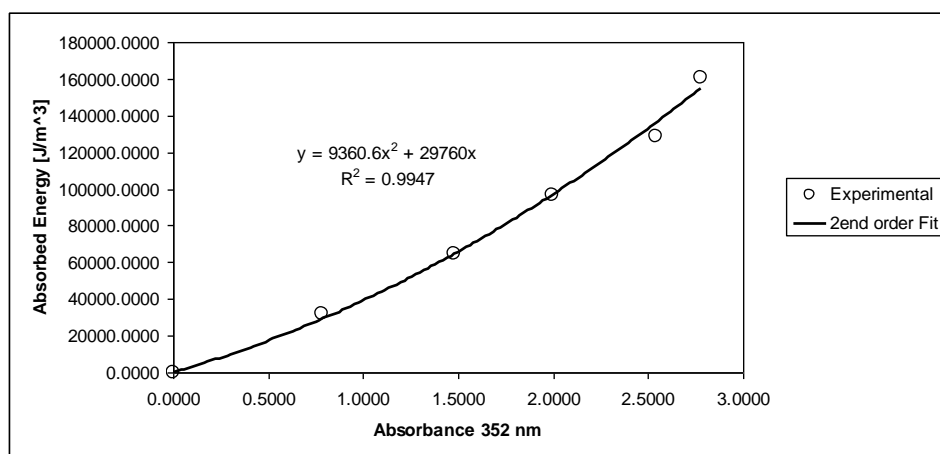


Figure 5-6: Absorbed Energy vs. Absorbance

5.3.6 Boundary conditions

The geometry for the Taylor-Couette flow was considered 2D axi-symmetric around the axis of rotation (x-axis) and the analysis was conducted including swirl (or rotation) flow. For numerical simulations of the flow in the annular region, laminar model was chosen using a numerical scheme of First Order Upwind and, once the convergence was reached, a Second Order Upwind scheme was selected. The following Table provides the boundary conditions used for these simulations.

Table 5-1: Boundary conditions

Material	Properties
Fluid	Density = 1000 kg/m^3 Viscosity = 0.001 kg/m / s Absorption Coefficient = $198 - 1985 \text{ 1/m}$ Refractive index = 1.37
Quartz	Absorption Coefficient = 39.3 1/m Refractive index = 1.505
Air	Default values

Edge	Boundary condition
Inlet	Mass Flow (ranges: 116-670 mL/min)
Outlet	Pressure outlet
Lamp	8.4 W
Wall (air domain)	em = 0.6 df = 0.5
Wall (quartz)	Rotating wall (40 rpm) Semi-transparent (df=0)

5.4 Results and Discussion

5.4.1 Model Verification

As Taylor number is less than critical value, no Couette vortices occur in the fluid domain. The flow is considered “stable”. In this condition, an analytical solution exists for the velocity profile which is a simplification of Navier-Stokes equation. The expression is the following:

$$u_r = R_i \Omega_i \frac{\frac{R_o}{r} - \frac{r}{R_o}}{\frac{R_o}{R_i} - \frac{R_i}{R_o}} \quad (5-13)$$

The model was compared at different Taylor numbers (below the critical value). It can be observed that the radial velocity profiles perfectly match the analytical solution provided

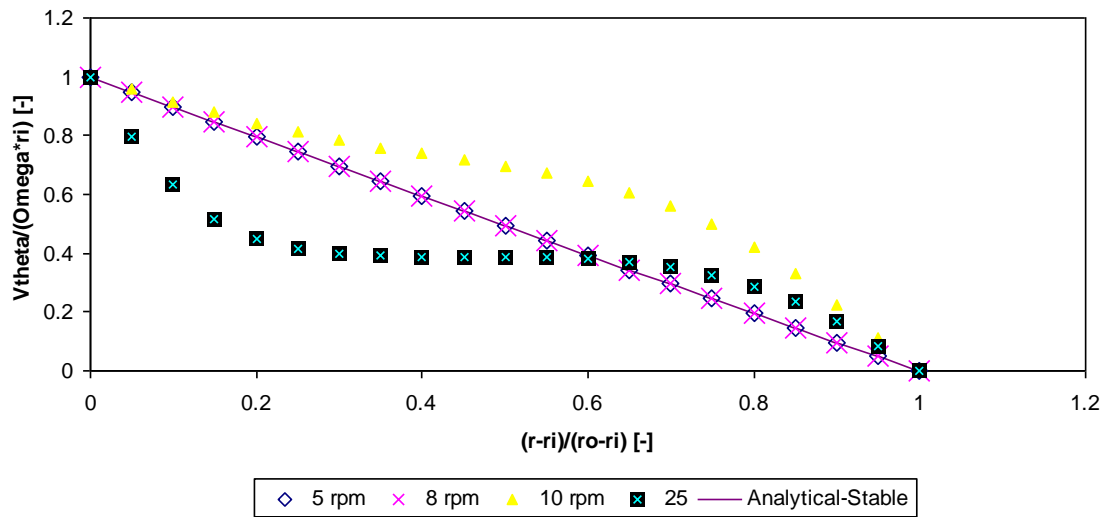


Figure 5-7: Stable Solution – Radial Velocity Profile Comparison

When Taylor number is increased above the critical value, the fluid is destabilized and vortices appear. This is the so-called “unstable” flow. In this case, there is no analytical solution for radial velocity. Moser (Moser et al., 1983) studied numerically a Taylor Couette reactor using CFD at high Taylor numbers. The normalized radial velocity profile was compared to Moser’s solution (Figure 5.8).

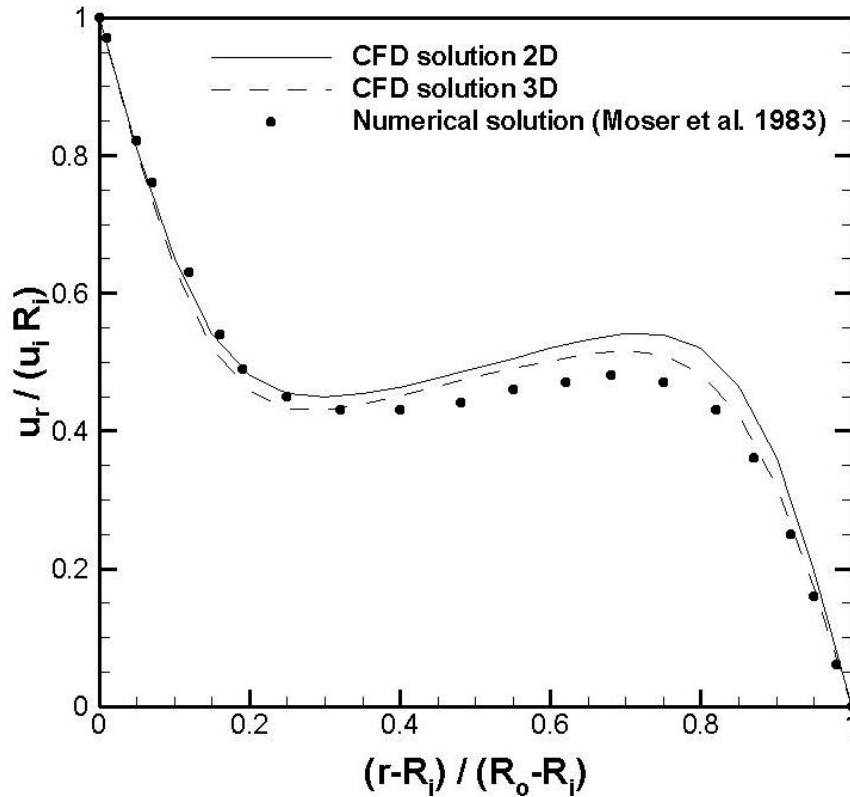


Figure 5-8: Unstable Solution – Radial Velocity Profile Comparison

From Figure 5.8 it can be noticed that 2D axi-symmetric CFD simulation matches well with the numerical data obtained by Moser especially close to the walls.

The Taylor Couette reactor was also drawn in 3D and meshed with cooper meshing scheme starting from the 2D mesh keeping the same aspect ratio. The radial velocity profile extracted from 3D geometry does not show improved accuracy. For this reason all the simulations were carried out using the grid independent 2D axi-symmetric geometry.

5.4.2 Model Validation – Tracer Test

The hydraulics study of Taylor Couette reactor was validated with a passive dye experiment. Methylene blue has been used as passive tracer and spiked in de-ionized water. 15mL samples were collected from the outlet and the absorption coefficient at 664nm was determined using Cary50 UV-Vis spectrophotometer.

Transient simulations were carried out using a user-defined-scalar as passive dye with diffusion coefficient 10^{-7} and spiked from the inlet. A third order MUSCL was used as solution method for the UDS and a surface monitor was considered at the outlet evaluating the concentration of the tracer. The transported fluid was considered water with default values with inlet mass flow rate equal to 116 ml/min and rotational speed equal to 40 rpm ($Ta = 1743$). The curve of breakthrough was calculated and compared with experimental data (Figure 5.9).

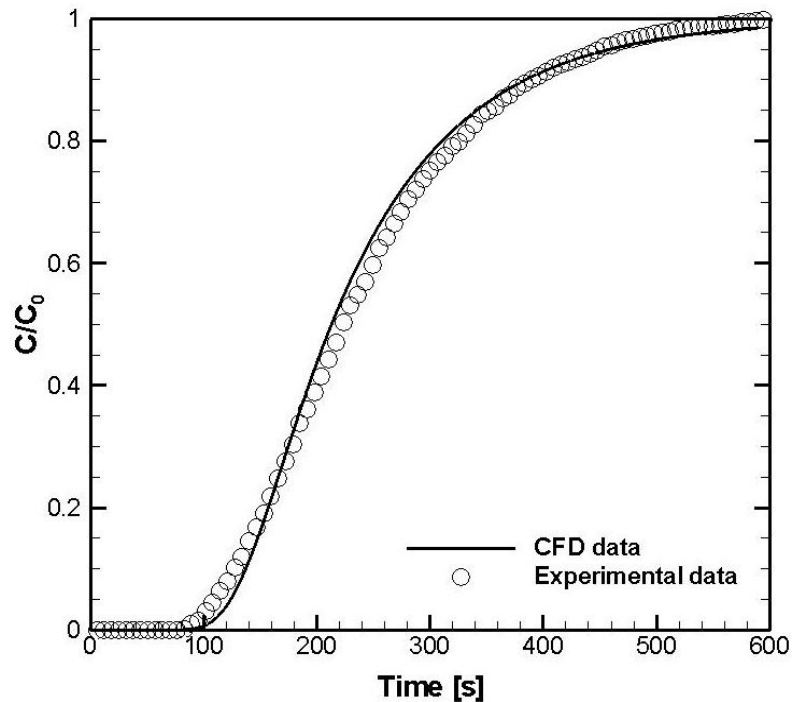


Figure 5-9: Breakthrough Curve with Passive Tracer

As can be seen from Figure 5.9 the match is good between experimental and numerical prediction. Moreover, the shape of the breakthrough curve is far from the ideal plug flow reactor. In this last case, the shape of the curve is assumed as a step function where the concentration of the tracer changes from 0 to 1 rapidly at time 177 s. This behaviour is due to axial flow dispersion that creates preferential fluid paths.

5.4.3 Model Validation – Steady State

Both hydraulics and incident radiation fields were validated with actinometric tests. Several simulations were carried out at steady state condition at different mass flow rates keeping the rotational speed constant at 40 rpm ($Ta = 1743$), and considering the fluid with optical properties described in attachment 1. The absorbed energy curve for triiodine was implemented in ANSYS FLUENT with a proper UDF file following collimated beam lab experiments. Third Order MUSCL as solution method for the active tracer. Figure 5.10 shows the results of steady state simulations compared with experimental data.

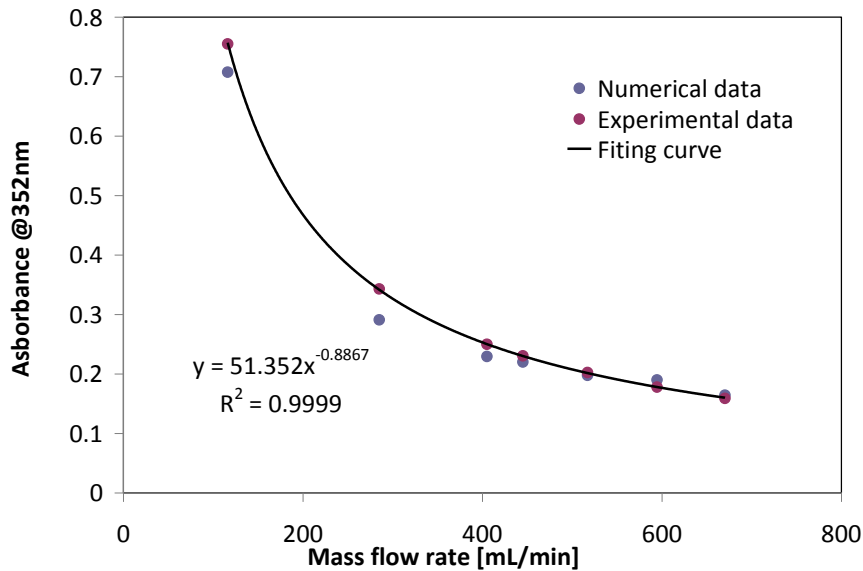


Figure 5-10: Steady State Model Validation

From Figure 5.10, it can be noticed that increasing the inlet mass flow rate the concentration of the active tracer at the outlet decreases as expected. The experimental data seems following a power law

$$\text{Absorbance} = 51.352 * (\text{Mass flow rate})^{-0.887} \quad (5-14)$$

There is good agreement between experimental and CFD data especially at high mass flow rates.

5.4.4 Model prediction

The validated model has been used to predict first order microbial kinetic inactivation in low UVT liquids. Steady state simulations were carried out at different D10 (the amount of energy required in order to inactivate 1 log reduction of microorganisms or the radiation dose that will reduce a microbial population by 90%) and different inlet mass flow rates. The inactivation of microorganism has been predicted using Eulerian framework. The absorption coefficient of fluid was 1985 1/m (UVT = 2.4×10^{-9}).

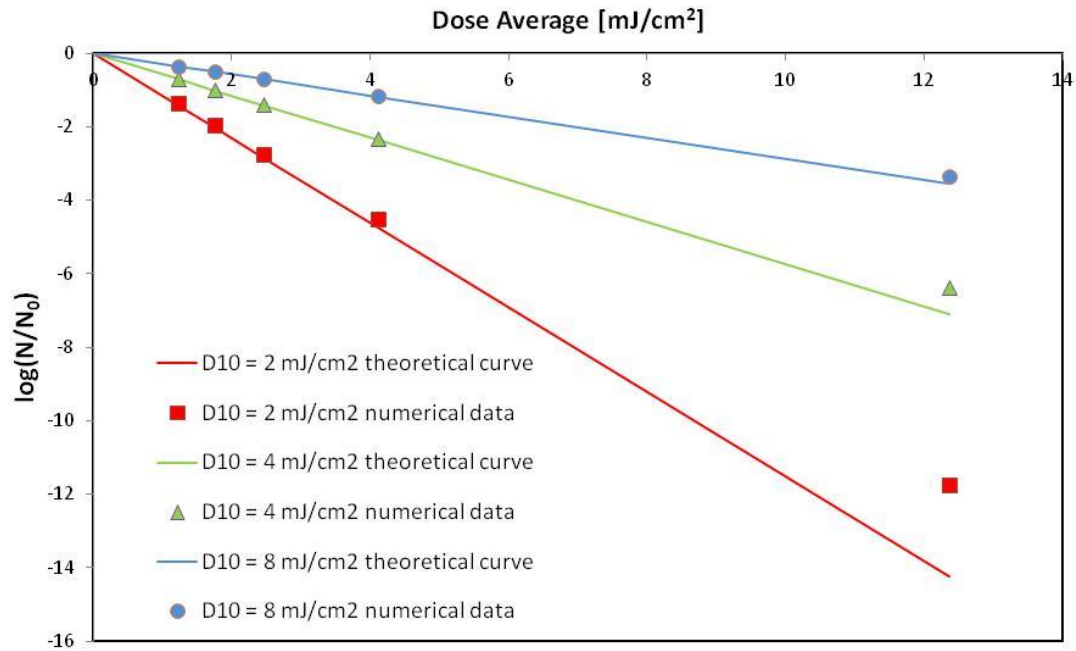


Figure 5-11: Prediction of First Order Inactivation Curve

As illustrated in Figure 5.11, the straight lines represent the theoretical first-order inactivation prediction curve (obtained from Equation 5-11) while the symbols (squares, triangles, circles) are the predicted inactivation obtained from CFD at different D_{10} . It can be noticed that CFD well predicts the microbial inactivation at low average dose. When the dose is increased the error also increased. This is due to axial flow dispersion, obtained at low flow rates, that creates preference patterns which makes a uniform dose distribution unachievable.

To better investigate the relation between D_{10} , UV dose and relative error, several simulations were carried out changing different microbial UV sensitivities ($0.25 - 16 \text{ mJ/cm}^2$), different UVT's of the fluid and different mass flow rates. The result is summarized in Figure 5.12.

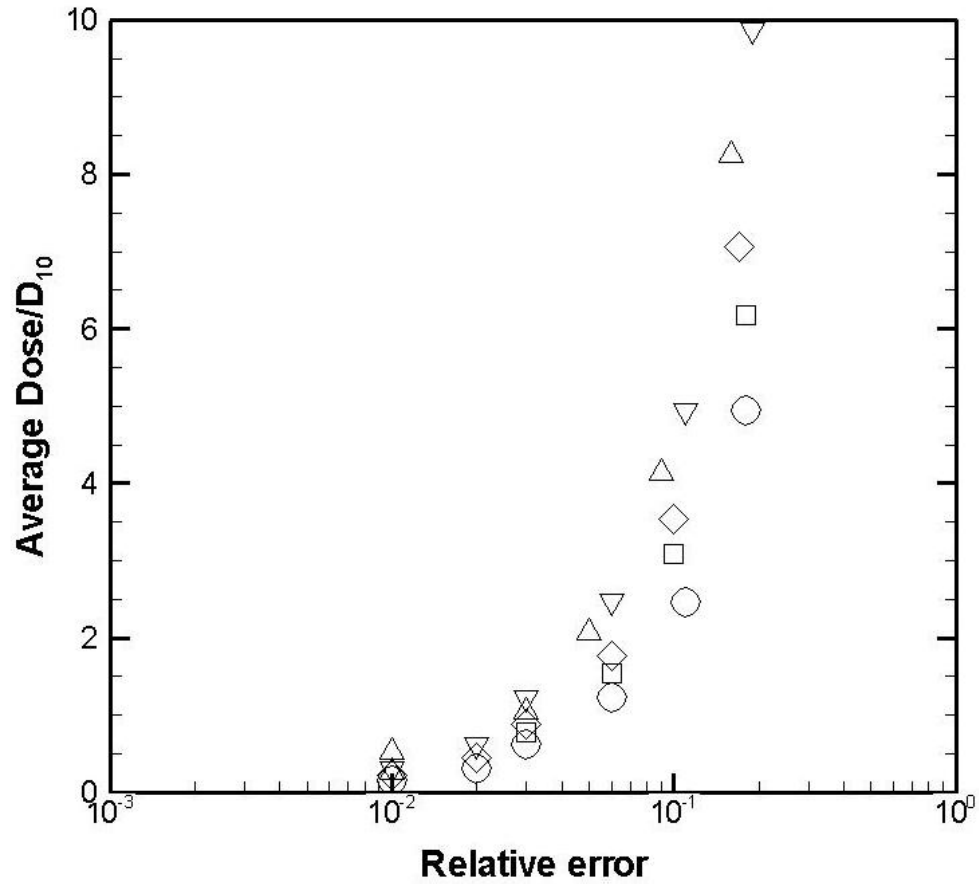


Figure 5-12: Average dose/D₁₀ vs. Relative error

All data were plotted in a graph where the y-axis represents the ratio of average dose and D₁₀ while x-axis represents the relative error. The data seems to be distributed and fitted well by a power law curve

$$\frac{\text{Average dose}}{D_{10}} = 52.019(\text{rel.error})^{1.1476} \quad (5-15)$$

From the above Figure, it can be concluded that in order to have an error of prediction less than 10% (relative error = 0.1), a ratio of average dose to D₁₀ less than 2

must be guaranteed. In this way, the axial dispersion is minimized and the behaviour of the Taylor Couette reactor can be compared to the collimated beam.

5.4.5 Taylor Couette –Milk Disinfection test

The Taylor Couette reactor was compared with Collimated beam reactor (CSTR – with uniform dose) and another CSTR reactor with regular lamp immersed in the fluid illustrated in appendix D.

The survival test figure 5.13 conducted to assure that disinfection is coming as a result of UV irradiance.

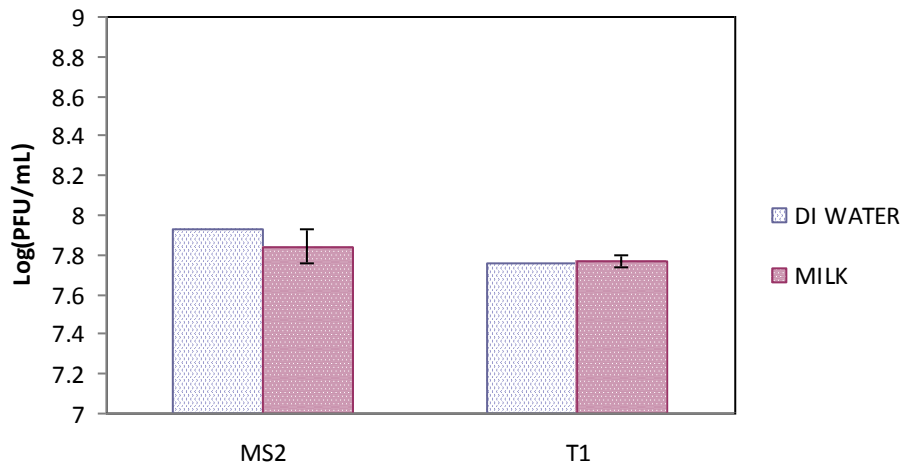


Figure 5-13:MS2/T1 Survival Test in Milk (96Hours).

The sensitivity tests figures 5.13 5.14 confirmed that no coating nor shielding course of actions were playing any role in the disinfection of milk.

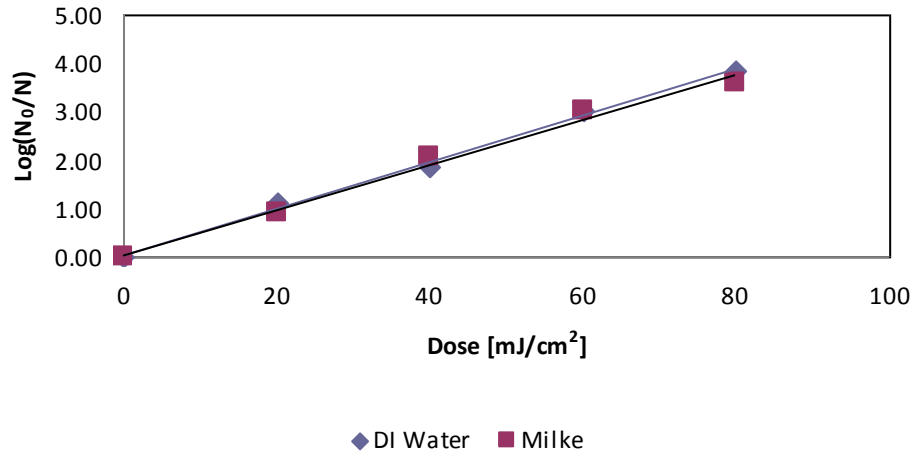


Figure 5-14:MS2-Milk Sensitivity Test

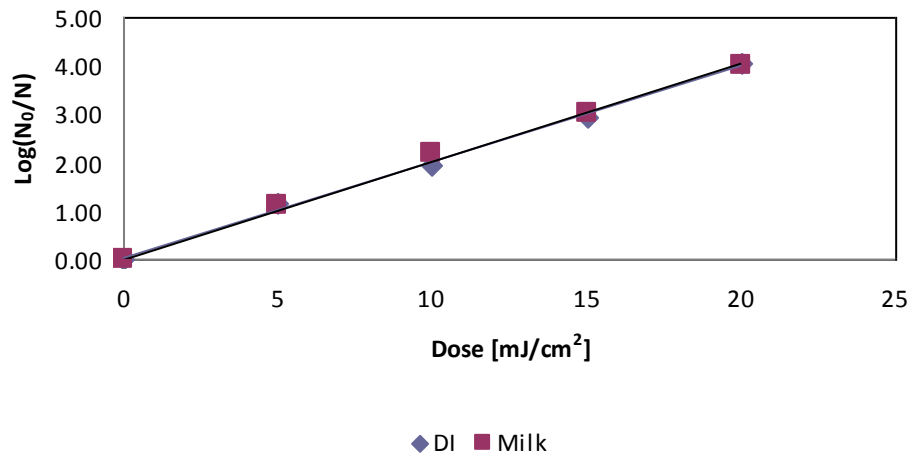


Figure 5-15:MS2-Milk Sensitivity Test

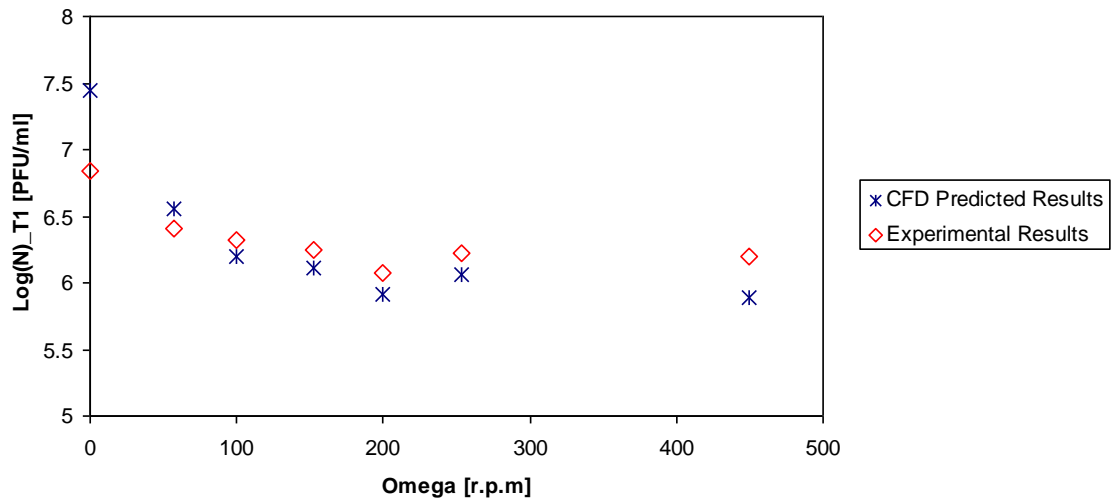


Figure 5-16:Log Inactivation Comparison CFD Vs Experimental Data

The deviation in the results which were mainly related to the variation in the UVT measurements which were summarized in appendix D

5.5 Penetration depth effect

The good agreement between experimental results and CFD prediction Figure 5.6 lead start numerical investigation of the mixing in Taylor Couette reactor the penetration depth was the main parameter of interest

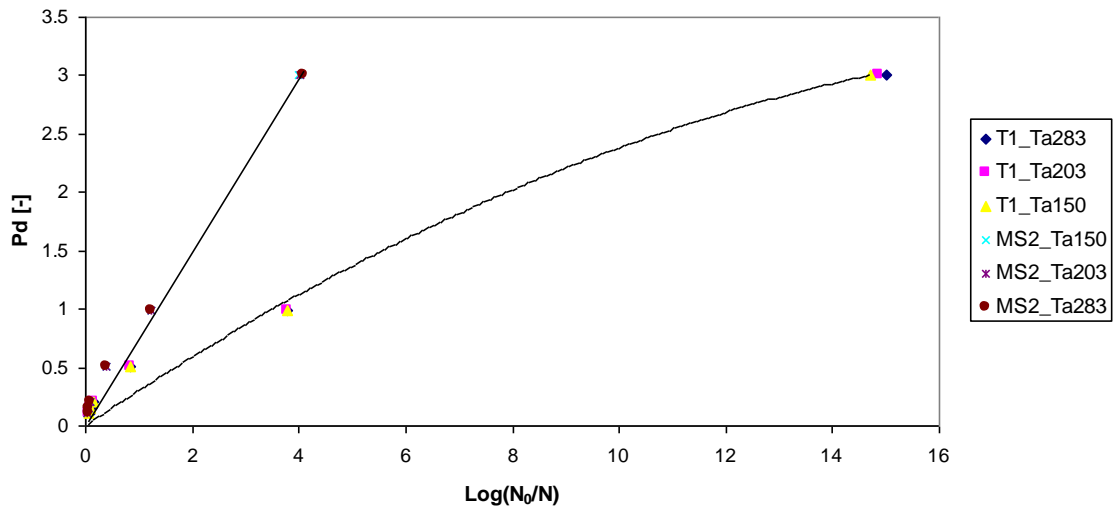


Figure 5-17: Dimensionless Penetration Depth Effects

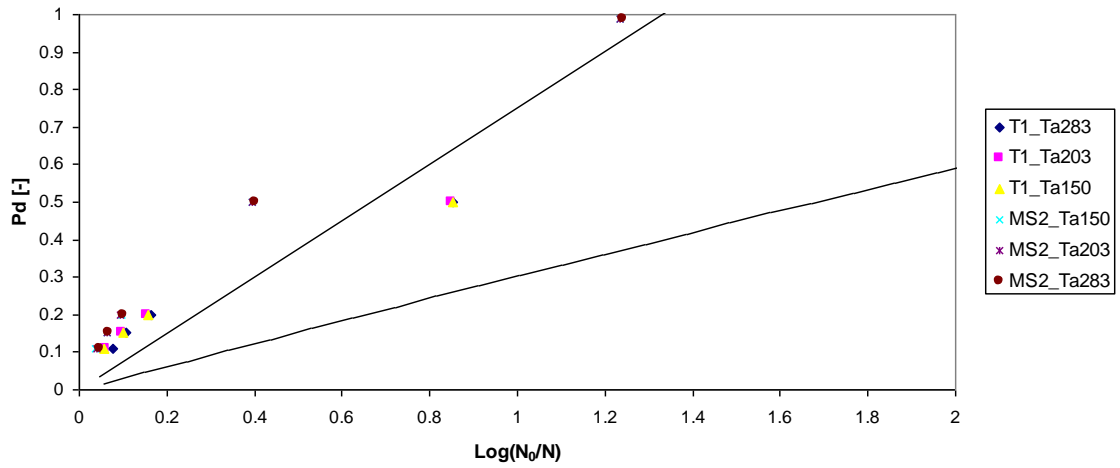


Figure 5-18: Dimensionless Penetration Depth Effects

Figure 5.17 (Magnified in 5.18) which compares disinfection in Taylor –Couette reactor for different dimensionless penetration depths (absorption coefficients), it is

shown that the log inactivation starts to deviate for two microbes for pd of 0.5 which means that the mixing in Taylor Couette reactor starts to be effective when light reach the middle of the gap. Moreover, the figure shows that as long as the light is reaching the middle of the cap in Taylor Couette reactor the inactivation starts to flow linear behaviour as shown in Figure 5.19 which illustrate the reduction equivalent dose calculated for the previous mentioned tests. Groups 1,2 and 3 represents penetration depth values of 0.1 0.15 0.2 respectively were groups 4, 5 and 6 represents penetration depth values of 0.5 1 and 3 respectively. As for groups 1, 2 and 3 the mixing was taking place partially on fluid elements occupying the irradiated zone to the dark zone, however there was the other part which was mixing fluid resides in the dark zone all the time. This had reflected in different values of reduction equivalent dose obtained from T1 and MS2 all the time. However once the UV light was capable of penetrating up to the center of the gap of the reactor the mixing started to be meaningful as the reduction equivalent dose of two different microorganism started to come together.

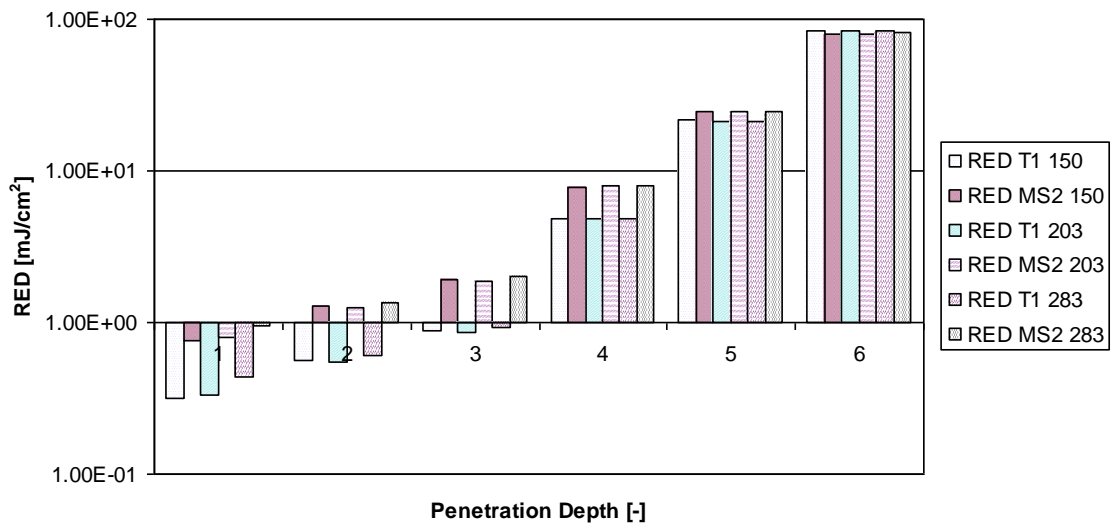


Figure 5-19: Penetration Depth Effects in Taylor Couette Reactor

As Taylor number increased, we were able to notice higher inactivation, which was a result of more visits of the fluid particles to the irradiated zone.

5.6 Modulate Taylor Couette reactor

The necessity of penetrating the UV light to the center of the gap remained barrier in the face of using Taylor Couette reactor as an effective small scale or laboratory device to disinfect UL-UVT fluids. The outer wall of Taylor Couette reactor modulated with sinusoidal way shape the mater enabled us from influence the TC votecies. As each vortex was passing through the narrow cross section area of the gap, the vortex used to get destroyed and fluid of low dark zone used to be mixed with one from irradiated zone then vortex used to be formed again and disinfection process used to take place over again. The previous mentioned procedure continued along the track of modulates Taylor Couette reactor and the result of the disinfection shown in figure 5.20. It includes simulation of groups 1,2 and 3 of figure 5.19 which represent penetration depth values of 0.1 0.15 0.2. The reduction equivalent dose came almost identical for all these penetration depth for Ta number 283. The matter which indicates the we were able the overcome mass transfer problem of UL-UVT fluids.

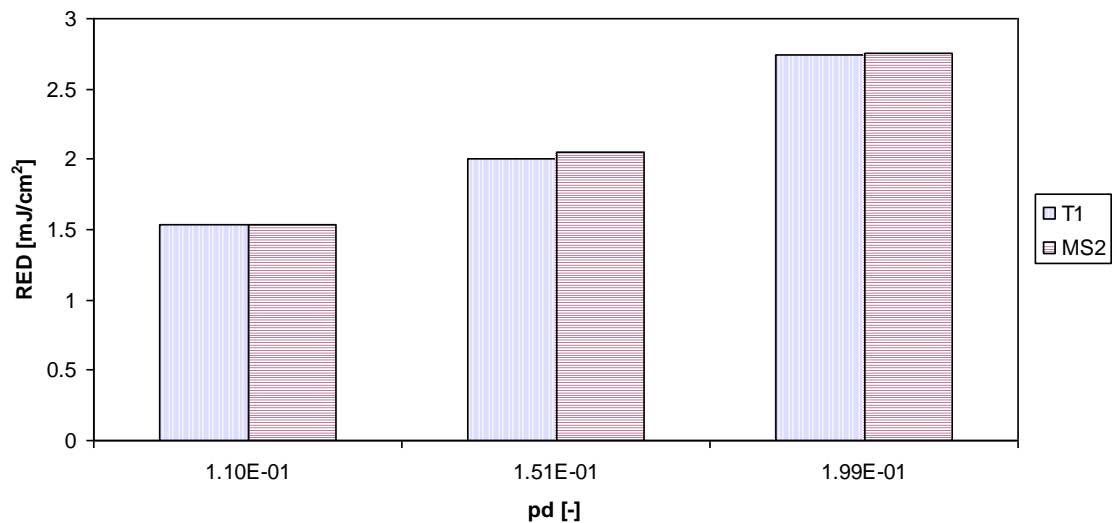


Figure 5-20: RED in Modulate Taylor Couette Reactor

5.7 Mixing efficiency

Electrical energy per order of disinfection EEO was used to provide qualitative estimation of disinfection efficiency in three different reactors.

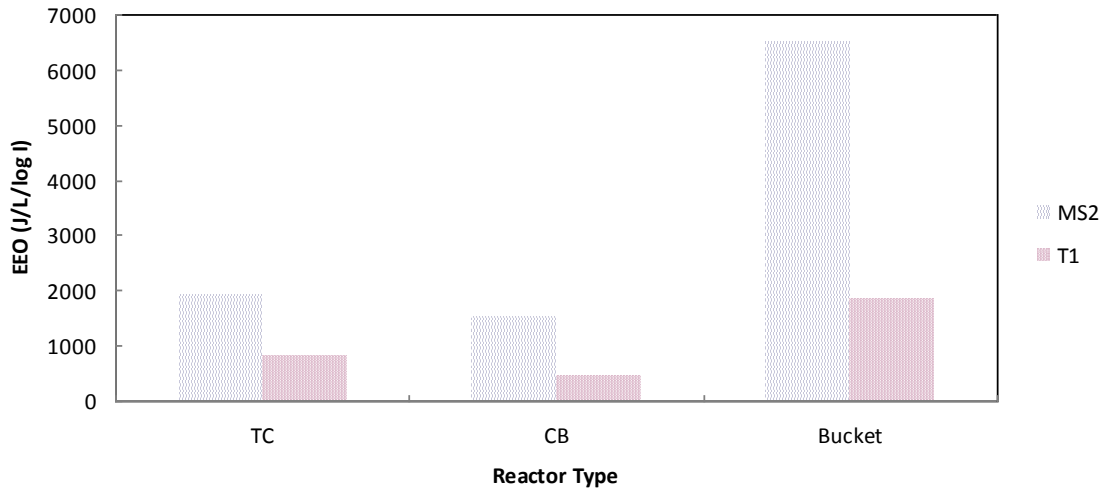


Figure 5-21: Energy Consumption per Different Reactors Raw Milk

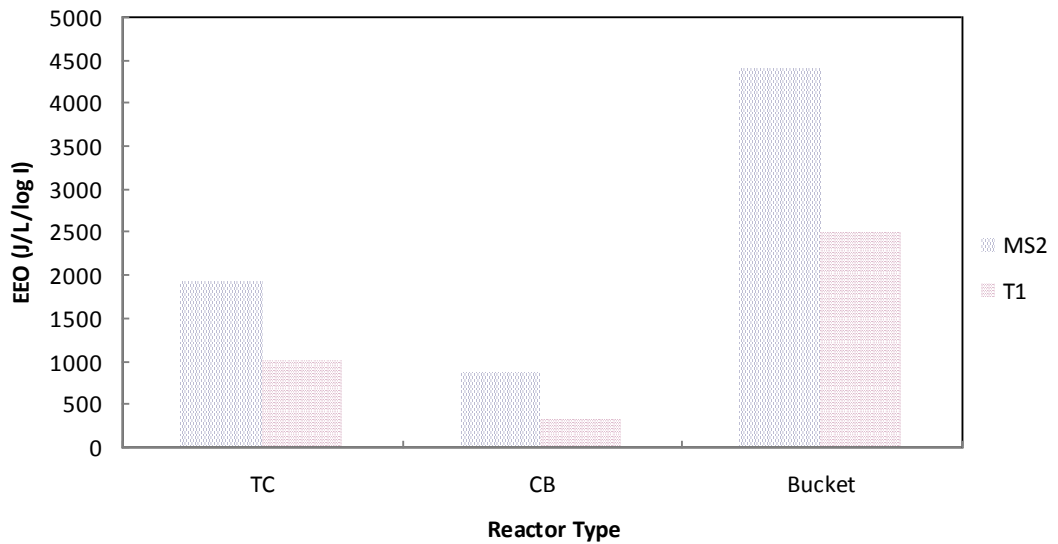


Figure 5-22: Energy Consumption per Different Reactors Pasteurized Milk

This comparison of the mixing in different types of reactors was mainly aimed to show advantage of Taylor Couette reactor mixing over ordinary PMR mixing type and the form of mixing should be considered to achieve desired disinfection level.

5.8 Conclusions

1. Numerical simulation was verified with reported data and validated with experimental results
2. Dimensional analysis provided us with insight on the conditions of Taylor Couette reactor for the predictions of microorganisms kinetics in the fluids
3. Penetration depth was found to be an important group parameters in disinfection very low transmittance fluids with UV light in Taylor Couette reactor
4. Modulated wavy wall Taylor Couette Reactor was found to overcome the limitation of straight walls one on mass transfer and was also found to be able to provide higher log inactivation and narrower dose distribution through combining more than one vortex pass the trough in one larger vortex formed in the crest of the wave the matter which can be explained as alternating between micro mixing and macro one over larger volume of the fluid

5.9 References

Ansys Fluent 12.0, Theory Guide (2009).

Kuo, J., Chen, C. L., Nellor, M., Standardized collimated beam testing protocol for water/wastewater ultraviolet disinfection. *Journal of Environmental Engineering*, 129, pp.774-779 (2003) .

Miller, R., Jeffrey, W., Mitchell, D., Elasri, M. Bacterial responses to ultraviolet light. *ASM News*, 65, pp.534-541 (1999).

Morowitz, H. J., Absorption effects in volume irradiation of microorganisms. *Science*, Washington D.C., 111, 229 (1950).

Moser, R. D., Moin, P., Leonard, A., A spectral numerical method for the Navier-Stokes equations with applications to Taylor-Couette flow. *Journal of Computational Physics*, 52, pp.524-544 (1983).

Severin, B. F., Suidan, M. T., Engelbrecht, R.S., Kinetic modeling of UV disinfection of water. *Water Research*, 17, pp.1669-1678 (1983).

Smith, G. P., Townsend, A. A., Turbulent Couette flow between concentric cylinders at large Taylor numbers. *Journal of Fluid Mechanics*, 123, pp.187-217 (1982).

Taylor, G. I., Stability of a viscous liquid contained between two rotating cylinders. *Philos. Trans. R. Soc. Lond. Ser. A*, 223, pp.289-343 (1923).

Vedantam, S., Joshi, J. B., Koganti, S. B., Three dimensional CFD simulation of stratified two fluid Taylor-Couette Flow. *The Canadian Journal of Chemical Engineering*, 84, pp.279-288 (2006).

Ye, Z., Forney, L. J., Koutchma, T., Giorges, A. T., Pierson, J. A., Optimum UV Disinfection between Concentric Cylinders. *Industrial & Engineering Chemistry Research*, 47, pp.3444-3452 (2008).

Chapter 6

6 Industrial Large Scale Reactor

6.1 Introduction

The impinging jet reactor (IJ) was built to treat fluids with UV transmission (UVT) below 1% per cm. The reactor forces fluid to flow directly on the lamp sleeve, so that all fluids will receive a similar UV dose. Consider the schematic representation of a single impinging jet reactor shown in Figure 6.1. The untreated fluid enters through the central cylindrical tube with radius z positioned at a certain distance w from the UV lamp. The fluid hits the wall and exits from the opposite direction.

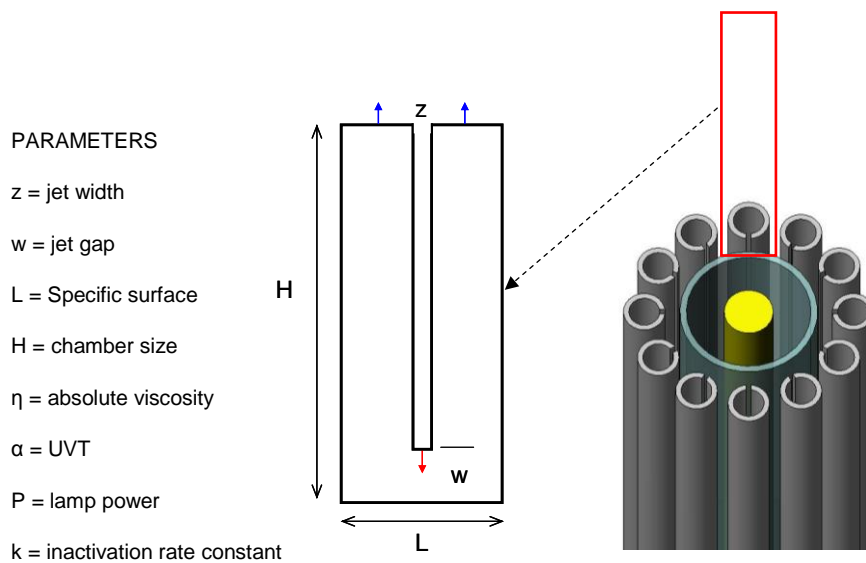


Figure 6-1: Simplified Model Geometry IJ Reactor U.S. Pat. No. 7,166,850

The dimensional analysis technique has been used to study the effect of the different parameters on the disinfection rate for the above-mentioned reactor and subsequently, the most affective PI-groups related to the disinfection rates were determined and finally the design of the reactor was optimized. The impinging jet reactor was selected to treat the effluent of a fish processing plant, which has very low UV transmittance and volumetric flow rate of 200 gpm. Appendix C

6.1.1 Measurement of UV Transmittance

This project has used ultra-thin cuvettes, with path length as low as 0.1 mm. In order to ensure that scattered light is correctly measured, we used the central sample port on an integrating-sphere spectrophotometer. The resulting measurements have shown that the disinfection test run can be correlated using the Collimated Beam apparatus. This gives confidence that these measurements are meaningful for simulation based on conventional calculation methods. Figure 6.2

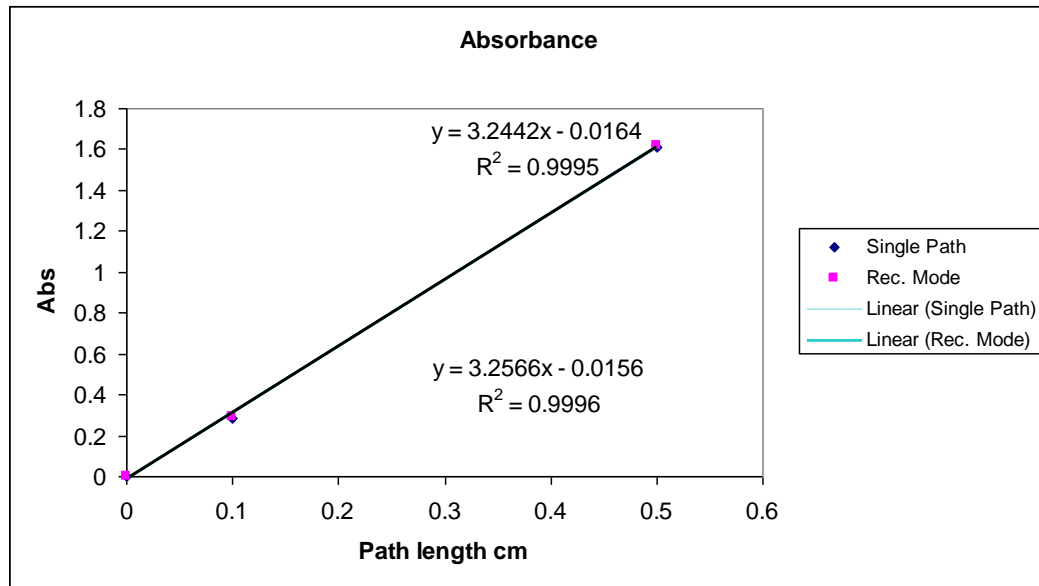


Figure 6-2: UVT measurement using DRA-30 Lab Sphere fixed on Varian Spectrophotometer Cary

6.1.2 Preliminary tests

6.1.2.1 Stability of Microorganism

Stability test MS2 and T1 in blood was came positive the matter which recommended these two microorganisms to carry out the test.

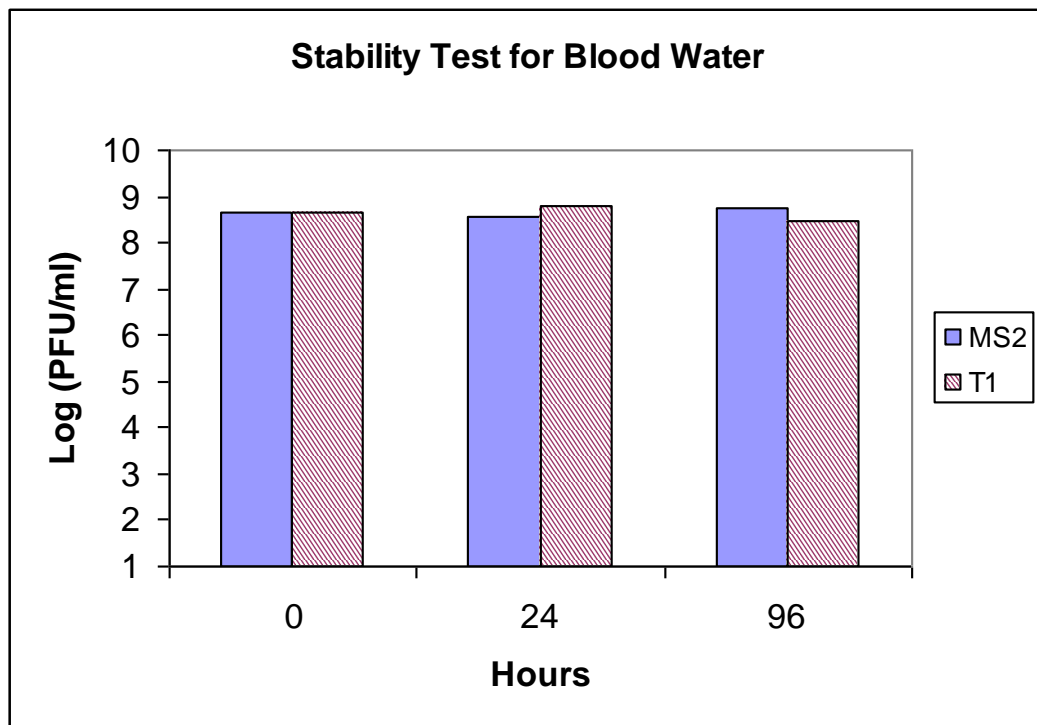


Figure 6-3:Blood Water Stability Test

6.1.2.2 Microorganism Inactivation Rate

The second test in variable needed to be determined was the inactivation rate constants for two challenging microorganisms .that illustrated in Figure 6.4

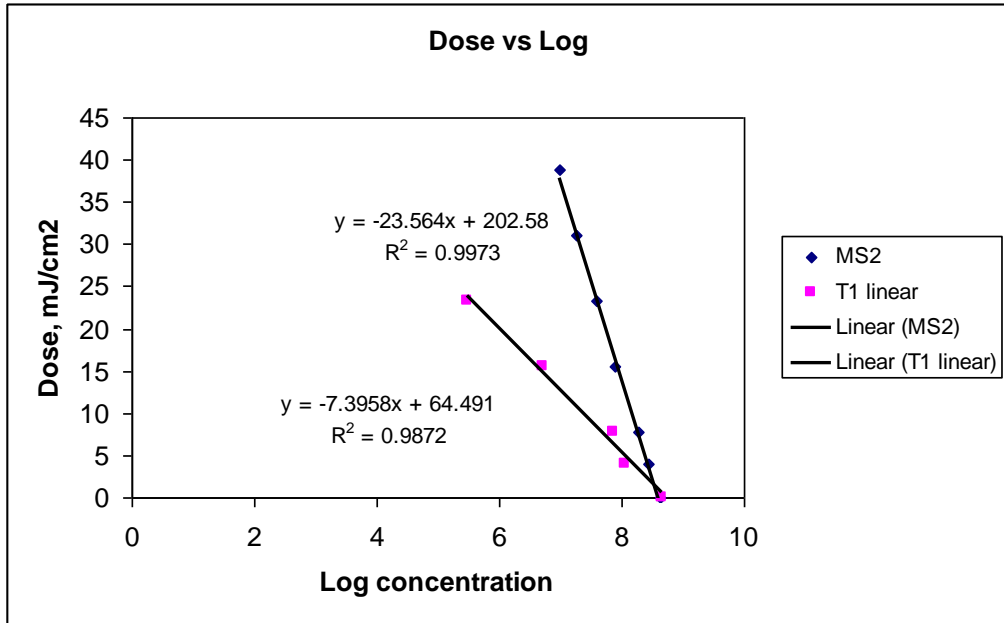


Figure 6-4:T1/MS2 UV disinfection Curves

The reduction equivalent dose of MS2 and T1 tested in IJ reactor came very close to each other, which was an indication of good mixing in the reactor. Figure 6.5.

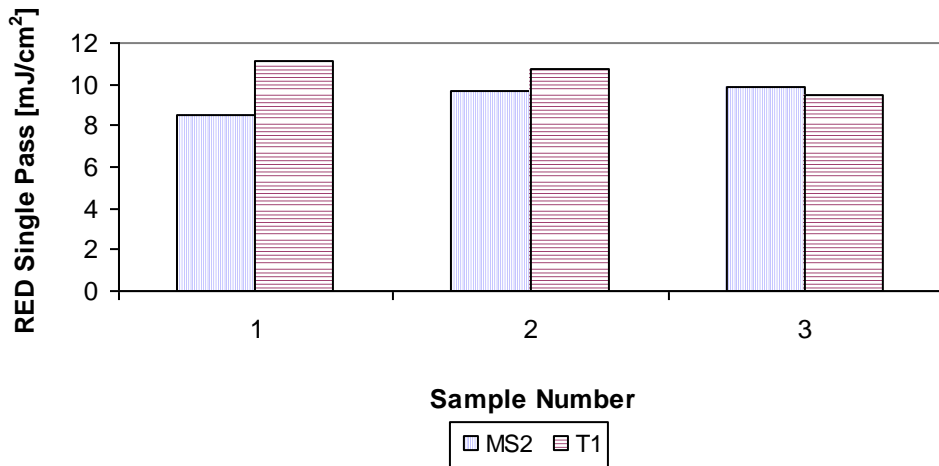


Figure 6-5:Reduction Equivalent Dose IJ Reactor

Based on the experiments and research activities carried out at Trojan Technologies, a 1 meter long single-lamp impinging jet reactor was manufactured Figure 6.6 and delivered to site for testing.



Figure 6-6:Impinging Jet Reactor

The reactor was tested in a recirculation mode as schematically illustrated in Figure 6.7 where N_a and N_b are the microbial concentrations in two nodes (a and b) of the hydraulic circuit, Q is the test flow rate, V is the volume of the recirculation tank. The methodology to interpret the bioassay results obtained in recirculation mode was developed by Trojan Technologies based on chemical reactor engineering principles and it is not included in this paragraph for confidentiality.

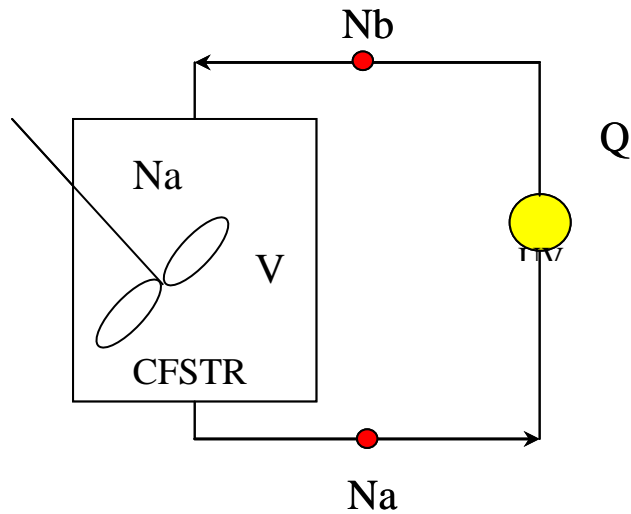


Figure 6-7:Experimental Layout used during Bioassay Experiment

6.1.3 The Pilot Test

The pilot reactor was set up in re-circulation mode at a flow rate of 50 gpm. For each test, the tank was filled to the desired level with effluent, spiked with the challenge organism (E. Coli or T1), and once the reservoir was well-mixed, the system was operated in recirculation mode with samples taken from both the inlet and outlet of the reactor every 10 minutes for 60 minutes.

Once the samples were cultured and counted, it was determined that the applied doses were too high to achieve meaningful results with E. Coli. As a result, only the T1 results were used to determine system performance. Recall that the E. Coli was also found to be unstable and to have increased UV resistance, so it is likely that the E Coli results would not have been reliable in any event. Results from of this typical performance test may be seen in Figure 6.8.

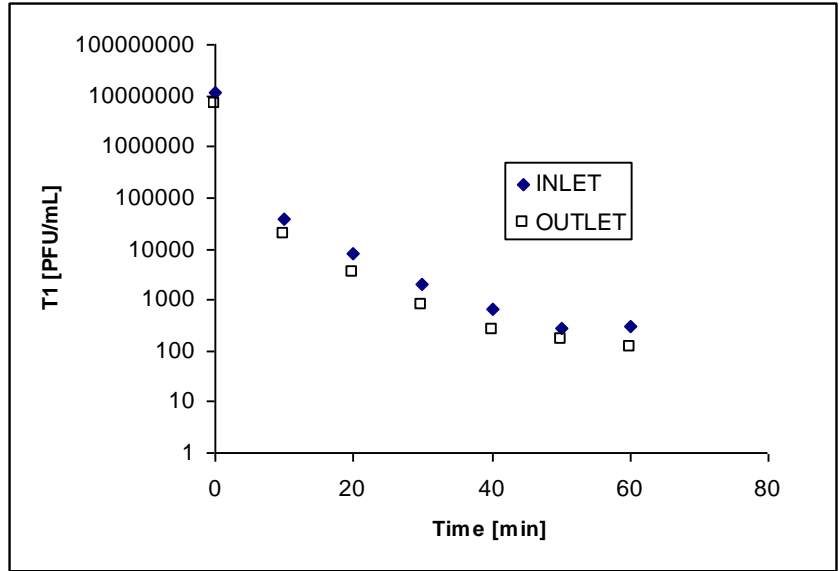


Figure 6-8:T1 Counts vs. Operating Time

The test results lead to deliver a system of 24 reactors arranged in 4 trains of 50 gpm flow rate work in parallel, each consists of 6 reactors connected in series to achieve the required disinfection level as will be shown later.

6.2 Full Scale System of Reactors Validation Tests

The complete effluent treatment system of the plant consists of an equalization tank, a dissolved air and polymer flotation system (DAF), a rotating screen filter, and the UV system. A flow diagram is shown below Figure 6.9.

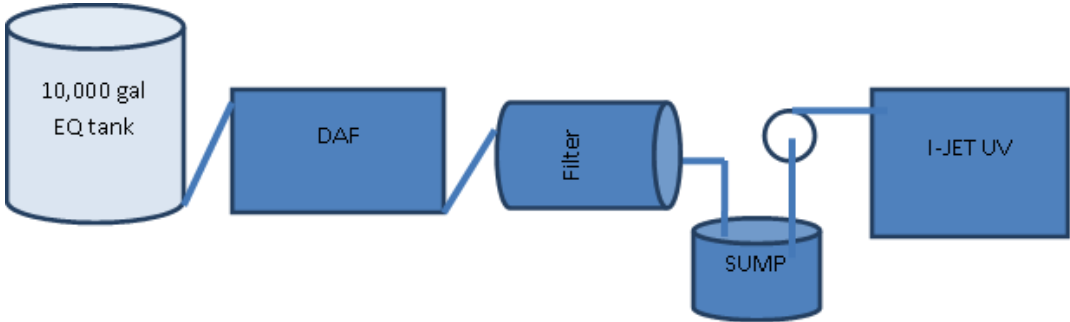


Figure 6-9: Schematic of Effluent’s Treatment System

The UV system consisted of 24 reactors arranged as 6 in series with 50 gpm nominal design flow rate and 4 trains in parallel to handle 200 gpm required effluent treatment capacity Figure 6.10.



Figure 6-10:IJ-UV Reactors

6.2.1 Test Objectives

- To identify the delivered dose from each reactor.
- To validate the performance of the system.
- To identify the number of reactors needed in series and in parallel to achieve the required dose at a certain flow rate for different UVT conditions.

6.3 Collimated Beam Test

6.4 Microorganism Selection

The work with IHN virus as targeted microorganism was not possible due to the risk of infection and the spread of it. T1 was selected as a surrogate for the following reasons:

- (a) T1 is nonpathogenic.
- (b) It has UV sensitivity value (D_{10}) of 5 mJ/cm^2 , which is close to the UV sensitivity of the targeted virus.
- (c) Due to the stability, seen in our previous work of T1 in the effluent of the plant Figure 6.11.
- (d) MS2 was not allowed to be used on the plant.

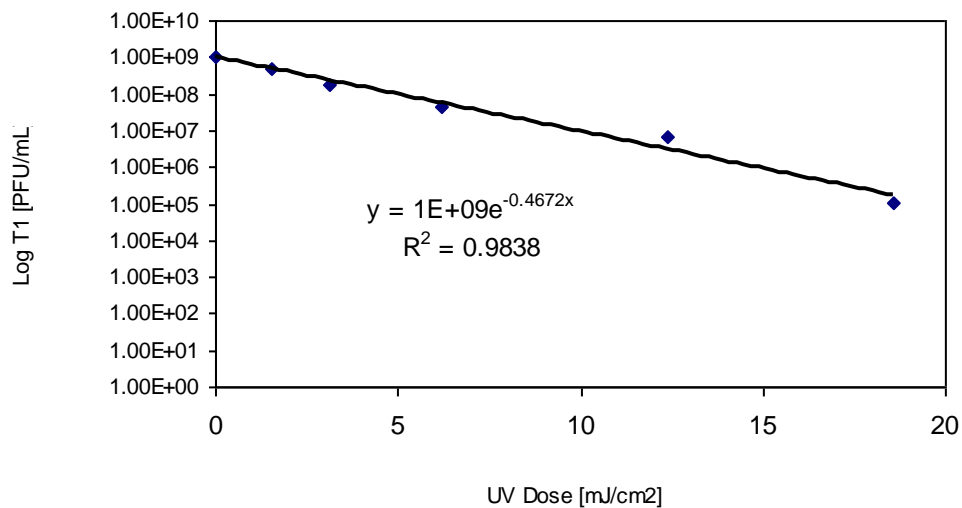


Figure 6-11:T1 Performance Curve for Walcan's Plant Effluent 2009

6.5 Target Microorganism Study

6.5.1 Determining the D_{10} of the Targeted Virus (IHNV)

Performing a collimated beam study on the targeted virus to determine its UV sensitivity is the first step in conducting a UV reactor validation study. The UV sensitivity (D_{10}) can be calculated as follows:

$$D_{10} = \frac{D_{CB}}{\text{Log } I} \quad (6-1)$$

Where:

D_{CB} : UV dose delivered by the collimated beam apparatus (mJ/cm^2)

$\text{Log } I$: Log inactivation of the microorganism observed with a UV dose of D_{CB} .

The Canadian Aquatic Health Sciences Centre performed testing on IHN and VHS viruses to estimate their resistance to UV disinfection. After a single set of experiments, they estimated that IHN and VHS viruses both had similar sensitivity. The dose per log, or D_{10} values were 1.9 for IHN, and 1.4 for VHS respectively Figure 6.12.

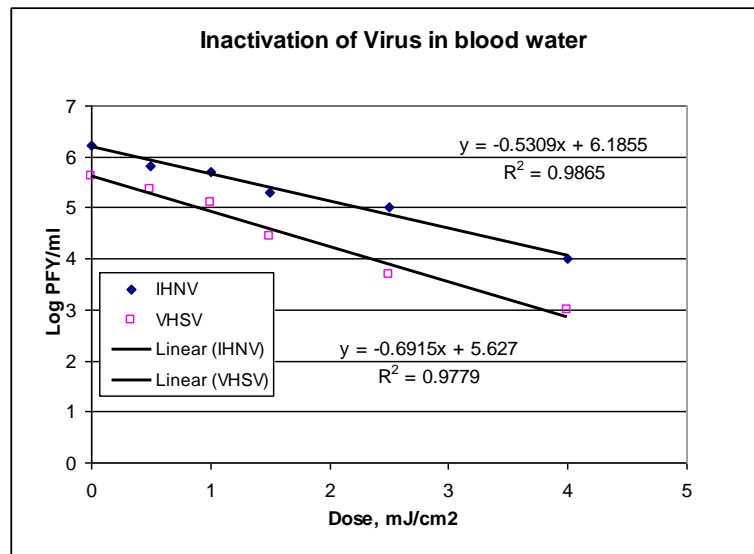


Figure 6-12: Dose-Response Curves for IHN and VHS Virus

6.5.2 Determining the Required Dose for the Treatment

The maximum concentration of IHN Virus was reported to be in the order of three logs by Garth Traxler, the researcher on IHN Virus at Pacific Biological Station-Fisheries and Oceans Canada. Thus, the required dose for 3-log reduction of IHN is approximately 6 mJ/cm².

6.5.3 Determining UV Dose–Response Curve of Test Microorganism

The log inactivation of a surrogate microorganism in a UV reactor is measured through lab analysis of the reactor inlet and outlet samples. A dose value termed as the reduction equivalent dose (RED), is then determined as the dose that achieve the same log inactivation in a collimated beam test.

Collimated beam testing was conducted to determine the D₁₀ of the test microorganism (T1). This test was done with Walcan’s effluent, and a control test was done with clean water. The control test showed a typical (for T1) linear dose response; however, the test with Walcan’s effluent showed a nonlinear dose response. This test was repeated and gave the same result Figure 6.13.

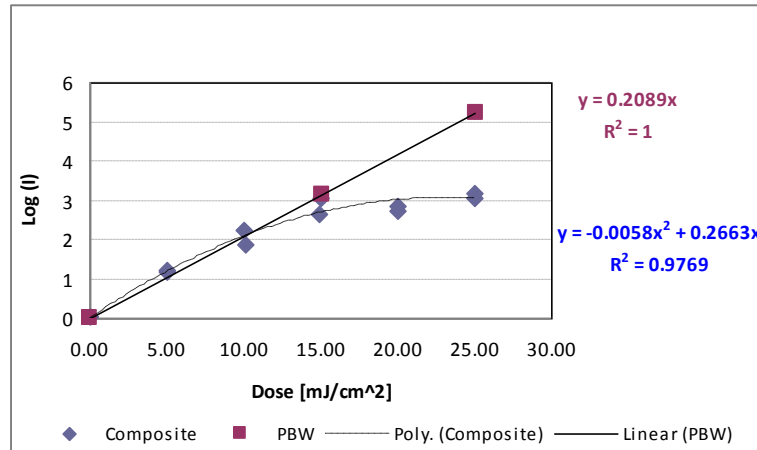


Figure 6-13:T1 Dose-Response Curves in Plant’s Effluent (“Composite”) and in Clean Water (“PBW”)

Previous experience with opaque fluids under a collimated beam test (CB) showed similar behavior when mixing is not sufficient or suspended materials are present in the fluid. An earlier (Figure 6.11-2009) (T1- CB) on the effluent, before the addition of the DAF system, showed a linear dose response, and so perhaps the nonlinear behavior is related to the presence of remaining DAF system chemicals. Since the T1 dose response was linear for up to 3 logs inactivation, and since there was less than 3 logs inactivation in the individual reactors, the linear model was used to calculate the RED for the reactor validation. The T1 dose response curve used in this work was obtained from a study in clean water Figure 13.

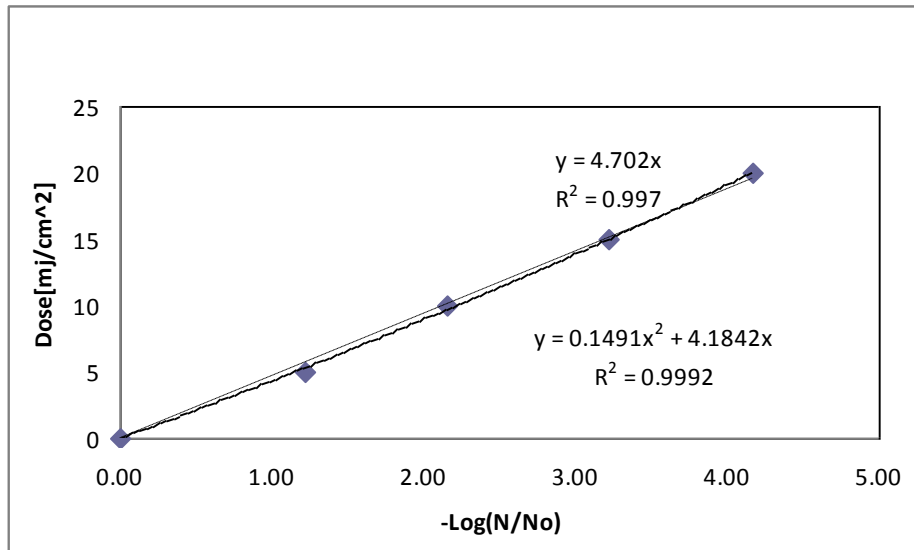


Figure 6-14:T1 Dose-Response Curve in Clean Water

6.5.4 Test Technical Details

In all the reactor tests, duration of three to five hydraulic retention times (HRTs, where one HRT is equal to the system volume divided by the volumetric flow rate) was allowed to pass, after the start of T1 injection, before samples were collected.

The flow rate for each test was measured by means of a bucket test in which the effluent was collected in a tank after exiting the reactors. The effluent piping was not changed between the bucket test and the performance test so that the flow rate would not be affected by a change in backpressure.

The (T1) dosing pump was connected to the inlet of the accelerating pump. All water samples were collected in triplicate.

6.5.5 Blank Test

A blank test was conducted with the UV lamps turned off to confirm that any disinfection in the UV reactors was a result of UV radiation only. Details of this test are in the Appendix C.

6.6 Short-Term Performance Test

The “short-term performance test” was designed to verify the flow rate at which the system should be operated to obtain the targeted dose. It was conducted with three flow rates (50, 75, and 100 gpm through train C). Samples were collected simultaneously at the inlet of the train and at each reactor outlet and from an additional downstream outlet after the sixth outlet to ensure good mixing downstream of the reactors, and thus good representation of the effluent.

The UV transmittance was kept almost constant during these three tests; it varied between 37 and 40 %/cm. The bundle slot size for this test was 0.4 mm.

6.7 Long-term performance test

The initial intent of the “long-term performance test” was to estimate the fouling rate of the lamp sleeves; the initial plan was for a 48-hour test with sampling every 2 hours from three locations. However, due to the huge fluctuation in the quality of water during the test, especially with regards to UV transmittance, it was decided to use the results of this test to study the effect of UV transmittance on the reactor disinfection

performance. The fouling study was conducted through direct measurement of the UV transmittance of the sleeves, as described later.

This test was conducted with two flow rates (50 gpm through train C and 84 gpm through train A; Figure 6.15). Samples were collected from each tested train at the inlet, the 3rd reactor outlet and 6th reactor outlet simultaneously.

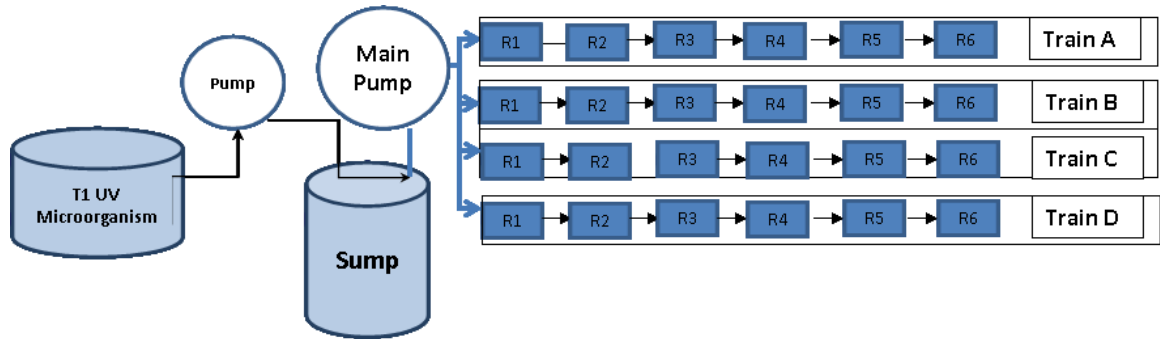


Figure 6-15:Schematic of Reactor Long-Term Test

The UV transmittance varied arbitrarily between 0 and 31.4 %/cm during the test, which was carried out for two days. The bundle slot width was 0.45 mm.

6.8 Results and Discussion

The T1 RED of the UV system was calculated from the following equation:

$$RED = a * \text{Log } I^2 + b * \text{Log } I \quad (6-2)$$

Where:

a, b: T1 Dose-Response curve coefficients determined from the clean water collimated beam test can be obtained from Figure 6.14.

Log I : Log inactivation of the challenge microorganism T1.

Note that although the T1 dose response was close to linear (in clean water), as mentioned earlier, a quadratic equation gave a slightly better fit to the data.

6.8.1 Short-Term Performance Test

The maximum delivered dose through the system was obtained for the flow rate of 50 gpm. A consistent increment in RED with reactor number was noticed except for outlets 5 & 6 for the 50 gpm flow rate; this latter observation is unexplained, but perhaps is related to clogging of the system.

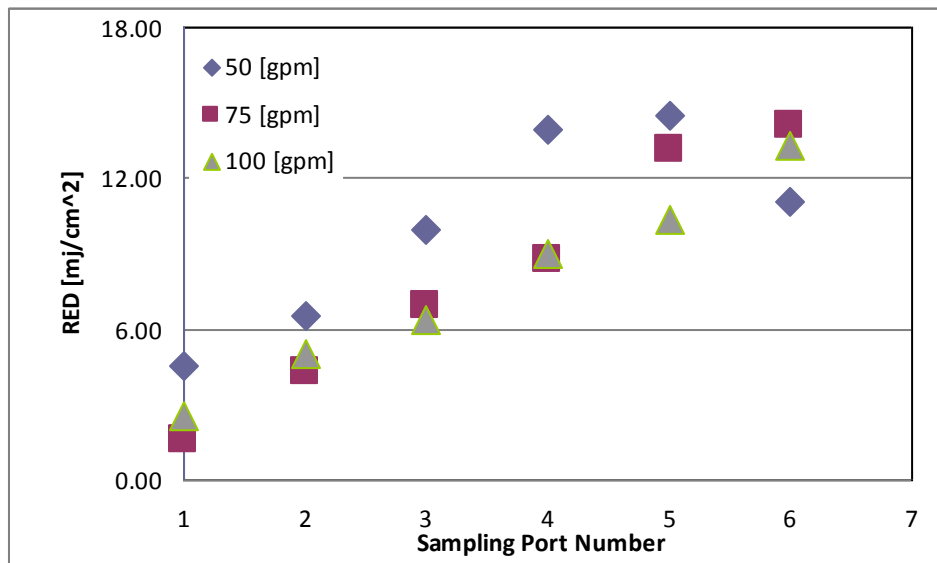


Figure 6-16:T1UV RED for 50, 75 & 100 gpm Flow Rates Measured at Six Outlets

6.8.2 Long-Term Performance Test

The delivered dose was calculated using equation 2. An important finding from this test was that the system was able to disinfect at very low UV transmittance (measured 0%/cm). In addition, as illustrated in Figures 16 & 17, the RED was higher at the lower flow rate, as expected.

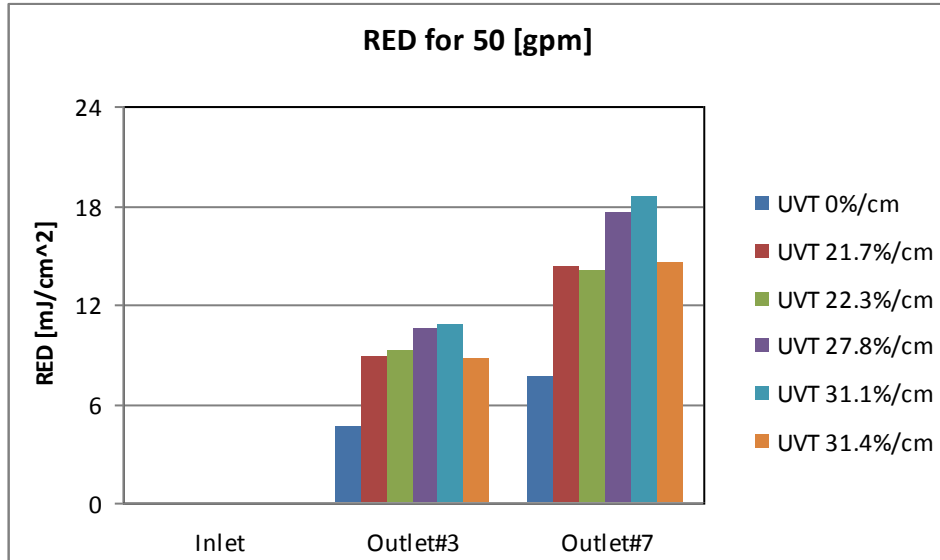


Figure 6-17:T1 RED for 50 gpm Flow Rate

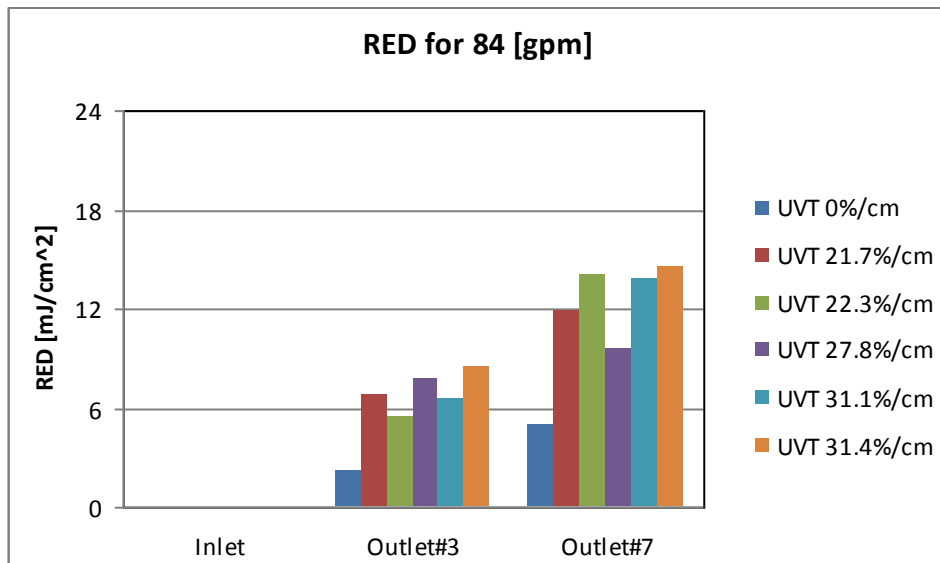


Figure 6-18:T1 RED for 84 gpm Flow Rate

6.9 Reactor Evaluation

In this part of our study we will quantify the UV dose delivery from multiple UV reactors in series. As part of this assessment, simulations results, which were performed on closed conduit reactors by Joel J. Ducoste, and Scott Alpert on reactors that were physically placed end to end or separated by a significant number of pipe diameters. Simulations were also performed with microorganisms that had different UV response kinetics. Results showed that UV dose delivery from multiple reactors in series may not consistently follow the sum of the individual UV dose delivered by each reactor. The results of the numerical simulations suggest that the summation of UV dose delivery from multiple reactors in series can only be achieved when sufficient mixing is accomplished upstream from each subsequent individual reactor.

Dr. Ducoste simulations show that for a microorganism with an inactivation rate constant of $(0.53 \text{ m}^2/\text{J}/\log I)$ the second reactor is expected to deliver 38% or 123% dose in case of no mixing is taking place between the reactors or enough mixing was taking place before the effluent of the first reactor enters the second reactor.

Table 6-1:: Log Inactivation

		Successive Reactors Disinfection Ratio					
Flow Rate gpm		R1	R2	R3	R4	R5	R6
50	Log(I)	3.07	3.29	3.67	N/A	3.51	3.42
	Ractor# n/Ractor #1	1.00	1.07	1.20	N/A	1.15	1.12

Table 6.1 indicate that our design was cable of continuously achieves higher log inactivation in every successive reactor in compare with the previous one. The explanation of table results was related to the parameters that impact the UV dose additive nature of multiple UV reactors in series.

As we provide mixing between reactors, disruption of effluent trajectories of microorganism will take place in between leaving previous reactor and entering second

one. Consequently, each successive UV reactor will be able to behave independently and more efficiently in terms of its ability to inactivate influent microorganisms.

6.10 Conclusions

1. Disinfection of very low transmittance fluid was achieved through impinging Jet reactor on commercial level.
2. Mixing was proved to be sufficient in impinging jet reactor.
3. Efficiency of very low transmittance fluids was calculated after neutralization of UV transmittance of the fluid .

6.11 References

Ducoste, J. J., Alpert, S., Assessing the UV Dose Delivered from Two UV Reactors in Series: Can You Always Assume Doubling the UV Dose from Individual Reactor Validations? Wef Proceedings (2009).

Fisheries and Oceans Canada <http://www.dfo-po.gc.ca/aquaculture/sustainable-durable/rapports-reports/2009-P26-eng.htm>

Gavi, E., Marchisio, D. L., Barresi A. A., CFD modelling and scale-up of confined Impinging Jet reactor, Chemical Engineering Science, 62 ,pp. 2228-2241 (2007).

Lior, N., Zuckerman, N., Heat transfer and Temperature distributions in the Fluid and Cooling Cylindrical Solid During radial Slot Jet Impingement Cooling. <http://www.seas.upenn.edu/~lior/documents/Heattransferandtemperatureristributioninthefluidandcooledcylindricalsolidduringradialslotjet.pdf>.

Olsson, E. E. M., Ahrne, L.M., Tragardh, A.C., Heat Transfer from a slot air jet on a circular cylinder , Journal of Food Engineering, 63, 4 ,pp. 393-401 (2004).

Puma, G. L., Dimensional Analysis of Photocatalytic reactors using Suspended Solid Photocatalysis , Chemical Engineering Research and Design, 83(A3) ,pp. 820-826 (2005).

Zhao, J.,Khayat R., Spread of non-Newtonian liquid jet over a horizontal plate , Journal of Fluid Mechanics, 613 ,pp. 411-443 (2008).

Chapter 7

Conclusions and Recommendations

Ultraviolet (UV) disinfection has been widely applied for drinking water and wastewater treatments because of its effective inactivation of many waterborne pathogens and its minimal formation of disinfection by-products. This Ph.D. dissertation illustrates a research study on the application of ultraviolet light photolysis for disinfection of very low UV transmittance (opaque) fluids such as milk and blood water.

All UV disinfection systems need validation to ensure their inactivation performances meet the regulation requirements. The most implemented method for validation is biosimetry, which involves bioassay to yield a simplified UV dose value. This dose value is called reduction equivalent dose (RED). However, RED depends on not only the performance of the reactor but also the UV sensitivity of the type of microorganisms used in the test. First, it was found that two UV absorbers (para Hydroxybenzoic acid (pHBA) and Super Hume) were capable of surviving complete set of tests. pHBA showed minimum scattering effects compared to Super Hume. However, Super Hume was best with respect to all other tests. The scattering of the low transmittance fluids for collimated beam played minor role in generating light gradient compared to the absorption. Proper mixing under Collimated was considered in light of combining the fluid hydraulics with the light gradient, the matter that brought wider concept than traditional mass mixing of fluids. It was found that pulsed irradiation was capable of delivering UV dose with narrower distribution.

Dimensional analysis technique was used to identify different dimensionless groups to reduce the number of parameters governing the disinfection of opaque fluids with UV light irradiation. Key parameters were determined that influence disinfection of very low transmittance fluids. The quality of the mixing, which is an essential component in the disinfection of opaque fluid process, was measured through reduction equivalent dose using two different UV sensitivity model microorganisms. The reduction equivalent

dose (RED) simulated results were validated with experimental results throughout our studies for all different reactors (Petri dish, Taylor Couette and Impinging Jet) considered in this study.

7.1 Major Contributions

The following are the significant contributions of this research study

- ❑ Experimental as well as simulation studies show that both laboratory scale as well as commercial scale reactor systems considered are capable of disinfecting fluids with very low UV transmittance.
- ❑ It was found that in addition to importance of ultraviolet light irradiation, mixing is an essential component in UV disinfection treatment system.
- ❑ It was shown with all three different scale reactor application (Petri dish, Taylor Couette reactor, and impinging jet reactor) that alternating between mixing and exposure to UV light is a necessary condition to get minimum dose distribution for efficient performance.
- ❑ We were able to identify the conditions which make collimated beam studies on fluids with low UV transmittance reliable.
- ❑ Role of penetration depth of UV light was established through classical Taylor Couette reactor.
- ❑ In order to overcome the mass transfer limitation, wavy wall Taylor Couette reactor was designed which utilized the formation of Taylor Couette vortices and its interaction to optimize the performance of classical Taylor Couette reactor.
- ❑ Underlying illuminated zone always existed in the very low UV transmittance fluids compared to the UV light source.

7.2 Other Key Contributions

- ❑ The development of the application of dimensional analysis technique was found out to be valuable to be applied in different physical industrial process. This method provided a quantitative assessment of the principal parameters in reduced numbers that influence the process under consideration.
- ❑ The development and characterization of the UV absorbers to be used for the animation of fluids with very low UV transmittance is an important addition to the validation of UV reactors especially when medium pressure lamps are used.
- ❑ The existence of thin illuminated zone at the edge of the quartz sleeves for impinging jet reactor was proved to be vital in UV disinfection application.

7.3 Recommendations for Future Work

Following are the recommendations for further studies:

- ❖ Wavy wall Taylor Couette reactor is going to be built to compare its performance with straight wall one and experimental validation with the simulated data as well.
- ❖ System of Impinging Jet reactor performance is needed to be tested with two or more microorganisms spiked together at the same time.
- ❖ Disinfection model of fluid with very low UV transmittance is possible to be developed once enough experimental data are collected.

APPENDIX

A. Appendix A: Dimensional Analysis of Annular Reactor

Table A.1: Reynolds' Number Designed Cases

Reynolds Number effects	Case Number				
Variables	1	2	3	4	5
Density	5.00E+02	5.00E+02	5.00E+02	5.00E+02	5.00E+02
Dynamic Viscosity	2.00E-03	2.00E-03	2.00E-03	2.00E-03	2.00E-03
Volumetric Flow Rate	1.00E-04	5.00E-04	1.00E-03	5.00E-03	1.00E-02
Inner Radius	5.00E-01	5.00E-01	5.00E-01	5.00E-01	5.00E-01
Outer Radius	6.00E-01	6.00E-01	6.00E-01	6.00E-01	6.00E-01
Reactor Length	1.00E+00	1.00E+00	1.00E+00	1.00E+00	1.00E+00
Absorption Coeff.	1.00E+02	1.00E+02	1.00E+02	1.00E+02	1.00E+02
Scattering Coeff.	1.00E+02	1.00E+02	1.00E+02	1.00E+02	1.00E+02
Lamp power	8.00E+00	4.00E+01	8.00E+01	4.00E+02	8.00E+02
Inactivation Rate constant1	1.00E-02	1.00E-02	1.00E-02	1.00E-02	1.00E-02
Inactivation Rate constant2	5.00E-03	5.00E-03	5.00E-03	5.00E-03	5.00E-03
Gap	1.00E-01	1.00E-01	1.00E-01	1.00E-01	1.00E-01
Cross section area	3.46E-01	3.46E-01	3.46E-01	3.46E-01	3.46E-01

Reactor Volume	3.46E-01	3.46E-01	3.46E-01	3.46E-01	3.46E-01
Residence time1	3.46E+03	6.91E+02	3.46E+02	6.91E+01	3.46E+01
Aver. Velocity	2.89E-04	1.45E-03	2.89E-03	1.45E-02	2.89E-02
Surface Area	3.14E+00	3.14E+00	3.14E+00	3.14E+00	3.14E+00
Boundary Intensity(Fluence Rate)	2.55E+00	1.27E+01	2.55E+01	1.27E+02	2.55E+02
Volumetric average Intensity	2.31E-01	1.16E+00	2.31E+00	1.16E+01	2.31E+01
Mass flow rate	5.00E-02	2.50E-01	5.00E-01	2.50E+00	5.00E+00
Reynolds Number	1.45E+01	7.23E+01	1.45E+02	7.23E+02	1.45E+03
Lamp Aspect Ratio	5.00E+00	5.00E+00	5.00E+00	5.00E+00	5.00E+00
Absorption Thickness	1.00E+01	1.00E+01	1.00E+01	1.00E+01	1.00E+01
Scattering Thickness	1.00E+01	1.00E+01	1.00E+01	1.00E+01	1.00E+01
Specific Dose	9.09E-02	9.09E-02	9.09E-02	9.09E-02	9.09E-02
UV Power	1.25E-01	1.25E-01	1.25E-01	1.25E-01	1.25E-01

Table A.2: Lamp Aspect Ratio Designed Cases

Lamp Aspect Ratio	Case Number				
	1	2	3	4	5
Variables	1.00E+00	2.00E+00	3.00E+00	4.00E+00	5.00E+00
Density	5.00E+02	5.00E+02	5.00E+02	5.00E+02	5.00E+02
Dynamic Viscosity	2.00E-03	2.00E-03	2.00E-03	2.00E-03	2.00E-03
Volumetric Flow Rate	1.00E-03	1.00E-03	1.00E-03	1.00E-03	1.00E-03
Inner Radius	5.00E-01	6.00E-01	7.00E-01	8.00E-01	9.00E-01
Outer Radius	6.00E-01	7.00E-01	8.00E-01	9.00E-01	1.00E+00
Reactor Length	1.00E+00	1.00E+00	1.00E+00	1.00E+00	1.00E+00
Absorption Coeff.	1.00E+02	1.00E+02	1.00E+02	1.00E+02	1.00E+02
Scattering Coeff.	1.00E+02	1.00E+02	1.00E+02	1.00E+02	1.00E+02
Lamp power	8.00E+00	8.00E+00	8.00E+00	8.00E+00	8.00E+00
Inactivation Rate constant1	1.00E-02	1.00E-02	1.00E-02	1.00E-02	1.00E-02
Inactivation Rate constant2	5.00E-03	5.00E-03	5.00E-03	5.00E-03	5.00E-03
Gap	1.00E-01	1.00E-01	1.00E-01	1.00E-01	1.00E-01
Cross section area	3.46E-01	4.08E-01	4.71E-01	5.34E-01	5.97E-01

Reactor Volume	3.46E-01	4.08E-01	4.71E-01	5.34E-01	5.97E-01
Residence time1	3.46E+02	4.08E+02	4.71E+02	5.34E+02	5.97E+02
Aver. Velocity	2.89E-03	2.45E-03	2.12E-03	1.87E-03	1.68E-03
Surface Area	3.14E+00	3.77E+00	4.40E+00	5.03E+00	5.65E+00
Boundary Intensity(Fluence Rate)	2.55E+00	2.12E+00	1.82E+00	1.59E+00	1.41E+00
Volumetric average Intensity	2.31E-01	1.96E-01	1.70E-01	1.50E-01	1.34E-01
Mass flow rate	5.00E-01	5.00E-01	5.00E-01	5.00E-01	5.00E-01
Dimensionless Group					
Reynolds Number	1.45E+02	1.22E+02	1.06E+02	9.36E+01	8.38E+01
Lamp Aspect Ratio	5.00E+00	6.00E+00	7.00E+00	8.00E+00	9.00E+00
Absorption Thickness	1.00E+01	1.00E+01	1.00E+01	1.00E+01	1.00E+01
Scattering Thickness	1.00E+01	1.00E+01	1.00E+01	1.00E+01	1.00E+01
Specific Dose	9.09E-02	9.23E-02	9.33E-02	9.41E-02	9.47E-02
UV Power	1.25E+00	1.25E+00	1.25E+00	1.25E+00	1.25E+00

Table A.3: Absorption Thickness Designed Cases

Absorption Thickness	Case Number			
Variables	1	2	3	4
Density	1.00E+03	5.00E+02	1.00E+02	5.00E+02
Dynamic Viscosity	1.00E-03	2.00E-04	2.00E-04	2.00E-04
Volumetric Flow Rate	5.00E-04	1.00E-03	5.00E-04	1.00E-03
Inner Radius	1.00E-01	5.00E-01	5.00E-02	5.00E-01
Outer Radius	1.10E-01	5.50E-01	5.50E-02	5.50E-01
Reactor Length	1.00E+00	1.00E+00	2.00E+00	2.00E+00
Absorption Coeff.	5.00E+01	2.00E+01	3.00E+02	4.00E+01
Scattering Coeff.	1.00E+02	2.00E+01	2.00E+02	2.00E+01
Lamp power	4.00E+01	1.60E+02	8.00E+02	1.60E+02
Inactivation Rate constant1	1.00E-02	1.00E-03	1.00E-03	1.00E-03
Inactivation Rate constant2	5.00E-03	5.00E-04	5.00E-04	5.00E-04
Gap	1.00E-02	5.00E-02	5.00E-03	5.00E-02
Cross section area	6.60E-03	1.65E-01	1.65E-03	1.65E-01
Reactor Volume	6.60E-03	1.65E-01	3.30E-03	3.30E-01
Residence time1	1.32E+01	1.65E+02	6.60E+00	3.30E+02

Aver. Velocity	7.58E-02	6.06E-03	3.03E-01	6.06E-03
Surface Area	6.28E-01	3.14E+00	6.28E-01	6.28E+00
Boundary Intensity(Fluence Rate)	6.37E+01	5.09E+01	1.27E+03	2.55E+01
Volumetric average Intensity	4.77E+01	3.07E+01	6.28E+02	1.05E+01
Mass flow rate	5.00E-01	5.00E-01	5.00E-02	5.00E-01
Dimensionless Group				
Reynolds Number	1.52E+03	1.52E+03	1.52E+03	1.52E+03
Lamp Aspect Ratio	1.00E+01	1.00E+01	1.00E+01	1.00E+01
Absorption Thickness	5.00E-01	1.00E+00	1.50E+00	2.00E+00
Scattering Thickness	1.00E+00	1.00E+00	1.00E+00	1.00E+00
Specific Dose	1.90E+00	9.52E-01	6.35E-01	4.76E-01
UV Power	6.25E-02	1.25E-01	1.88E-01	2.50E-01

Table A.4:UV Power designed Cases

UV Power	Case Number				
Variables	1	2	3	4	5
Density	1.00E+03	1.00E+03	1.00E+03	1.00E+03	1.00E+03
Dynamic Viscosity	1.00E-03	1.00E-03	1.00E-03	1.00E-03	1.00E-03
Volumetric Flow Rate	1.00E-03	1.00E-03	1.00E-03	1.00E-03	1.00E-03
Inner Radius	5.00E-01	5.00E-01	5.00E-01	5.00E-01	5.00E-01
Outer Radius	6.00E-01	6.00E-01	6.00E-01	6.00E-01	6.00E-01
Reactor Length	1.00E+00	1.00E+00	1.00E+00	1.00E+00	1.00E+00
Absorption Coeff.	1.00E+02	1.00E+02	1.00E+02	1.00E+02	1.00E+02
Scattering Coeff.	1.00E+02	1.00E+02	1.00E+02	1.00E+02	1.00E+02
Lamp power	1.00E+01	2.00E+01	3.00E+01	4.00E+01	5.00E+01
Inactivation Rate constant1	1.00E-02	1.00E-02	1.00E-02	1.00E-02	1.00E-02
Inactivation Rate constant2	5.00E-03	5.00E-03	5.00E-03	5.00E-03	5.00E-03
Gap	1.00E-01	1.00E-01	1.00E-01	1.00E-01	1.00E-01
Cross section area	3.46E-01	3.46E-01	3.46E-01	3.46E-01	3.46E-01
Reactor Volume	3.46E-01	3.46E-01	3.46E-01	3.46E-01	3.46E-01
Residence time1	3.46E+02	3.46E+02	3.46E+02	3.46E+02	3.46E+02
Aver. Velocity	2.89E-03	2.89E-03	2.89E-03	2.89E-03	2.89E-03

Surface Area	3.14E+00	3.14E+00	3.14E+00	3.14E+00	3.14E+00
Boundary Intensity(Fluence Rate)	3.18E+00	6.37E+00	9.55E+00	1.27E+01	1.59E+01
Volumetric average Intensity	2.89E-01	5.79E-01	8.68E-01	1.16E+00	1.45E+00
Mass flow rate	1.00E+00	1.00E+00	1.00E+00	1.00E+00	1.00E+00
Dimensionless Group					
Reynolds Number	5.79E+02	5.79E+02	5.79E+02	5.79E+02	5.79E+02
Lamp Aspect Ratio	5.00E+00	5.00E+00	5.00E+00	5.00E+00	5.00E+00
Absorption Thickness	1.00E+01	1.00E+01	1.00E+01	1.00E+01	1.00E+01
Scattering Thickness	1.00E+01	1.00E+01	1.00E+01	1.00E+01	1.00E+01
Specific Dose	9.09E-02	9.09E-02	9.09E-02	9.09E-02	9.09E-02
UV Power	1.00E+00	5.00E-01	3.33E-01	2.50E-01	2.00E-01

B. Appendix B: Taylor Couette Reactor

B.1 Case Designs Two Different Dimensional Designs with Identical PI Groups

Variables	Case Number	
	1	2
Density	1.00E+03	1.00E+02
Dynamic Viscosity	1.00E-03	2.00E-04
Volumetric Flow Rate	5.00E-04	5.00E-04
Inner Radius	1.00E-01	5.00E-02
Outer Radius	1.10E-01	5.50E-02
Reactor Length	1.00E+00	2.00E+00
Absorption Coeff.	1.00E+02	2.00E+02
Scattering Coeff.	1.00E+02	2.00E+02
Lamp power	4.00E+01	8.00E+02
Inactivation Rate constant1	1.00E-02	1.00E-03
Inactivation Rate constant2	5.00E-03	5.00E-04
Gap	1.00E-02	5.00E-03

Cross section area	6.60E-03	1.65E-03
Reactor Volume	6.60E-03	3.30E-03
Residence time1	1.32E+01	6.60E+00
Aver. Velocity	7.58E-02	3.03E-01
Surface Area	6.28E-01	6.28E-01
Boundary Intensity(Fluence Rate)	6.37E+01	1.27E+03
Volumetric average Intensity	3.83E+01	7.67E+02
Mass flow rate	5.00E-01	5.00E-02
Omega	1.31E+00	1.05E+01
r.p.m	1.25E+01	1.00E+02
Reynolds Number	1.52E+03	1.52E+03
Lamp Aspect Ratio	1.00E+01	1.00E+01
Absorption Thickness	1.00E+00	1.00E+00
Scattering Thickness	1.00E+00	1.00E+00
Specific Dose	9.52E-01	9.52E-01
UV Power	1.25E-01	1.25E-01
Ta	4.14E+02	4.14E+02

B.2 Disinfection Results

Design	Design	Microbs Inlet Count	Dose	Microb#1 outlet count	Microb#2 outlet count	Log(l) Microb#1	Log(l) Microb#2	Total disinfection
1	1	1.00E+08	5.98E+03	4.56E+06	1.79E+07	1.34E+00	7.47E-01	9.49E-01
2	2	1.00E+08	5.98E+03	4.67E+06	1.82E+07	1.33E+00	7.41E-01	9.43E-01

B.3 Milk Disinfection Test with Taylor Couette Reactor



Raw Milk



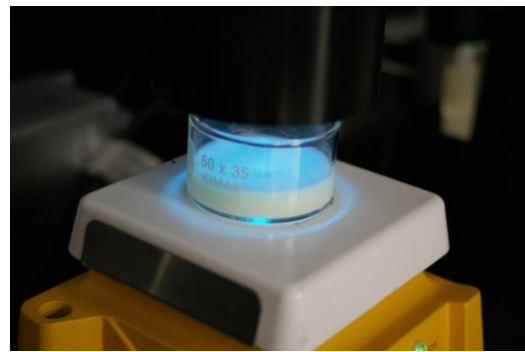
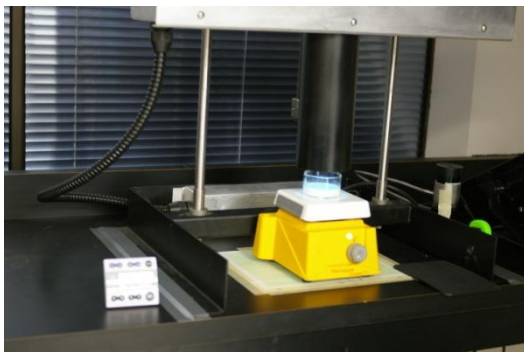
Pasteurized



Mixing tank for TC Reactor



TC reactor set up



Collimated beam test



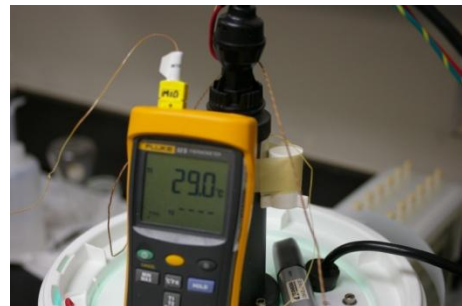
Collimated beam test



PMF Reactor_1



PMF Reactor_2



PMF Reactor_3

PMF Reactor_4

B.4 UVT measurements' with integrating sphere

UVT	Pasteurized Milk with MS2 & T1				
	Path Length Cm	Absorbance	Abs. Coeff./cm	UVT	UVT%
	0	0			
	0.01	0.12725	12.725	1.9E-13	1.9E-11
	1				1.88E-10
UVT	Raw Milk with MS2 & T1				
	Path Length Cm	Absorbance	Abs. Coeff./cm	UVT	UVT%
	0	0			
	0.01	0.126	12.6	2.5E-13	2.5E-11
	1				2.51E-10

C. Appendix C: Impinging Jet Validation test

C.1 Blank Test

A blank test was conducted with the UV lamps turned off to confirm that any disinfection in the UV reactors was a result of UV radiation only. T1UV was injected as during the performance testing, and samples were collected from three positions (inlet, reactor #3 outlet and additional outlet #7 downstream of reactor #6 outlet), in triplicate.

A statistical analysis was done to confirm the similarity of the results:

$$\mu_{inlet} - \mu_{Outlet} = 0 \text{ (Null hypothesis)}$$

$$s_p^2 = \frac{(n_{Inlet} - 1)STDEV_{Inlet}^2 + (n_{Outlet} - 1)STDEV_{Outlet}^2}{(n_{Inlet} - 1) + (n_{Outlet} - 1)}$$

$$T = \frac{(Average_{Inlet} - Average_{Outlet})}{\sqrt{s_p^2 \left(\frac{1}{n_{Inlet}} + \frac{1}{n_{Outlet}} \right)}}$$

Blank Test

Log(Inlet Concentration [pfu/ml])	Log(Outlet#3 Concentration [pfu/ml])	Log(Outlet#7 Concentration [pfu/ml])
5.86	5.98	5.96
5.87	5.97	5.85
5.94	5.85	5.72

Average	5.89	5.93	5.84
STDEV	0.042	0.072	0.117

Null Hypothesis Results

	Inlet & Outlet#3	Inlet & Outlet#7
s_p^2	0.0035	0.0078
T	-0.898	0.664

Since the T value, for both outlets, is well within the 5% significance level bounds, the null hypothesis is justified, and so no significant difference was detected between the inlet and either outlet. The following statements are therefore confirmed:

- No disinfection was detected in the reactors in the absence of UV radiation.
- The mixing of T1UV between the injection port and the reactor inlet was sufficient to produce representative results. (A difference in T1UV concentration, between the reactor inlet and outlet, would have been an indication of insufficient mixing).

C.2 RED Bias Factor

If the UV sensitivities of the challenge microorganism and target pathogen are not the same, the RED delivered under the same reactor operating conditions will differ. The RED bias is a correction factor that accounts for the difference between the UV sensitivity of the target pathogen and of the challenge microorganism.

The magnitude of the RED bias depends on the following factors:

- The dose distribution of the UV reactor
- The difference between the inactivation kinetics of the challenge microorganism and the target pathogen.

If the challenge microorganism is more resistant to UV light than the target pathogen, the RED measured during validation will be *greater* than the RED that would be measured for the target pathogen. In this case, the RED bias would be greater than 1.0. If the challenge microorganism is less resistant (more sensitive) to UV light than the target pathogen, the RED measured during validation will be *less*

than the RED that would be measured for the target pathogen. In this case, the RED bias should be assigned a value of 1.0.

Validation testing is sometimes performed using two challenge microorganisms whose UV sensitivities bracket those of the target pathogen (i.e., one challenge microorganism is less resistant than the target pathogen and the other is more resistant than the target pathogen).

C.3 Dimensional Variables IJ reactor

Impinging Jet – Variables (All)

	Variables	Symbols	Dimensions	Units
1	Slot size	S	m	L
2	Jet Gap	δ	m	L
3	Jet Specific Width	w	m	L
4	Chamber Depth	R_o	m	L
5	Reactor Length	Z	m	L
6	Absorption Coeff.	α	m⁻¹	L⁻¹
7	Scattering Coeff.	σ	m⁻¹	L⁻¹
8	Scattering anisotropy.	g	-	
9	UV Power	P_{UV}	Kg m² sec⁻³	M L² T⁻³
10	Fast Inactivation Rate	K_d	Sec² Kg⁻¹	T² M⁻¹
11	Slow Inactivation Rate	K_p	Sec² Kg⁻¹	T² M⁻¹
12	Free Microbial Conc.	N_d	Counts /m³	Counts /L³
13	Microbial Conc. In Particles	N_p	Counts /m³	Counts /L³
14	Dynamic Viscosity	μ	Kg m⁻¹ Sec⁻¹	M L⁻¹ T⁻¹
15	Density	ρ	Kg m⁻³	M L⁻³
16	Volumetric flow rate	Q	m³ Sec⁻¹	L³ T⁻¹

C.4 Tanks Connections



Reactor Trains A, C Exits.



Reactor Trains A, C Exit Connections at the Flow Rate Measuring Tank.

C.5 Dimensional Groups

<p>Impinging Jet – Systems of Equations</p> $\Pi_n = R_i Q \rho N_d (\text{Dimensional Variable})_n$ $\Pi_n = [L]^a \left[\frac{L^3}{T} \right]^b \left[\frac{M}{L^3} \right]^c \left[\frac{\text{Count}}{L^3} \right]^d (\text{Unit})$ $[L]^a \left[\frac{L^3}{T} \right]^b \left[\frac{M}{L^3} \right]^c \left[\frac{\text{Count}}{L^3} \right]^d (\text{Unit}) = M^0 L^0 T^0 \text{Count}^0$	<p>Impinging Jet – Systems of Equations</p> $\Pi_1 = S Q \rho N_d (\delta)$ $\begin{cases} [M]: c = 0 \\ [L]: a + 3b - 3c - 3d + 1 = 0 \\ [T]: -b = 0 \\ [\text{Counts}]: d = 0 \end{cases} \implies a = -1$ $\Pi_1 = S Q^0 \rho^0 N_d^0 \delta = \delta / S$	<p>Impinging Jet – Systems of Equations</p> $\Pi_2 = S Q \rho N_d (w)$ $\begin{cases} [M]: c = 0 \\ [L]: a + 3b - 3c - 3d + 1 = 0 \\ [T]: -b = 0 \\ [\text{Counts}]: d = 0 \end{cases} \implies a = -1$ $\Pi_2 = S Q^0 \rho^0 N_d^0 w = w / S$
<p>Impinging Jet – Systems of Equations</p> $\Pi_3 = S Q \rho N_d (R_o)$ $\begin{cases} [M]: c = 0 \\ [L]: a + 3b - 3c - 3d + 1 = 0 \\ [T]: -b = 0 \\ [\text{Counts}]: d = 0 \end{cases} \implies a = -1$ $\Pi_3 = S Q^0 \rho^0 N_d^0 R_o = R_o / S$	<p>Impinging Jet – Systems of Equations</p> $\Pi_4 = S Q \rho N_d (z)$ $\begin{cases} [M]: c = 0 \\ [L]: a + 3b - 3c - 3d + 1 = 0 \\ [T]: -b = 0 \\ [\text{Counts}]: d = 0 \end{cases} \implies a = -1$ $\Pi_4 = S Q^0 \rho^0 N_d^0 z = z / S$	<p>Impinging Jet – Systems of Equations</p> $\Pi_5 = S Q \rho N_d (\alpha)$ $\begin{cases} [M]: c = 0 \\ [L]: a + 3b - 3c - 3d - 1 = 0 \\ [T]: -b = 0 \\ [\text{Counts}]: d = 0 \end{cases} \implies a = 1$ $\Pi_5 = S Q^0 \rho^0 N_d^0 \alpha = \alpha / S$
<p>Impinging Jet – Systems of Equations</p> $\Pi_6 = S Q \rho N_d (\sigma)$ $\begin{cases} [M]: c = 0 \\ [L]: a + 3b - 3c - 3d - 1 = 0 \\ [T]: -b = 0 \\ [\text{Counts}]: d = 0 \end{cases} \implies a = 1$ $\Pi_6 = S Q^0 \rho^0 N_d^0 \sigma = \sigma / S$	<p>Impinging Jet – Systems of Equations</p> $\Pi_7 = S Q \rho N_d (P_{UV})$ $\begin{cases} [M]: c + 1 = 0 \\ [L]: a + 3b - 3c - 3d + 2 = 0 \\ [T]: -b - 3 = 0 \\ [\text{Counts}]: d = 0 \end{cases} \implies \begin{matrix} a = 4 \\ b = -3 \\ c = -1 \end{matrix}$ $\Pi_7 = S^4 Q^{-3} \rho^{-1} N_d^0 P_{UV} = \frac{P_{UV} \cdot S^4}{\rho \cdot Q^3}$	<p>Impinging Jet – Systems of Equations</p> $\Pi_8 = S Q \rho N_d (K_d)$ $\begin{cases} [M]: c - 1 = 0 \\ [L]: a + 3b - 3c - 3d = 0 \\ [T]: -b + 2 = 0 \\ [\text{Counts}]: d = 0 \end{cases} \implies \begin{matrix} a = -3 \\ b = 2 \\ c = 1 \end{matrix}$ $\Pi_8 = S^{-3} Q^2 \rho^1 N_d^0 K_d = \frac{\rho \cdot K_d \cdot Q^2}{S^3}$
<p>Impinging Jet – Systems of Equations</p> $\Pi_9 = S Q \rho N_d (K_p)$ $\begin{cases} [M]: c - 1 = 0 \\ [L]: a + 3b - 3c - 3d = 0 \\ [T]: -b + 2 = 0 \\ [\text{Counts}]: d = 0 \end{cases} \implies \begin{matrix} a = -3 \\ b = 2 \\ c = 1 \end{matrix}$ $\Pi_9 = S^{-3} Q^2 \rho^1 N_d^0 K_p = \frac{\rho \cdot K_p \cdot Q^2}{S^3}$	<p>Impinging Jet – Systems of Equations</p> $\Pi_{10} = S Q \rho N_d (N_p)$ $\begin{cases} [M]: c = 0 \\ [L]: a + 3b - 3c - 3d - 3 = 0 \\ [T]: -b = 0 \\ [\text{Counts}]: d + 1 = 0 \end{cases} \implies \begin{matrix} a = 0 \\ d = -1 \end{matrix}$ $\Pi_{10} = S^0 Q^0 \rho^0 N_d^{-1} N_p = \frac{N_p}{N_d}$	<p>Impinging Jet – Systems of Equations</p> $\Pi_{11} = S Q \rho N_d (\mu)$ $\begin{cases} [M]: c + 1 = 0 \\ [L]: a + 3b - 3c - 3d - 1 = 0 \\ [T]: -b - 1 = 0 \\ [\text{Counts}]: d = 0 \end{cases} \implies \begin{matrix} a = 1 \\ b = -1 \\ c = -1 \end{matrix}$ $\Pi_{11} = S^1 Q^{-1} \rho^{-1} N_d^0 \mu = \frac{\mu \cdot S}{\rho \cdot Q}$

C.6 Mixing effect Joel J. Ducoste, Scott Alpert simulation

Assessing the UV Dose Delivered from Two UV Reactors in Series

Monte Carlo Simulations First order microbial rate, k	Two reactors in series				
	Reactor 1 RED(1)	0% mixing Ratio		100% mixing Ratio	
		RED(2)	RED(2)/RED(1)	RED(2')	RED(2')/RED(1)
0.001	43.5	82.7	1.90	86.9	2.0
0.064	35.8	61.4	1.72	72.4	2.02
0.1	33	54.5	1.65	67	2.03
0.2	27.8	41.8	1.50	56.6	2.04
0.4	21.4	29.6	1.38	45.4	2.12
0.53	18.7	25.8	1.38	41.7	2.23
1	13.7	19.9	1.45	35.9	2.62
5	8.4	14.4	1.71	30.4	3.62
10	7.7	13.7	1.78	29.7	3.86
20	7.4	13.3	1.80	29.3	3.96

Joel J. Ducoste, and Scott Alpert
Can You Always Assume Doubling the UV Dose from Individual Reactor Validations?"
IUVA September 2011

C.7 Reactor Efficiency

The role of the UV transmittance was neutralized through comparing the available energy for disinfection after disregarding the absorbed portion by the fluids the matter which made us eliminated the residence time within the reactor and consider only small volume close to the lamp were the disinfection is taking place. The impinging jet reactor was compared with ideal reactor (PFR) and the results shown in figure E.7.

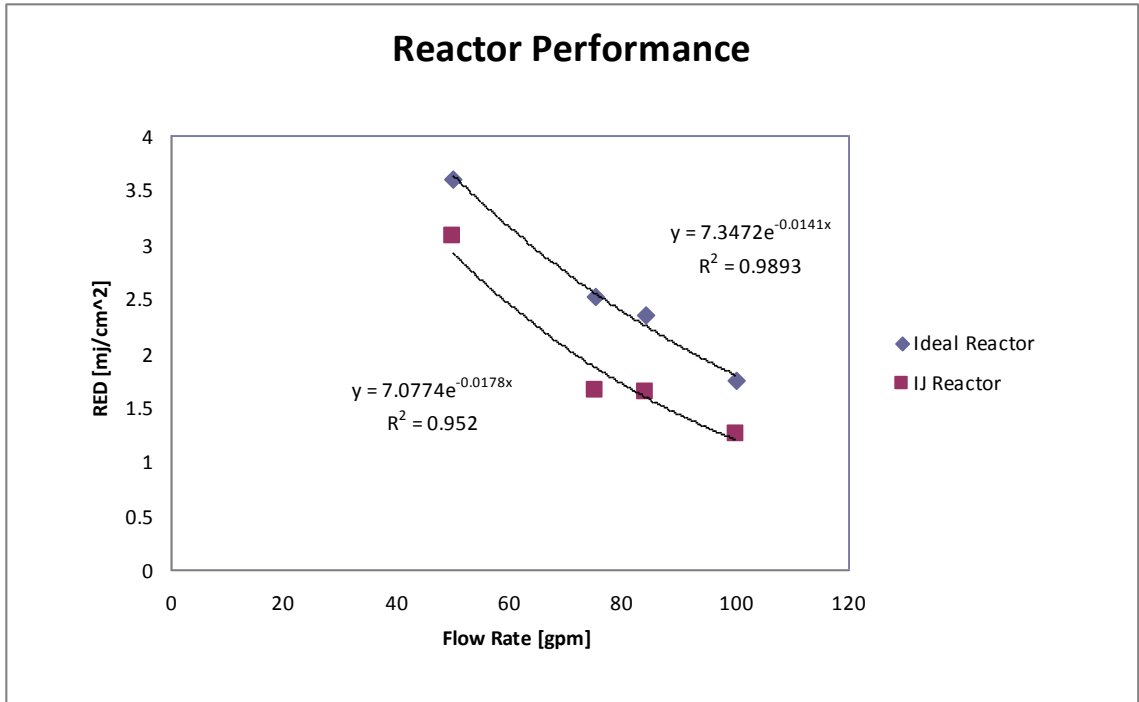


Figure C.7: T1 RED for 84 gpm IJ Flow Rate compared with ideal reactor for Efficiency Estimation.

Curriculum Vitae

Housyn Mahmoud

Education

2012 PhD, Chemical Engineering

The University of Western Ontario, London, ON, Canada.

Thesis: Disinfection of low transmittance UV fluids: Fundamentals and applications.

2006 Master of Engineering, Mechanical Engineering

The University of Western Ontario, London, ON, Canada.

Project Title: Modeling Taylor Vortices by Double Fourier Series

1997 Diploma in Fluid Mechanics , Mechanical Engineering

Damascus University, Damascus, Syria.

1994 Bachelor of Engineering science , Mechanical Engineering

Damascus University, Damascus, Syria.

Research and Professional Experience

2008 - 2012 Mitacs Fellow and Graduate Research/Teaching Assistant

Department of Chemical and Biochemical Engineering

The University of Western Ontario, London, ON, Canada.

2008-2012 Research Scientist/Trojan Technologies

Research and Development Department, Trojan Technologies (Danaher), London, Ontario.

Applied dimensional analyses on ultra violet UV disinfection of low transmittance fluid.

Simulated the fluence rate distribution of UV lamp inside the UV reactor with Matlab.

Conducted bioassay tests on UV systems to validate numerical simulations.

Proposed improvement on UV reactor design based on bioassay tests.

2007 - 2008 Graduate Research Assistant/Teaching Assistant

Department of Chemical and Biochemical Engineering

The University of Western Ontario, London, ON, Canada.

2004 - 2006 Graduate Research Assistant/Teaching Assistant

Department of mechanical and Material Engineering

The University of Western Ontario, London, ON, Canada.

Refereed Conference Proceedings

- ❑ **Mahmoud, H.**, , Ray, A. K. Disinfection of Opaque fluids with UV light at 8th World Congress of Chemical Engineering, August 2009, Montreal, Canada.
- ❑ **Mahmoud, H.**, , Khayat, R. Non isothermal effects in fiber spinning . CANSAM 2007, Toronto , Ontario, May 2007.

Scholarship and Awards

- ❑ Mitacs 2009-2012.

Technical Expertise

- ❑ Experience in commercial CFD software “ANSYS Fluent” (Turbulent and laminar flow modeling, radiation DO modeling applied for UV batch reactors).
- ❑ Specialized knowledge of numerical methods, heat transfer, and UV disinfection.
- ❑ Programming skills: MATLAB, Fortran.

Professional Organizations

- ❑ Professional Engineers of Ontario since 2011.